

Physical Oceanographic Conditions on the Newfoundland and Labrador Shelf during 2024

Jonathan Coyne, Frédéric Cyr, Steve Snook, Charlie Bishop, Peter S. Galbraith,
Jean-Luc Shaw, Nancy Chen, and Guoqi Han

Northwest Atlantic Fisheries Centre

Fisheries and Oceans Canada

80 East White Hills Road

St. John's, NL

A1C 5X1, Canada

2025

Canadian Technical Report of Hydrography and Ocean Sciences 401



Fisheries and Oceans
Canada

Pêches et Océans
Canada

Canada

Canadian Technical Report of Hydrography and Ocean Sciences

Technical reports contain scientific and technical information of a type that represents a contribution to existing knowledge but which is not normally found in the primary literature. The subject matter is generally related to programs and interests of the Oceans and Science sectors of Fisheries and Oceans Canada.

Technical reports may be cited as full publications. The correct citation appears above the abstract of each report. Each report is abstracted in the data base *Aquatic Sciences and Fisheries Abstracts*.

Technical reports are produced regionally but are numbered nationally. Requests for individual reports will be filled by the issuing establishment listed on the front cover and title page.

Regional and headquarters establishments of Ocean Science and Surveys ceased publication of their various report series as of December 1981. A complete listing of these publications and the last number issued under each title are published in the *Canadian Journal of Fisheries and Aquatic Sciences*, Volume 38: Index to Publications 1981. The current series began with Report Number 1 in January 1982.

Rapport technique canadien sur l'hydrographie et les sciences océaniques

Les rapports techniques contiennent des renseignements scientifiques et techniques qui constituent une contribution aux connaissances actuelles mais que l'on ne trouve pas normalement dans les revues scientifiques. Le sujet est généralement rattaché aux programmes et intérêts des secteurs des Océans et des Sciences de Pêches et Océans Canada.

Les rapports techniques peuvent être cités comme des publications à part entière. Le titre exact figure au-dessus du résumé de chaque rapport. Les rapports techniques sont résumés dans la base de données *Résumés des sciences aquatiques et halieutiques*.

Les rapports techniques sont produits à l'échelon régional, mais numérotés à l'échelon national. Les demandes de rapports seront satisfaites par l'établissement auteur dont le nom figure sur la couverture et la page de titre.

Les établissements de l'ancien secteur des Sciences et Levés océaniques dans les régions et à l'administration centrale ont cessé de publier leurs diverses séries de rapports en décembre 1981. Vous trouverez dans l'index des publications du volume 38 du *Journal canadien des sciences halieutiques et aquatiques*, la liste de ces publications ainsi que le dernier numéro paru dans chaque catégorie. La nouvelle série a commencé avec la publication du rapport numéro 1 en janvier 1982.

Canadian Technical Report
of Hydrography and Ocean Sciences 401

2025

Physical Oceanographic Conditions on the Newfoundland and Labrador Shelf during 2024

Jonathan Coyne¹, Frédéric Cyr^{1,2}, Steve Snook¹, Charlie Bishop¹, Peter S. Galbraith³, Jean-Luc Shaw³, Nancy Chen⁴, and Guoqi Han⁴

¹ Northwest Atlantic Fisheries Centre
Fisheries and Oceans Canada
80 East White Hills Road
St. John's, NL, A1C 5X1, Canada

² Fisheries and Marine Institute of Memorial University of Newfoundland and Labrador
155 Ridge Road
St. John's, NL, A1C 5R3, Canada

³ Maurice-Lamontagne Institute
Fisheries and Oceans Canada
850 Rte de la Mer
Mont-Joli, QC, G5H 3Z4, Canada

⁴ Institute of Ocean Sciences
Fisheries and Oceans Canada
9860 West Saanich Road
Sidney, BC, V8L 4B2, Canada

© His Majesty the King in Right of Canada, as represented by the Minister of the Department of
Fisheries and Oceans, 2025

Cat. No. Fs97-18/401E-PDF

ISBN 978-0-660-78138-9

ISSN 1488-5417

<https://doi.org/10.60825/1d14-x857>

Correct citation for this publication:

Coyne, J., Cyr, F., Snook, S., Bishop, C., Galbraith, P.S., Shaw, J.-L., Chen, N., and Han, G.
2025. Physical Oceanographic Conditions on the Newfoundland and Labrador Shelf during
2024. Can. Tech. Rep. Hydrogr. Ocean Sci. 401: iv + 61 p. <https://doi.org/10.60825/1d14-x857>

Contents

1	Introduction.....	1
2	Meteorological conditions	3
3	Sea ice conditions	8
4	Icebergs.....	16
5	Satellite sea-surface temperature	17
5.1	Marine heatwaves	24
6	Ocean conditions on the Newfoundland and Labrador shelf.....	27
6.1	Long-term observations at Station 27	27
6.2	Standard hydrographic sections	37
6.2.1	Temperature and Salinity Variability.....	37
6.2.2	Cold Intermediate Layer Variability	41
6.3	Bottom observations in NAFO sub-areas.....	44
6.3.1	Spring Conditions	44
6.3.2	Fall Conditions.....	48
6.3.3	Summary of bottom temperatures.....	51
7	Labrador Current transport	52
8	Summary	55
8.1	Highlights of 2024.....	57
9	Acknowledgements.....	57
	References.....	58

ABSTRACT

Coyne, J., Cyr, F., Snook, S., Bishop, C., Galbraith, P.S., Shaw, J.-L., Chen, N., and Han, G. 2025. Physical Oceanographic Conditions on the Newfoundland and Labrador Shelf during 2024. Can. Tech. Rep. Hydrogr. Ocean Sci. 401: iv + 61 p. <https://doi.org/10.60825/1d14-x857>

An overview of physical oceanographic conditions in the Newfoundland and Labrador (NL) Region during 2024 is presented in support of the Atlantic Zone Monitoring Program (AZMP). The winter North Atlantic Oscillation (NAO) index, a key indicator of the direction and intensity of the winter wind field patterns over the Northwest (NW) Atlantic was positive (+0.8) in 2024. Since 2014, all years except 2021 were positive (historically indicative of colder conditions). All environmental parameters presented in this report were indicative of warmer than normal conditions in 2024 (normal being defined as the average over the 1991–2020 climatological period). Sea surface temperature anomalies were tied for the warmest on record (with 2012), establishing new monthly and seasonal records among the Grand Banks NAFO divisions. 2024, 2023, and 2022 were the first, fourth, and third warmest annual SSTs on record respectively. While the transport on the Labrador and northeastern Newfoundland Slope was normal, the transport on the Scotian Slope was above normal for the second year in a row and at its highest value since its monitoring started in 1993 (+2.3 SD). The NL Climate index was at +1.1, making 2024 the 4th warmest year since 1951.

RÉSUMÉ

Coyne, J., Cyr, F., Snook, S., Bishop, C., Galbraith, P.S., Shaw, J.-L., Chen, N., and Han, G. 2025. Physical Oceanographic Conditions on the Newfoundland and Labrador Shelf during 2024. Can. Tech. Rep. Hydrogr. Ocean Sci. 401: iv + 61 p. <https://doi.org/10.60825/1d14-x857>

Un sommaire des conditions océanographiques physiques pour la région de Terre-Neuve et Labrador (TNL) en 2023 est présenté dans le cadre du Programme de Monitorage de la Zone Atlantique (PMZA). L'Oscillation Nord-Atlantique (ONA), un indicateur clé pour la direction et l'intensité des champs de vents hivernaux au-dessus de l'Atlantique nord-ouest, était positif (+0.8) en 2024. Depuis 2014, toutes les années sauf 2021 étaient positives (normalement indicatif de conditions froides). Tous les indices environnementaux présentés dans rapport étaient indicatifs de conditions plus chaudes que la normale en 2024 (normale étant définie comme la moyenne sur la période climatologique 1991-2021), à l'exception l'ONA. Les températures de surface de la mer étaient à leur plus chaud niveau enregistrés (à égalité avec 2012), incluant de nombreux records mensuels et saisonniers pour les différentes divisions de l'OPANO analysées. Les années 2024, 2023 et 2022 ont été respectivement les première, quatrième et troisième années les plus chaudes enregistrées pour la température de surface de la mer. Alors que le transport le long du talus de TNL était normal, le transport le long du talus néo-écossais était au-dessus de la normale pour une deuxième année consécutive et à son plus haut niveau jamais enregistré depuis le début de ce monitorage en 1993 (+2.3 É-T). L'indice du climat de TNL était à +1.1, faisant de 2024 la quatrième année la plus chaude depuis 1951.

1 Introduction

This manuscript presents an overview of the 2024 environmental and physical oceanographic conditions in the Newfoundland and Labrador (NL) Region (Figure 1), in support of the Fisheries and Oceans Canada (DFO) Atlantic Zone Monitoring Program (AZMP; Therriault et al., 1998, Galbraith, Blais, et al., 2024). This report complements similar reviews of the environmental conditions in the Gulf of St. Lawrence (Galbraith, Chassé, et al., 2024) and the Scotian Shelf and Gulf of Maine (Hebert et al., 2024). Physical oceanographic conditions for the NL region in 2023 were presented in Cyr et al., (2024).

The information presented in this report is derived from various sources:

1. Ice data from the Canadian Ice Service, while meteorological data are from Environment and Climate Change (ECCC) Canada and other sources cited in the text;
2. Sea Surface Temperatures (SSTs, Galbraith et al., 2021). These correspond to a blend of Advanced Very High Resolution Radiometer (AVHRR) data from Pathfinder version 5.3 (1982–2014), the Maurice Lamontagne Institute (1985–2013) and the GHRSST NOAA/STAR L3S-LEO-Daily (2007–present). See Galbraith et al., (2025) for a description;
3. Observations made throughout the year at monitoring Station 27 near St. John's, NL;
4. Measurements made along standard AZMP cross-shelf sections (see map Figure 1);
5. Oceanographic observations made during spring and fall multi-species resource assessment surveys;
6. Other multi-source historical data (ships of opportunity, international campaigns, surveys from other DFO regions, the Argo program, etc.).

All vertical profiles of temperature and salinity used in this report (e.g. points 3-6 above) are available at <https://doi.org/10.20383/102.0739> [consulted 2025-01-20] (Coyne et al., 2023). Bottom temperatures and salinity presented in Section 6.3 are also available at <https://doi.org/10.20383/103.0969> [consulted 2025-02-11] (Coyne & Cyr, 2025).

Time series of temperature and salinity anomalies, as well as other climate indices were constructed by subtracting the average computed over a standard climatological period from 1991 to 2020. When a variable is measured throughout the seasonal cycle (e.g. air temperature, Station 27 observations), the annual anomaly is calculated as the average of monthly anomalies. Unless otherwise specified, annual or seasonal anomalies were normalized by dividing the values by the standard deviation (SD) of the data time series over the climatological period. A value of 2, for example, indicates that the index was 2 SD higher than its long-term average. As a general guide, anomalies within ± 0.5 SD are considered to be normal.

The normalized values of water properties and derived climate indices are presented as “scorecards”, which are color-coded gradations of 0.5 SD (Figure 2). Shades of blue represent cold environmental conditions and red represent warm conditions. In some instances, such as for the North Atlantic Oscillation (NAO), or for ice and cold intermediate layer (CIL) properties, negative anomalies indicate warm conditions, and are therefore colored red. Most of the colormaps used in this report are taken from the *cmocean* colormaps package for oceanography (Thyng et al., 2016).

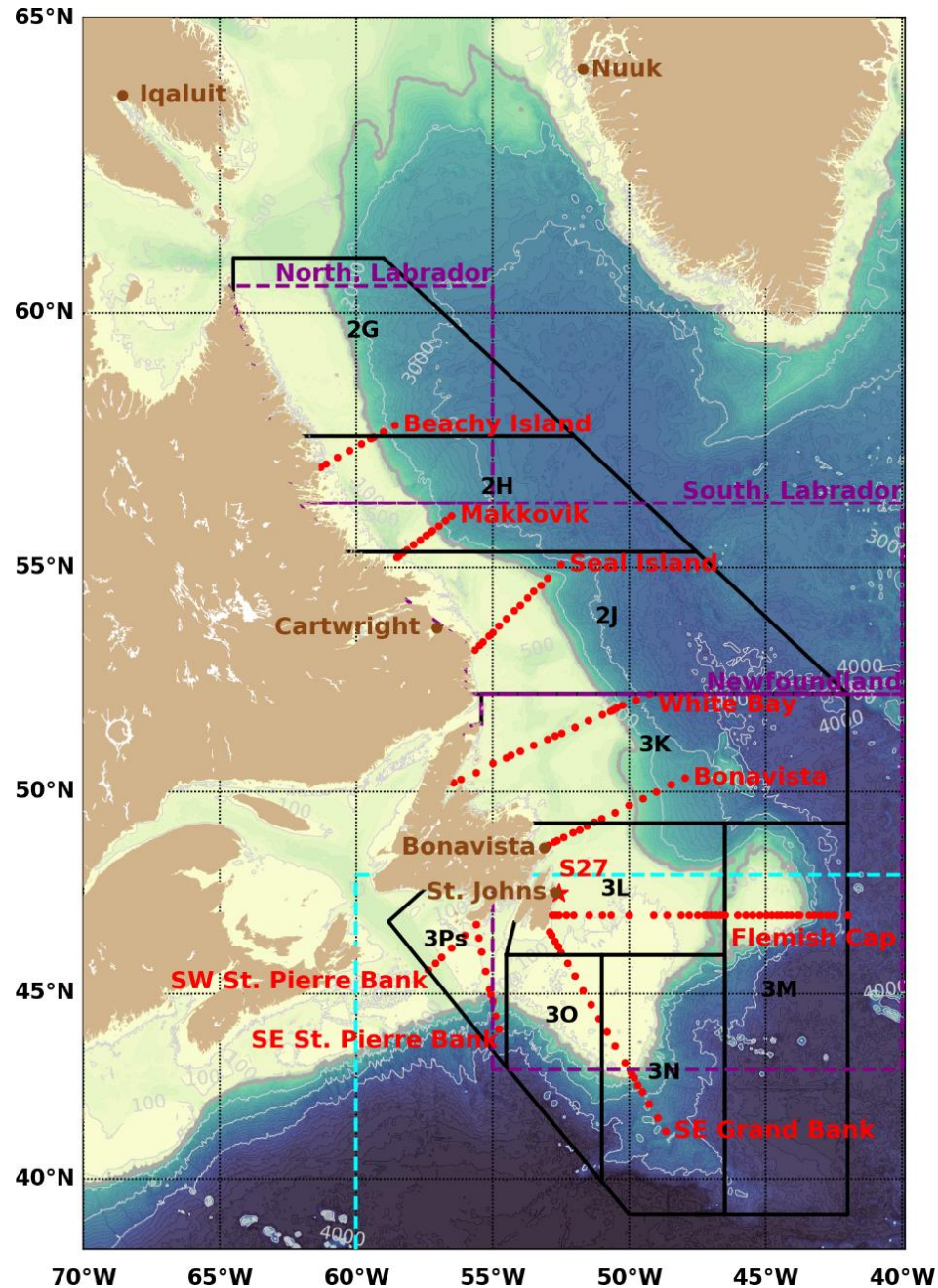


Figure 1: Map of the Northwest Atlantic Ocean, including important bathymetric features (the gray isobaths are identified on the figure). NAFO Divisions (sub-areas 2 and 3) on the Newfoundland and Labrador (NL) shelf are drawn. (black boxes) The AZMP hydrographic sections are shown with red dots, and their names labeled in red text on the figure. Long-term AZMP hydrographic Station 27 is highlighted with a red star. The five stations used for the air temperature time series are shown in brown. The three regions used for sea ice calculations (Northern Labrador shelf, Southern Labrador shelf and Newfoundland shelf) are drawn with dashed magenta lines. The region used by the International Ice Patrol for iceberg sightings south of 48°N is drawn in dashed cyan. The shelf break is delimited by a thicker and darker gray contour corresponding to the isobath 1,000 m (used to clip the SST and bottom temperature).

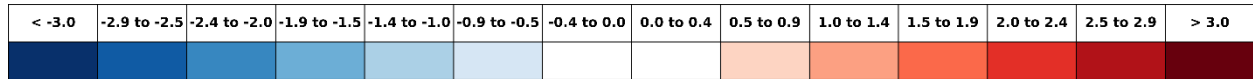


Figure 2: Color scale used for the presentation of normalized anomalies. Color levels are incremented by 0.5 standard deviations (SD), where blue is below normal and red above normal. Values between 0 and ± 0.5 SD remain white indicating normal conditions. Anomalies are rounded to the nearest tenth.

2 Meteorological conditions

The North Atlantic Oscillation (NAO; see Figure 3 for time series since 1951 and Figure 4 for tabulated values since 1980) refers to the anomaly in the sea-level pressure (SLP) difference between the subtropical high (average location near the Azores) and the subpolar low (average location near Iceland). Several definitions of the NAO exist, though the one used here is from the National Center for Environmental Information of the National Oceanic and Atmospheric Administration (NOAA) available [online](#). The winter NAO (defined here as the average of monthly values from December to March) is considered a measure of the strength of the winter westerly and northwesterly winds over the Northwest Atlantic. A high NAO index (positive phase) occurs during an intensification of the Icelandic Low and Azores High. Except for some years for which the SLP patterns are spatially shifted (e.g., 1999, 2000, and 2018), positive winter NAO years favor strong northwesterly winds, cold air and sea surface temperatures (SSTs), and heavy ice conditions on the NL shelves (Colbourne et al., 1994; Drinkwater et al., 1994; Petrie et al., 2007). The winter NAO was positive in 2024 (+0.8; first row in Figure 4). While the lowest winter NAO index value was reached in 2010, all years between 2012 and 2024 (except 2013 and 2021) were positive, including the record high of +1.6 in 2015.

The Arctic Oscillation (AO) is a larger-scale index intimately linked with the NAO. During a positive phase, the Arctic air outflow to the Northwest Atlantic increases, resulting in colder winter air temperatures over much of NL and adjacent shelf regions. The AO was neutral in 2024 at +0.1 (Figure 4). In 2020, the AO was at its highest value since 1990 at +0.8. A record low was reached in 2010 when it was below normal at -1.0 (warm air temperatures).

The Atlantic Multidecadal Oscillation (AMO) is also provided in Figure 4. This index, based on the Sea Surface Temperature of the Atlantic Ocean, evolves as part of a 65–80 year cycle that influences the regional climate and has consequences on the ocean circulation in the North Atlantic (Kerr, 2000). The AMO has been in a slightly positive phase since the late 1990s (Figure 4). No update to the AMO has been made available since January 2023.

Air temperature anomalies (winter and annual values) from five coastal communities around the Northwest Atlantic (Nuuk, Greenland; Iqaluit on Baffin Island, Nunavut; Cartwright, Labrador; Bonavista and St. John's in Newfoundland; see Figure 1) are shown in Figure 4 as normalized anomalies between 1980 and 2024, and in Figure 5 and Figure 6 as monthly and annual (cumulative for all stations) anomalies, respectively. Except for Nuuk for which data are obtained from the Danish Meteorological Institute, the air temperature data from Canadian sites are from the second generation of Adjusted and Homogenized Canadian Climate Data (AHCCD), which accounts for shifts in station location and changes in observation methods (Vincent et al., 2012). Because the AHCCD product was not ready for the year 2024, historical data from the Government of Canada [Monthly Climate Summaries](#) have been used for that year.

In 2024, the air temperature exhibited consistently positive anomalies that were generally coherent between all sites (excluding Nuuk annual air temperature which was neutral) (Figure 4). Temperature anomalies were positive for every month (excluding May), with February to April being especially warm (Figure 5). Averaged over the year, the air temperatures were above normal, making 2024 the 2nd warmest

year since 1950 at +1.4 SD (Figure 6). 2010 was the warmest year at +2.1 SD, and all of the 6 warmest years have occurred since 2005.

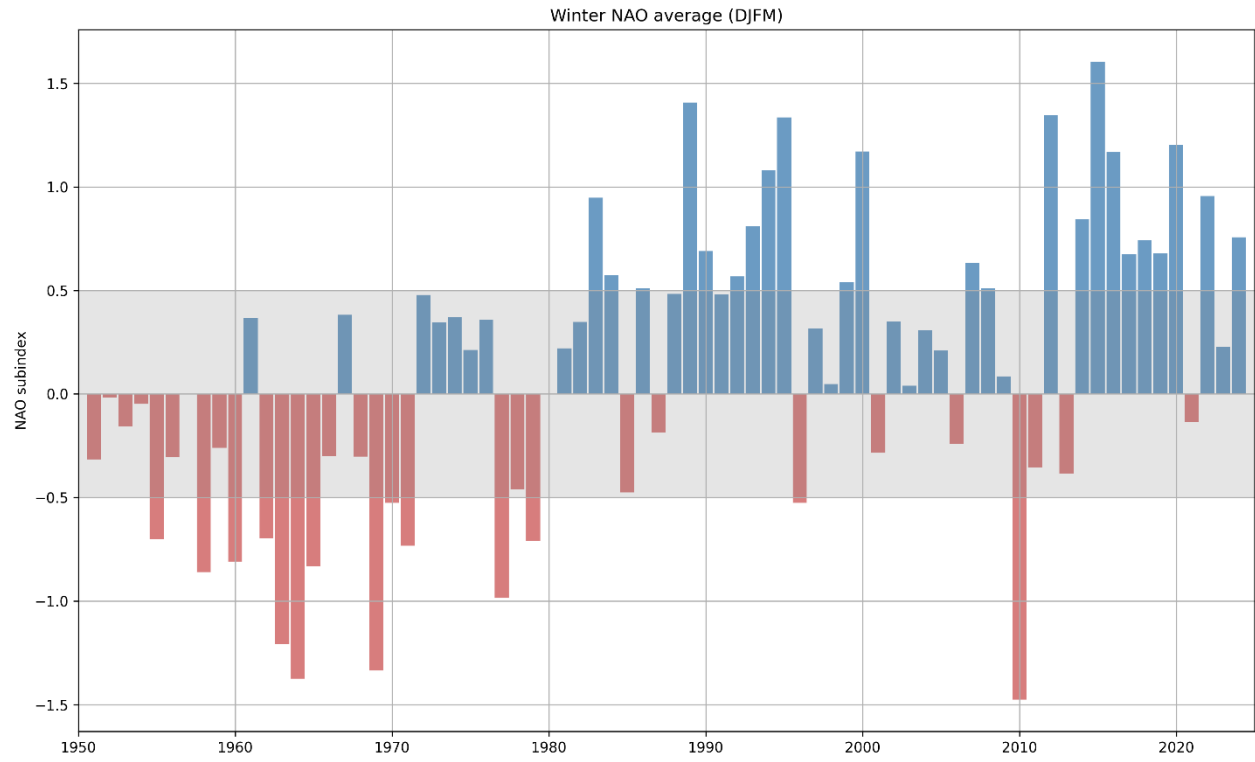


Figure 3: Winter North Atlantic Oscillation (NAO) Index calculated by averaging the December to March values since 1951 (which correspond to the average of December 1950 and January-March 1951). The NAO Index used here is from the National Center for Environmental Information of the NOAA. This index is used as part of the NL climate index mentioned in the summary (Figure 4646).

	-- Climate indices --																														x	sd															
	80	81	82	83	84	85	86	87	88	89	90	91	92	93	94	95	96	97	98	99	00	01	02	03	04	05	06	07	08	09	10	11	12	13	14	15	16	17	18	19	20	21	22	23	24	x	sd
NAO _{winter}	0.0	0.2	0.3	0.9	0.6	-0.5	0.5	-0.2	0.5	1.4	0.7	0.5	0.6	0.8	1.1	1.3	-0.5	0.3	0.0	0.5	1.2	-0.3	0.4	0.0	0.3	0.2	-0.2	0.6	0.5	0.1	-1.5	-0.4	1.3	-0.4	0.8	1.6	1.2	0.7	0.7	0.7	1.2	-0.1	1.0	0.2	0.8		
AO	-0.6	-0.4	0.3	0.0	-0.2	-0.5	0.1	-0.5	0.0	1.0	1.0	0.2	0.4	0.1	0.5	-0.3	-0.5	0.0	-0.3	0.1	0.0	-0.2	0.1	0.2	-0.2	-0.4	0.1	0.3	0.2	-0.3	-1.0	0.5	-0.2	0.0	-0.1	0.6	-0.1	0.3	0.2	-0.1	0.8	-0.1	0.1	0.0	0.1		
AMO	0.0	-0.1	-0.2	-0.1	-0.2	-0.3	-0.3	-0.0	0.0	-0.1	-0.1	-0.2	-0.3	-0.2	-0.2	0.1	-0.1	0.0	0.3	0.1	0.0	0.1	0.0	0.2	0.2	0.3	0.2	0.1	0.1	0.0	0.3	0.1	0.1	0.3	0.3	0.0	0.1	0.3	0.2	0.2	0.2	0.2					
	-- Winter Air Temperature --																																														
Nuuk	0.8	0.2	0.0	-3.0	-3.6	0.4	2.2	-0.4	0.4	-1.4	-0.6	-1.1	-1.4	-2.5	-0.7	-1.3	0.4	0.1	-0.3	0.1	0.2	0.1	0.9	1.3	0.3	0.6	1.0	-1.5	0.6	2.3	1.3	-0.1	0.5	0.1	-1.0	0.1	0.1	-0.5	1.1	-0.5	0.9	0.0	0.2	0.6	-7.2	2.2	
Iqaluit	0.4	0.8	0.9	-2.3	-2.0	0.6	1.7	-1.3	-0.4	-1.7	-1.1	-1.7	-0.9	-2.1	-0.8	-0.2	0.2	0.1	-1.9	-0.3	0.2	0.4	-0.2	0.3	0.8	-0.6	0.4	1.1	-1.0	-0.1	2.2	2.1	0.6	0.6	0.5	-1.2	0.2	0.4	0.1	0.6	0.3	2.7	0.4	-0.1	1.3	-23.9	3.0
Cartwright	0.4	0.8	0.1	-1.3	-1.0	-0.2	0.0	-0.2	-0.1	-1.3	-1.3	-1.4	-1.6	-1.5	-1.1	-0.8	0.4	0.1	0.7	0.3	0.2	-0.1	0.3	0.1	1.6	-0.1	0.6	0.8	-0.9	0.1	2.7	2.0	0.0	0.8	-0.8	-1.2	0.3	-0.2	0.2	-0.3	-0.9	2.2	-0.6	0.1	1.7	-12.0	2.6
Bonavista	-0.3	0.6	-0.2	-0.3	-0.4	-1.0	-0.5	-0.9	-0.2	-1.5	-2.4	-1.5	-1.8	-2.1	-1.7	-1.0	0.4	-0.2	0.1	0.8	1.0	-0.3	0.1	-0.9	0.9	0.4	1.5	0.2	-0.5	0.4	1.0	1.9	0.8	0.6	-1.2	0.1	0.6	0.0	1.1	-0.7	0.0	2.0	0.8	0.9	1.4	-3.2	1.3
St.Johns	-0.6	0.6	-0.4	0.6	0.4	0.8	-0.3	1.3	0.4	1.7	2.4	1.3	1.9	1.9	1.5	-1.0	0.1	-0.1	1.1	1.2	0.8	0.0	-1.0	0.7	0.5	1.4	-0.1	0.4	0.9	0.9	2.0	0.7	0.4	-1.0	0.5	0.6	-0.1	1.2	-0.8	0.0	2.1	1.3	0.8	0.8	-3.0	1.2	
	-- Annual Air Temperature --																																														
Nuuk	0.4	-0.2	-1.6	-2.4	-2.1	1.0	-0.2	-0.4	0.0	-1.7	-1.2	-0.7	-2.0	-2.2	-1.1	-0.6	0.1	-0.2	0.0	-0.3	0.1	0.5	-0.1	1.1	0.4	1.0	0.6	0.4	-0.1	0.3	2.8	-0.6	0.9	0.5	0.1	-1.5	1.0	0.2	-0.9	1.0	-0.6	0.8	-0.1	0.5	0.2	-1.0	1.3
Iqaluit	0.4	1.2	-1.3	2.1	1.6	0.9	-1.1	-1.2	-0.4	-1.6	-1.7	0.9	2.3	2.3	-0.7	0.3	0.3	0.6	-0.2	-0.5	0.2	0.4	-0.5	0.6	0.2	0.7	1.3	-0.1	-0.4	0.2	2.9	0.3	0.4	0.0	0.2	-1.7	0.1	0.5	0.6	0.9	0.5	2.3	0.4	0.0	1.0	-8.3	1.5
Cartwright	-0.2	0.9	-1.3	-0.6	-1.1	0.7	-1.0	0.3	-0.4	0.6	-1.2	-1.5	-1.3	-1.3	-0.6	0.5	0.3	0.4	0.5	0.8	0.4	0.5	-0.4	0.3	0.9	0.7	1.5	0.0	0.0	0.3	2.2	0.5	1.1	0.4	-0.1	3.0	-0.4	0.1	0.2	-1.1	0.4	1.5	0.2	0.8	1.8	0.2	1.4
Bonavista	-1.1	0.6	-1.0	0.1	-0.4	-1.3	-0.9	-0.3	0.2	-0.2	-0.7	-1.7	-1.7	-1.6	-0.6	-0.7	0.5	-0.9	0.6	0.5	0.9	0.5	-0.2	0.2	0.7	0.8	1.2	0.6	0.4	0.2	1.3	-1.6	1.4	0.7	-0.1	-0.7	0.3	0.9	-2.1	-0.5	0.9	1.6	1.7	0.7	2.2	5.0	1.0
St.Johns	-1.6	0.8	-1.3	0.3	0.1	-2.0	-1.3	-0.9	-0.1	-0.9	-0.8	-1.8	-2.2	-1.8	-0.7	-1.0	0.1	-1.4	0.4	1.8	0.8	0.1	-0.7	0.1	0.3	0.5	1.4	-0.4	0.6	0.7	1.3	0.1	1.5	0.7	0.1	-1.0	0.2	0.1	-0.2	-0.7	0.8	1.4	2.1	0.4	1.7	5.5	0.8

Figure 4: Scorecard of large-scale indices (winter NAO, AO and AMO) and normalized air temperature anomalies (winter and annual) for five cities between 1980 and 2024. Means and standard deviations for the air temperatures during the 1991–2020 period are provided in the last column (in °C). No means or standard deviations are provided for the large-scale indices (grayed boxes).

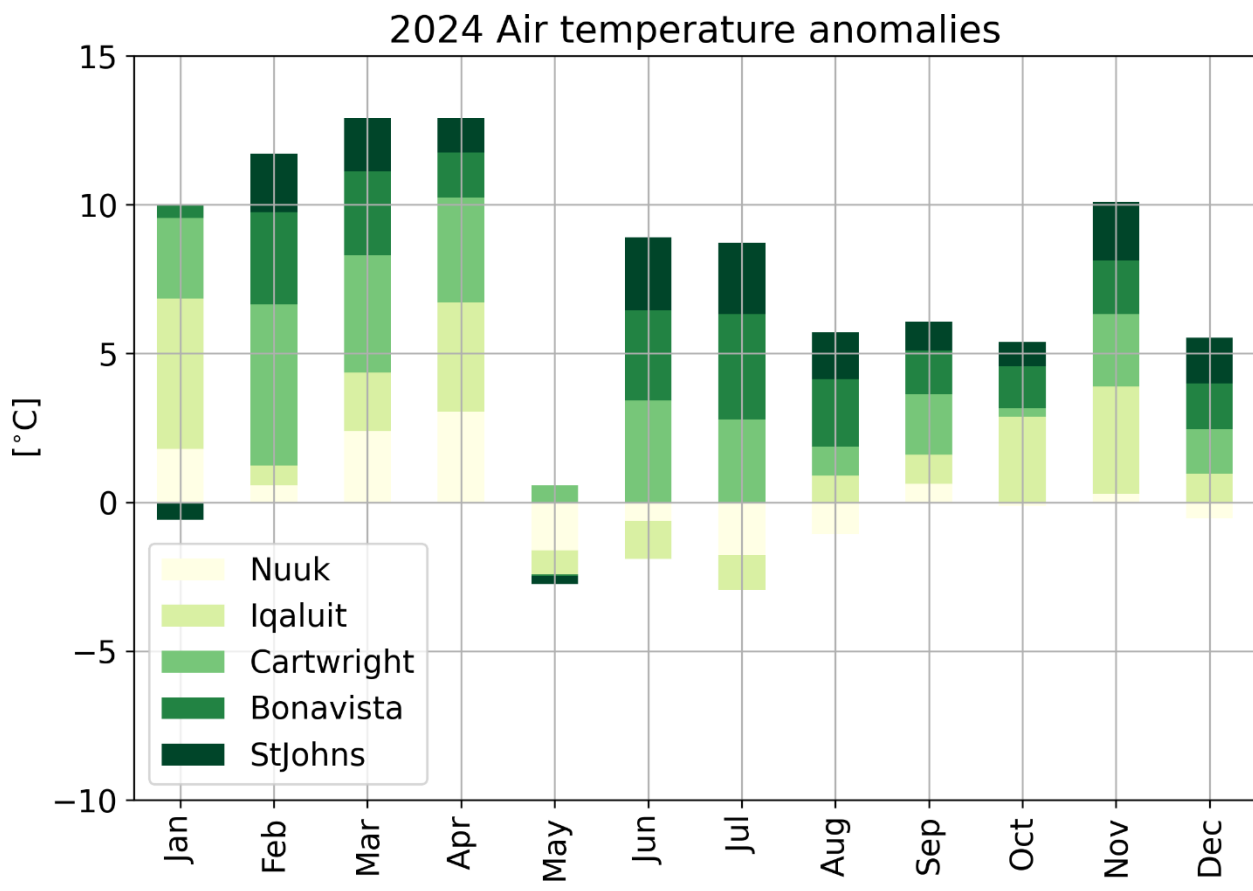


Figure 5: Cumulative monthly air temperature anomalies at Nuuk, Iqaluit, Cartwright, Bonavista and St. John's for 2024.

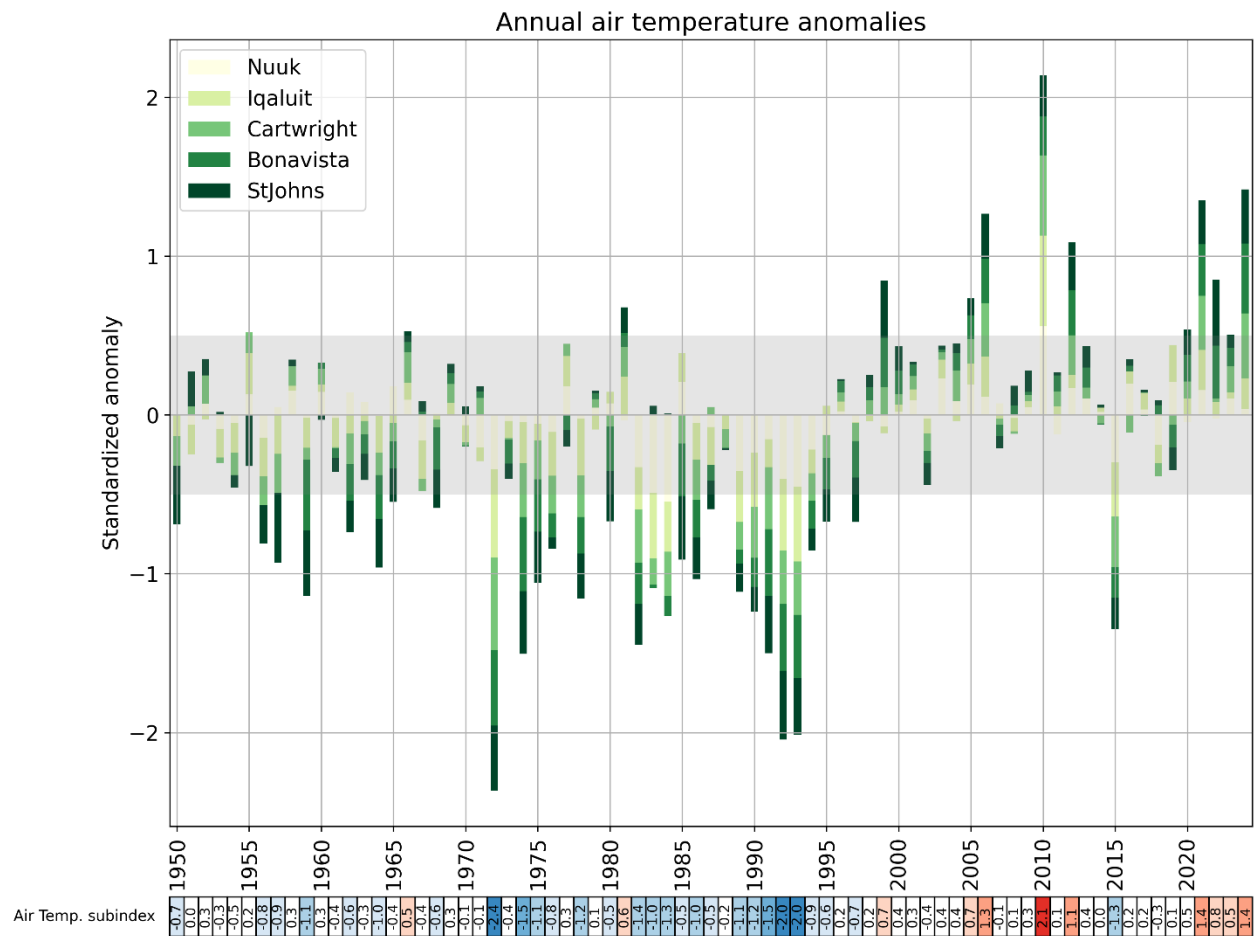


Figure 6: Normalized annual air temperature anomalies for Nuuk, Iqaluit, Cartwright, Bonavista and St. John's. This figure shows the average of the five stations, in which the length of each bar corresponds to the relative contribution of the individual station to the average. The shaded area corresponds to the 1991–2020 average ± 0.5 SD, a range considered normal. The numerical values of this time series are reported in a color-coded scorecard at the bottom of the figure. The bottom scorecard is the average of these five time series, and is used to construct the NL climate index presented in the summary (Figure 4646).

3 Sea ice conditions

Ice cover area, volume and seasonal duration are estimated from ice cover products obtained from the Canadian Ice Service (CIS) as detailed in Galbraith, Sévigny, et al., (2024) for the Gulf of St. Lawrence. These products consist of Geographic Information System (GIS) charts covering the East Coast and Hudson Bay system, the latter providing coverage of the Northern Labrador Shelf. The East Coast region has weekly charts available for 1969–2024 and daily charts for 2009–2024 while only weekly charts are available for the Hudson Bay system for 1980–2024. All vector charts were further converted into regular 0.01° latitude by 0.015° longitude grids (approximately 1 km resolution), with ice concentrations and growth stages attributed to each grid point. Average thicknesses (and therefore regional volumes) are estimated from standard thicknesses associated with each stage of ice growth from new ice (stage 1, <10 cm: 5 cm), nilas (stage 2, <10 cm: 5 cm), gray ice (stage 4, 10–15 cm: 12.5 cm), gray-white ice (stage 5, 15–30 cm: 22.5 cm), thin first-year ice (stage 7, 30–70 cm: 50 cm), medium first-year ice (stage 1•, corresponding to 70–120 cm: 95 cm) and thick first-year ice (stage 4•, corresponding to >120 cm: 160 cm). Prior to 1983, the CIS reported ice categories with fewer classifications, where a single category of first-year ice (≥30 cm) was used with a suggested average thickness of 65 cm. We have found this value leads to underestimates of the seasonal maximum thickness and volume based on high interannual correlations between the estimated volume of the weekly seasonal maximums and its area or sea ice season duration. The comparisons of the slope of these correlations pre- and post-1983 provided estimates of first-year ice thickness of 85 cm in the Gulf of St. Lawrence and 95 cm on the Newfoundland and Labrador Shelf for this single first-year ice category, which were used instead of the suggested 65 cm.

Several products were computed to describe the sea ice cover inter-annual variability. The day of first and last occurrence, ice season duration (Figure 7) and the distribution of ice thickness during the week of maximum volume (Figure 8) are presented as maps. These two figures combine information from the East Coast sea ice charts and Hudson Bay system charts, leading to a slight jump in the climatology maps of first occurrence and duration. This occurs because there are often missing weeks in the Hudson Bay charts around the period of first occurrence on the northern Labrador Shelf. Therefore, anomalies of these two parameters have more uncertainty than the rest. Regional scorecards of anomalies for the first and last day of ice, duration of the sea ice season and maximum ice volume are presented in Figure 9 for the Labrador and Newfoundland shelves. Here, the areas defined as the Northern and Southern Labrador shelves and the Newfoundland Shelf are depicted in Figure 1, with the Newfoundland Shelf and Gulf of St. Lawrence delimited at the Eastern end of the Strait of Belle Isle. Evolution of the estimated ice volume during the 2023-24 ice season is presented in Figure 10 for the three regions in relation to the climatology and historical extremes. The Northern Labrador Shelf progression is shown using weekly data extracted from Hudson Bay charts, while the others are shown using daily data extracted from East Coast charts. Time series of seasonal maximum ice volume, area (excluding thin new ice) and ice season duration are presented for the Northern (top) and Southern (middle) Labrador Shelf and for the Newfoundland Shelf (bottom) in Figure 11. The December-to-April air temperature anomaly at Cartwright showed the best correlation with sea ice properties and is included with reversed scale in the Newfoundland Shelf panel. The durations shown in Figure 9 and Figure 11 are different products. The first corresponds to the number of weeks where the volume of ice anywhere within the region exceeded 5% of the climatological maximum, while the second is the average duration at every pixel of Figure 7, which is much shorter than the first. An overview of sea ice conditions (area and season duration) for NL since 1969 is presented in Figure 12 as the average of normalized anomalies.

Ice typically starts forming in December along the Labrador coast and appears only by late February at the southernmost extent of sea ice presence (Figure 7). The last occurrence is usually in late June to early July on the Labrador coast, leading to sea ice season durations of 23 weeks or more. There has been a declining trend in ice cover severity since the early 1990s (Figure 9) second and first lowest values in

2010 and 2011, with a rebound in 2014, third lowest value in 2021, and ending with the 6th lowest in 2024. On the Newfoundland Shelf, the sea ice metrics of annual maximum ice area, volume, and ice cover duration are all well-correlated with each other ($R^2 = 0.72$ to 0.75; Figure 11). The strongest correlation with air temperature was found between the December-April air temperature anomaly at Cartwright and the sea ice metrics of the Newfoundland Shelf ($R^2 = 0.64$ to 0.78), indicative of the advective nature of the Newfoundland shelf sea ice; i.e. strong ice cover is associated with cold air temperatures in the source area. Sensitivity of the Newfoundland Shelf ice cover to increases in air temperature (e.g. through climate change) can thus be estimated using 1969–2024 co-variations between winter air temperature at Cartwright and sea ice parameters, which indicate losses of 14 km³, 25,000 km² and eight days of sea ice season for each 1°C increase in winter air temperature.

In 2024, the sea ice cover first appeared at generally later than normal dates (Figure 7), leading to regional thresholds marking the beginning of the season that were crossed later than normal (Figure 9). The last occurrence was earlier than normal (Figure 7) but some ice lingered into July on the Northern Labrador Shelf (Figure 10) leading to a near-normal date crossing the regional threshold (Figure 9). Estimated sea ice volumes progressed below normal throughout the season in the three regions (Figure 10). The maximum ice volumes reached during the season were below normal on the Labrador Shelf, at 54 km³ (-1.6 SD; record low) and 53 km³ (-1.7 SD; second lowest) on the northern and southern parts respectively, and also below normal on the Newfoundland Shelf at 14 km³ (-1.4 SD; third lowest). The December-to-June seasonal averages followed the same pattern at 29 km³ (-1.5 SD) and 20 km³ (-1.3 SD) on the Northern and Southern Labrador Shelves and 3 km³ (-1.1 SD) on the Newfoundland Shelf (Figure 9). From North to South, the pixel average durations were below normal at 93 (-1.5 SD), 72 (-1.1 SD) and 17 days (-1.4 SD) (Figure 7 and Figure 11). The maximum area reached within each region (excluding ice less than 15 cm thick) was below normal at 82 000 km² (-0.8 SD), 109 000 km² (-0.6 SD) and 40 000 km², -1.3 SD).

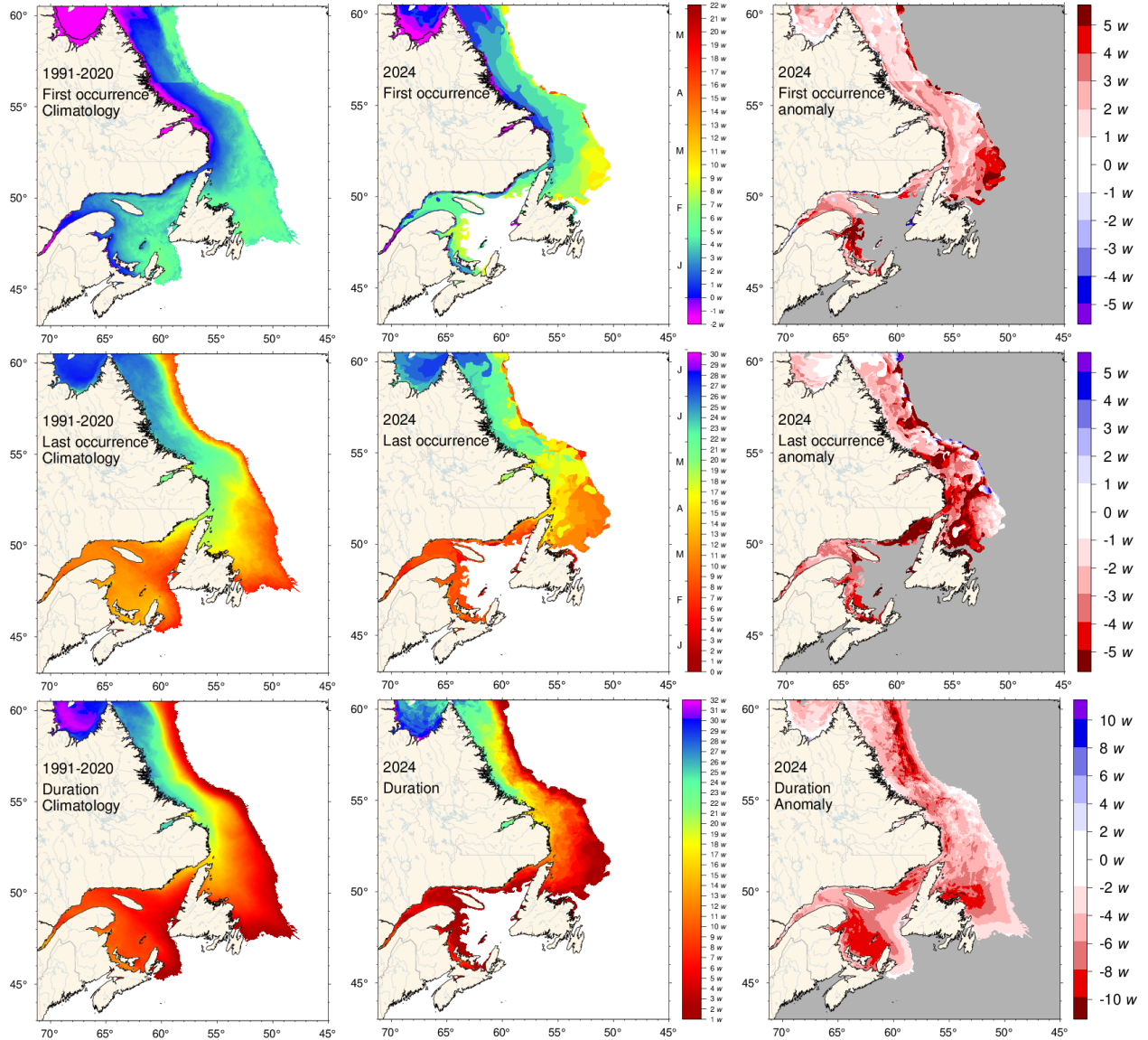


Figure 7: First (top) and last (middle) occurrence of ice and ice season duration (bottom) based on weekly data. The 1991–2020 climatologies are shown (left) as well as the 2024 values (middle) and anomalies (right). First and last occurrences are defined here as the first and last weekly chart in which any amount of ice is recorded for each pixel and are illustrated as day-of-year. Ice duration sums the number of weeks with ice cover for each pixel. Climatologies are shown for pixels that had at least 15 years out of 30 with occurrence of sea ice, and therefore also show the area with 50% likelihood of having some sea ice at any time during any given year. The duration anomaly map includes pixels with no ice cover where some was expected based on the climatology.

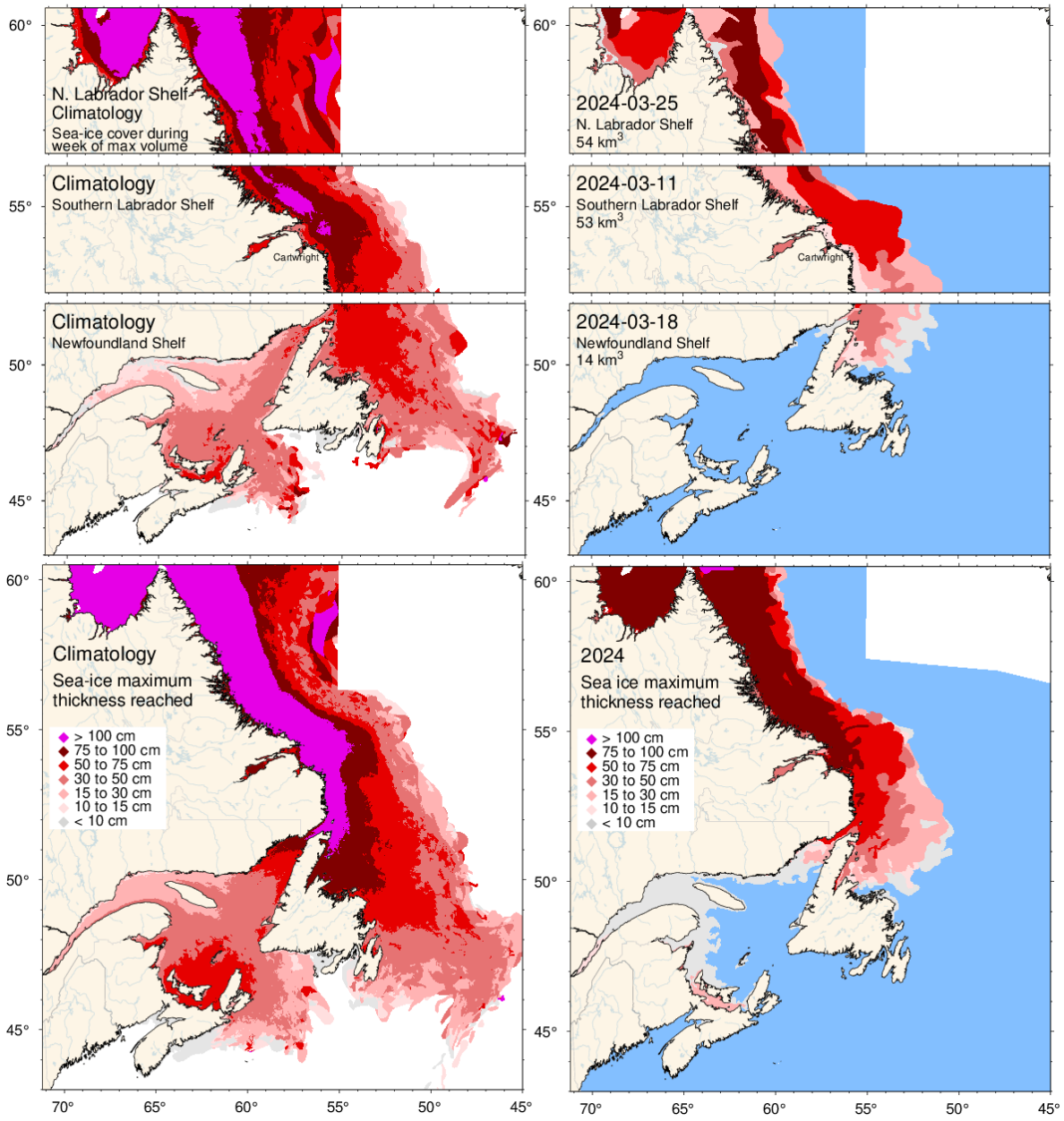


Figure 8: Ice thickness map for 2024 for the week with the maximum annual volume on the Newfoundland and Labrador Shelf (three upper right panels) and similarly for the 1991–2020 climatology of the weekly maximum (three upper left panels). Note that these maps reflect the ice thickness distribution on that week. The maximum ice thickness observed at any given location during the year is presented in the lower panels, showing the 1991–2020 climatology and 2024 distribution of the thickest ice recorded during the season at any location.

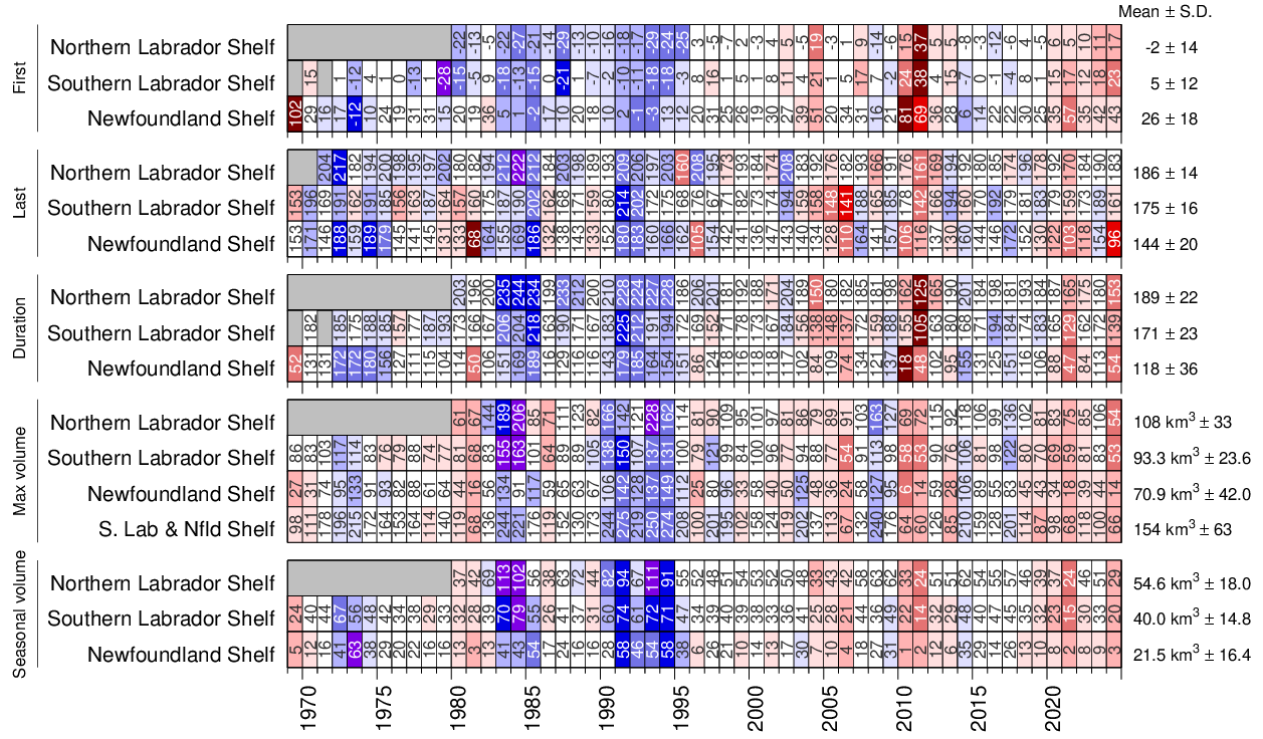


Figure 9: First and last day of ice occurrence, ice duration, maximum seasonal ice volume and average seasonal (DJFMAMJ) ice volume by region. The moment when ice was first and last observed in days from the beginning of each year is indicated for each region, and the color code expresses the anomaly based on the 1991–2020 climatology, with blue (cold) representing earlier first occurrence and later last occurrence. The threshold is 5% of the climatological average of the seasonal maximum ice volume. Numbers in the table are the actual day of the year or volume, but the color coding is according to normalized anomalies based on the climatology of each region. Duration is the numbers of days that the threshold was exceeded. Seasonal average volumes (lowermost scorecard) are reported in the ICES Report on Ocean Climate (Cyr & Galbraith, 2023).

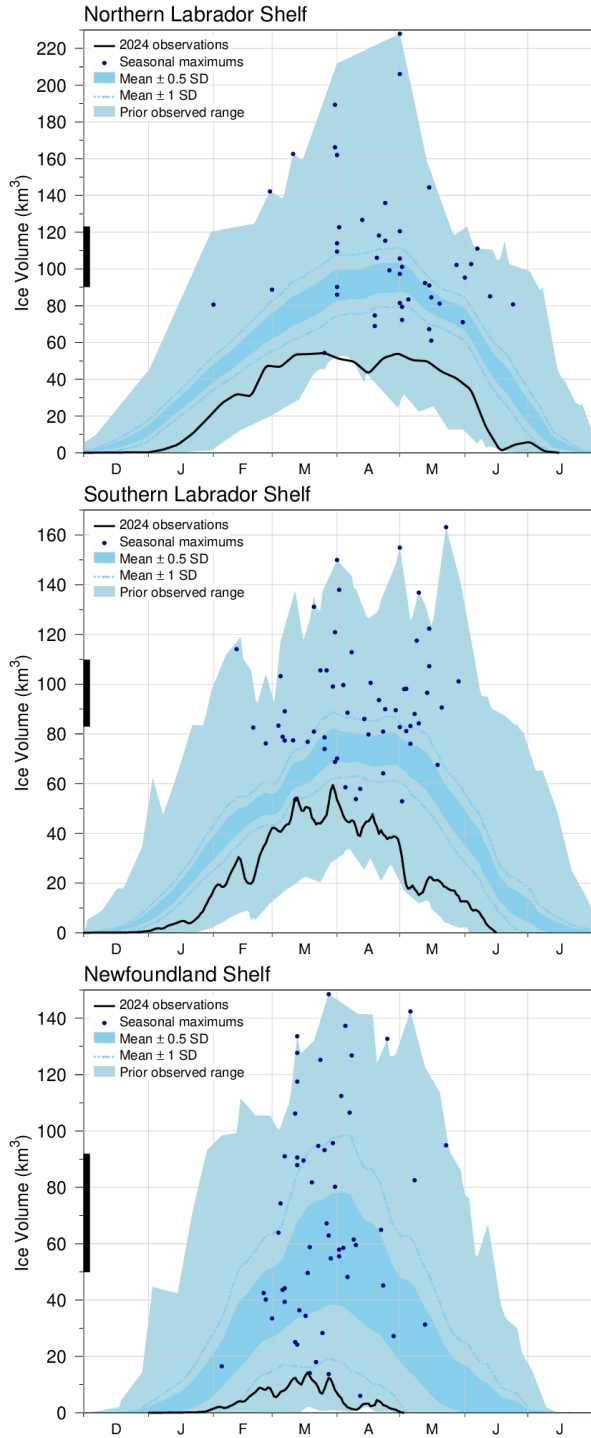


Figure 10: Time series of the 2023–24 mean ice volume (black lines) for the Northern Labrador Shelf (top), Southern Labrador Shelf (middle), and Newfoundland Shelf (bottom), the 1991–2020 climatological mean volume ± 0.5 and ± 1 SD (dark blue area and dashed line respectively), the minimum and maximum span of 1969–2023 observations (light blue), and the date and volumes of 1969–2023 seasonal maximums (blue dots). The black thick line on the left indicates the mean volume ± 0.5 SD of the annual maximum ice volume distribution.

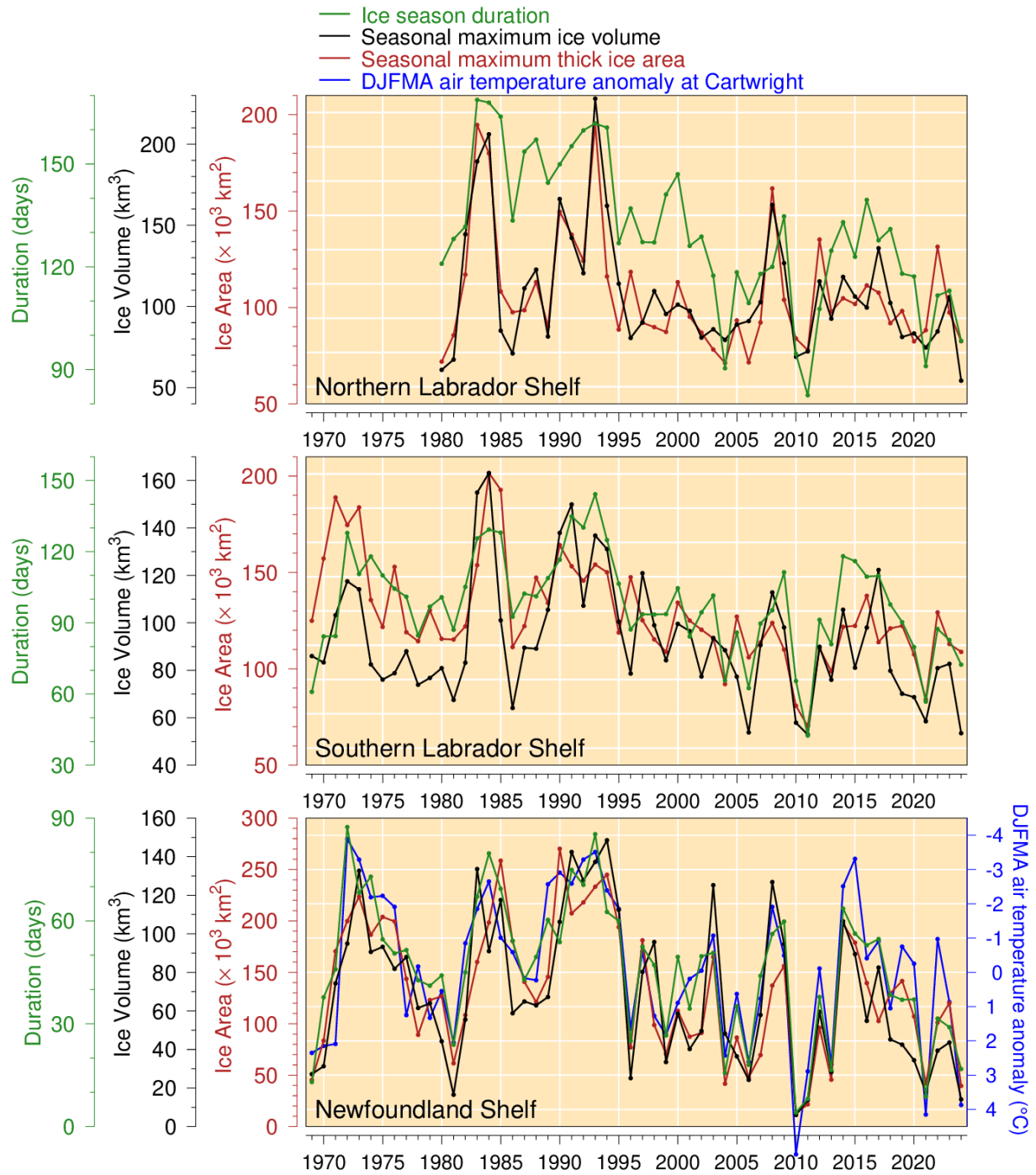


Figure 11. Regional average sea ice metrics and NL sea ice index. Seasonal maximum ice volume (black lines) and area (excluding ice less than 15 cm thick; red lines), and ice season duration (green lines) for the Northern and Southern Labrador Shelf (first and second panels, respectively) and the Newfoundland Shelf (third), and December-to-April air temperature anomaly at Cartwright (blue line).

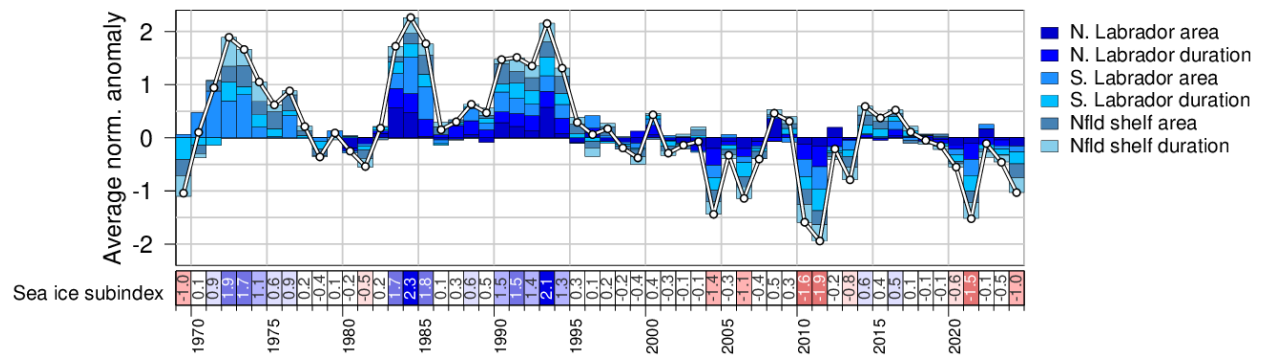


Figure 12. Newfoundland and Labrador sea ice index established by accumulating the normalized anomalies of seasonal maximum area and duration of sea ice for Newfoundland and Labrador shelves (red and green time series in Figure 11). This sea ice index contributes to the NL climate index described in the summary (Figure 4646).

4 Icebergs

Iceberg counts obtained from the International Ice Patrol of the US Coast Guard indicate that 22 icebergs drifted south of 48°N onto the Northern Grand Banks during 2024 (Figure 13), mostly during April (18 icebergs) (Figure 14) (Report of the International Ice Patrol in the North Atlantic - 2024 Season, 2024). This number is much lower than the climatological (1991–2020) average of 771. Some years have seen even lower numbers. For example, only one iceberg was observed in 2010 and 2021, two in 2011 and 13 in 2013. Only two years (1966 and 2006) in the 120-year time series have reported no icebergs south of 48°N . More than 1,500 icebergs have been observed in some years during the cold periods of the early 1980s and 1990s, including the all-time record of 2,202 in 1984, along with a recent high number of 1,515 in 2019. Years with low iceberg numbers on the Grand Banks generally correspond to higher-than-normal air temperatures, lighter-than-normal sea ice conditions, and warmer-than-normal ocean temperatures on the NL Shelf. As such, the normalized anomaly of the number of icebergs (scorecard at the bottom of Figure 13) is used as one component of the NL climate index presented in the summary.

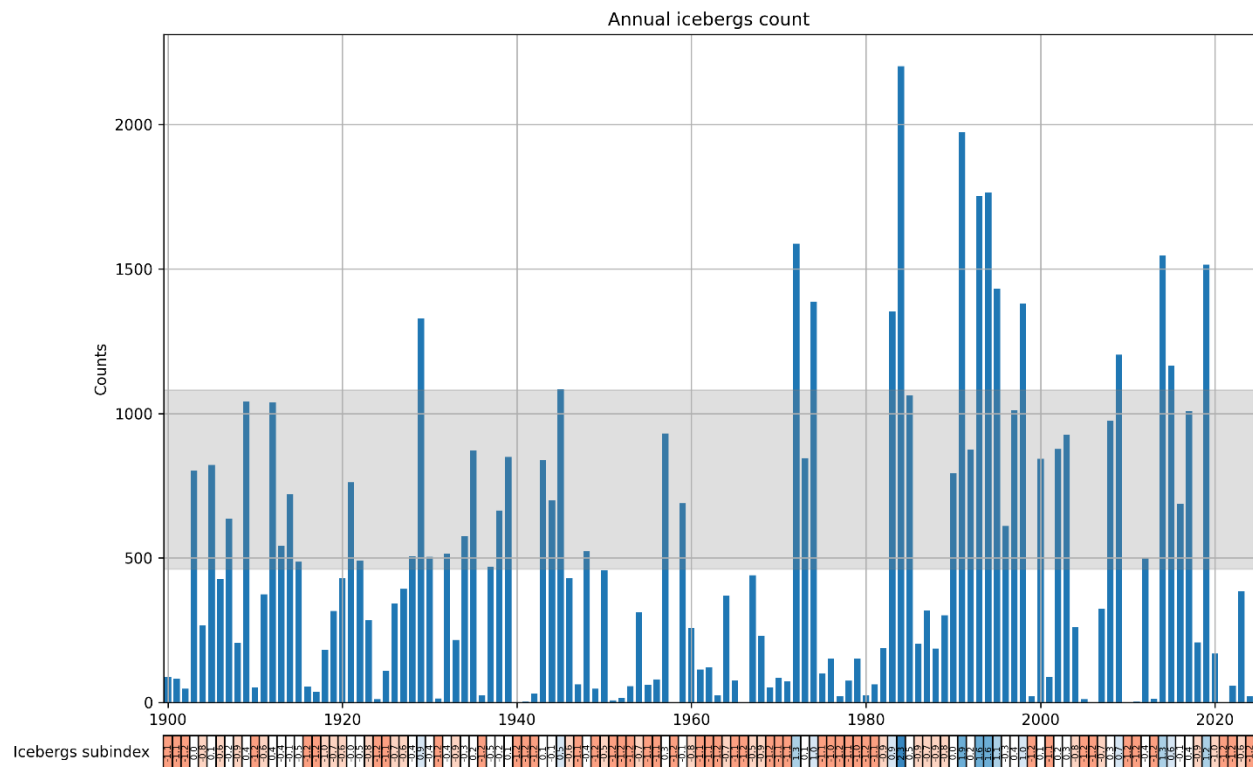


Figure 13: Annual iceberg count crossing south of 48°N on the northern Grand Bank. The shaded area corresponds to the 1991–2020 average $\pm 0.5 \text{ SD}$. The data are from the International Ice Patrol (International Ice Patrol, 2020). The normalized anomaly of this time series is color-coded in the bottom scorecard. This iceberg sub-index contributes to the NL climate index described in the summary (Figure 4646).

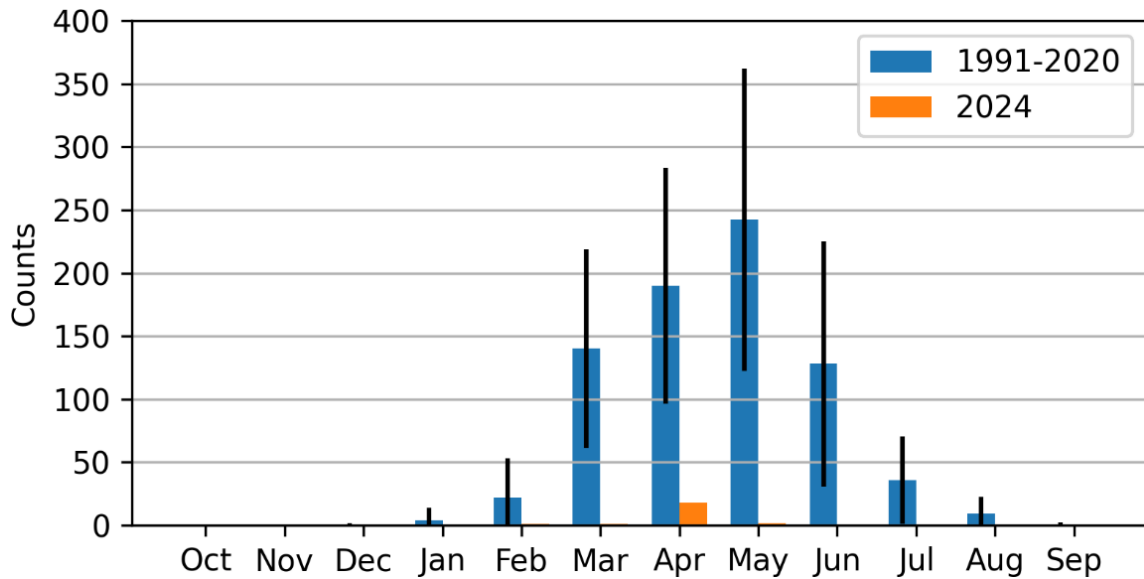


Figure 14: Monthly count of icebergs crossing south of 48°N on the northern Grand Banks during the annual iceberg season (from October to September). The 1991–2020 climatological average is in blue (with the black vertical bars corresponding to ± 0.5 SD) and the counts for the year 2024 are in orange. One iceberg was detected in February, one in March, and two in May (not visible in the figure). The data is collected from the international Ice Patrol (Report of the International Ice Patrol in the North Atlantic - 2024 Season, 2024).

5 Satellite sea-surface temperature

The satellite-based sea surface temperature product is again revised this year. It blends data from Pathfinder version 5.3 (4 km resolution for 1982–1985 and sparsely to 2020; Casey et al., 2010), Maurice Lamontagne Institute (MLI; 1.1 km resolution for 1985–2000 and sparsely to 2013; Larouche & Galbraith, 2016) with the NOAA STAR CoastWatch Advanced Clear-Sky Processor for Ocean (ACSPO) L3S-LEO-Daily “super-collated” v2.81 product (0.02 degree resolution for 2000 to current; (Jonasson et al., 2024). Details of the regional calibration are found in Galbraith et al., (2025). Monthly (and weekly) temperature composites are calculated from averaged available daily anomalies to which monthly (or weekly) climatological average temperatures are added as in Galbraith et al. (2021). Because the SST blend is different than in previous reports, certain previously reported records have changed although the patterns remain the same. In particular, 2012 would have previously been reported as the warmest year rather than 2021.

Weekly, monthly and annual temperature anomalies relative to the 1991–2020 climatology are calculated for NAFO divisions cropped at the shelf break (see Figure 15 or Figure 16). Monthly mean sea-surface temperatures from AVHRR imagery are presented as maps (Figure 15), temperature anomaly maps against the 1991–2020 climatology (Figure 16), and spatial averages and anomalies (Figure 17). Since the NOAA/LEO data differ from previously published regional monthly averages, we also include the monthly and seasonal time series since 1981 for all regions (Figure 18 and Figure 19).

In 2024, monthly average SSTs were largely above normal in ice-free areas across the region with the warmest normalized anomalies occurring in October in 2GHJ and 3P, and during summer in other areas (Figure 17). Several new monthly warm records were established across the different NAFO divisions and for the different months. The largest departure from the average temperature was reached on the southern Grand Banks (Division 3N), reaching +4.17 °C in July.

Seasonal SSTs averaged over the ice-free months were also significantly above normal across the NL Shelf (between +0.7 to +2.4 SD above average for the different NAFO divisions; Figure 17 bottom scorecards at the bottom of panels). Seasonal records were reached in 3K, 3L and 3N and all other regions had above normal seasonal temperatures. It is thus not surprising that the spatially weighted average over the NL region was also warm at +2.0 SD above average making 2024 virtually tied with 2012 for the warmest year of the series (Figure 20).

Note that air temperature has been found to be a good proxy of sea surface temperature. The warming trend observed in air temperature since the 1870s of about 1°C per century is also expected to have occurred in surface water temperatures across Atlantic Canada (Galbraith et al., 2021).

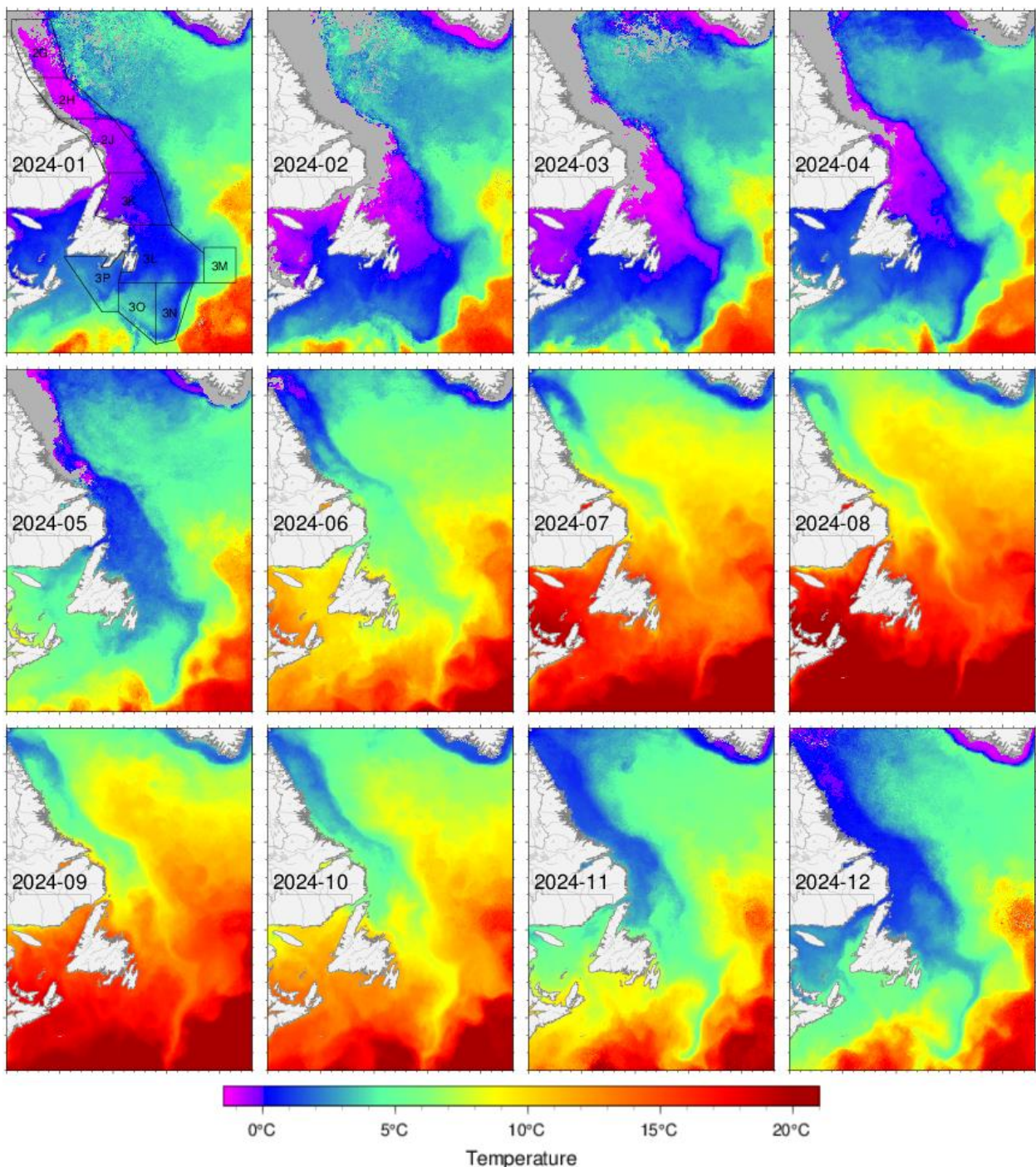


Figure 15. Sea-surface temperature monthly averages for 2024 as observed with satellite remote sensing. Grey areas have no data for the period due to ice cover or clouds. The NAFO divisions 2GHJ3KLMNOP cropped at the shelf break that are used for SST averages are shown in the month of January.

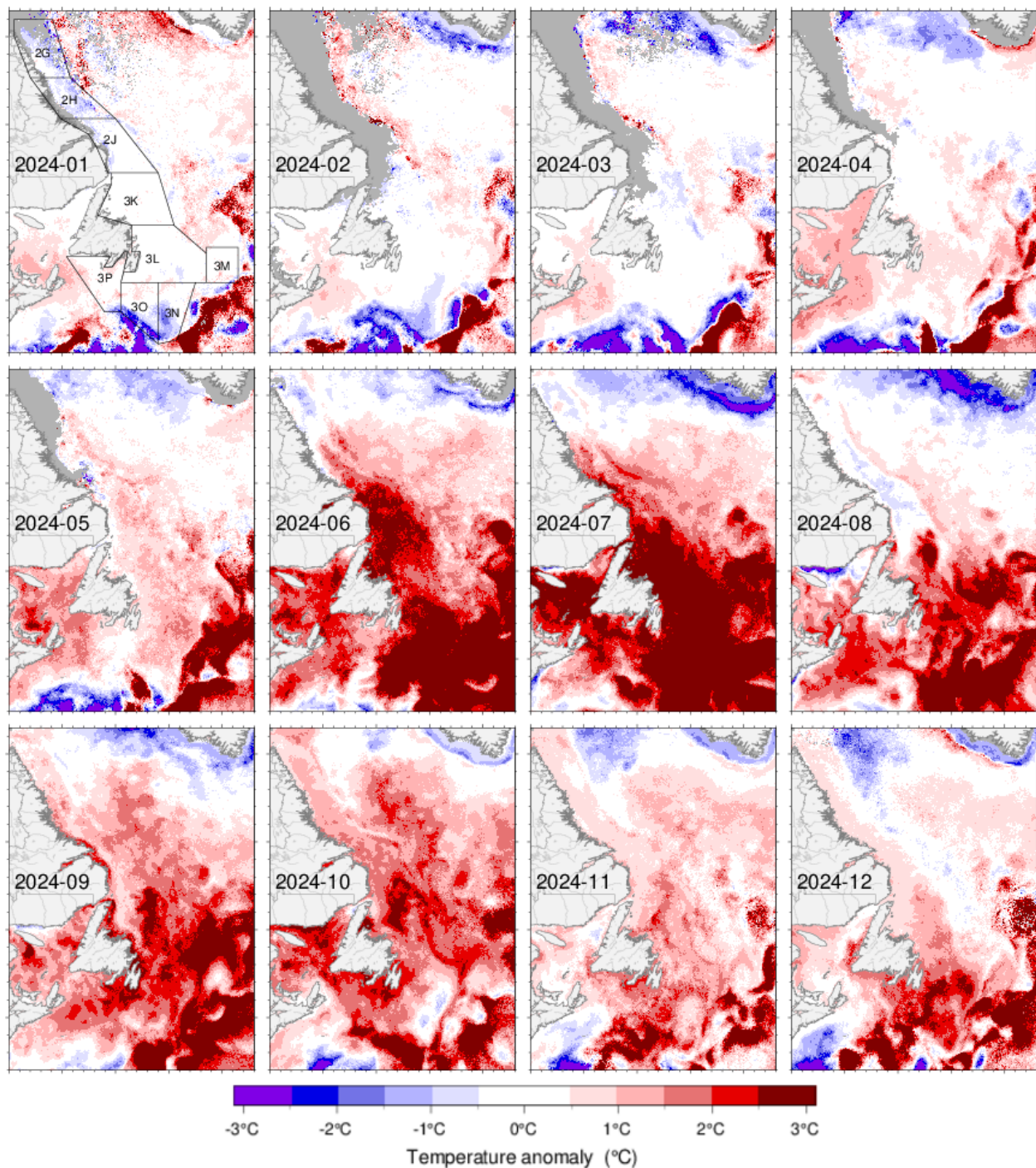


Figure 16. Sea-surface temperature monthly anomalies for April–December 2024 based on monthly climatologies calculated for the 1991–2020 period observed with satellite remote sensing. The NAFO divisions 2GHJ3KLMNOP cropped at the shelf break that are used for SST averages are shown in the month of January.

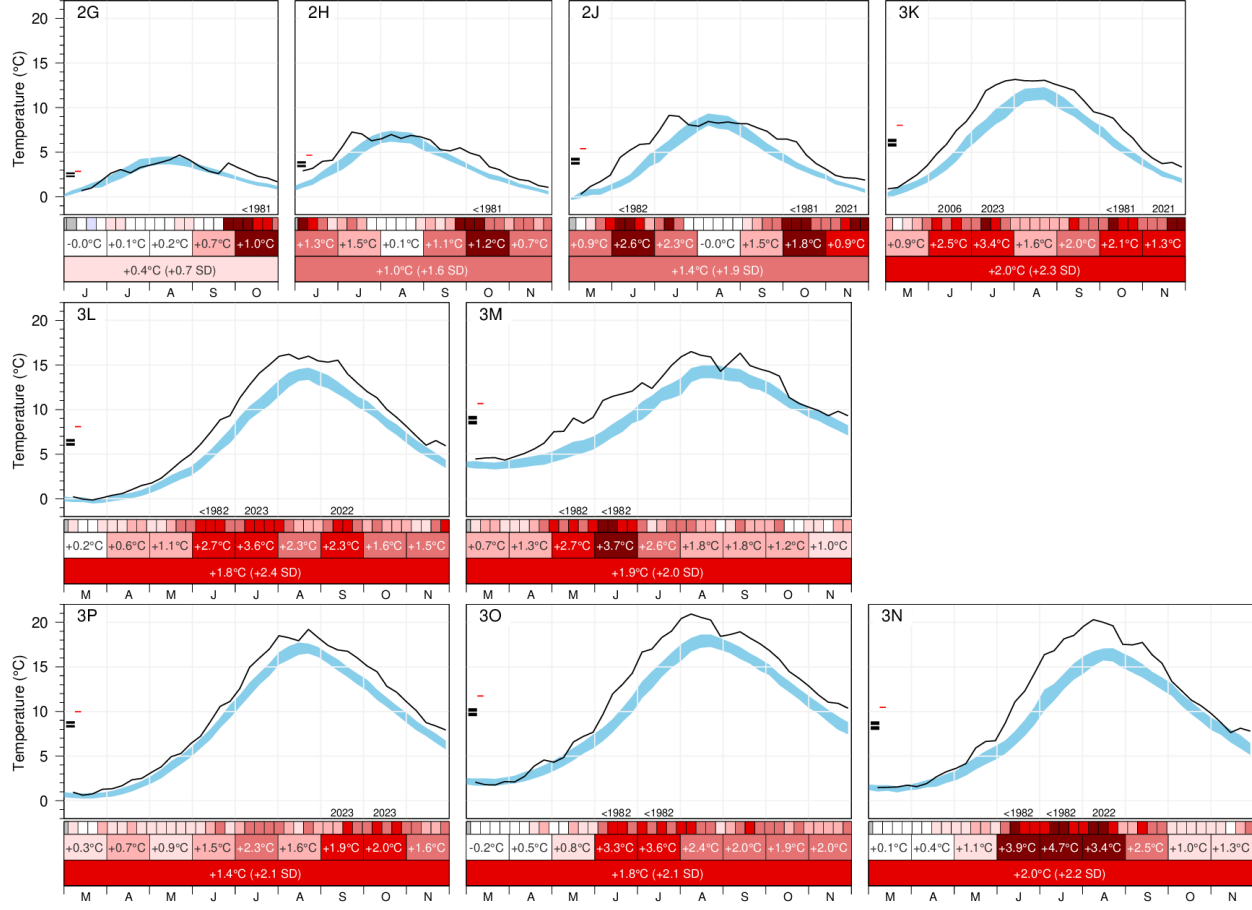


Figure 17: Weekly evolution of AVHRR Sea surface temperature evolution in 2024 for NAFO divisions 2GHJ3KLMNOP (black lines) during the ice-free season (season-length variable). Broken lines indicate that the threshold for the number of good pixels was not reached during these weeks (no data). The blue area represents the 1991–2020 climatological weekly mean ± 0.5 SD. Scorecards representing the weekly, monthly and seasonal averages (in $^{\circ}\text{C}$) appear at the bottom of each panel and are color-coded according to the normalized anomalies (top, middle and bottom row, respectively), with data gaps in grey. The two black ticks along the y-axis correspond to the seasonal climatological average ± 0.5 SD, while the red tick represents the 2024 seasonal average.

		0.0												0.01°C													
		-0.8												-0.79°C													
		-0.4												-0.50°C ± 0.08													
2G		J	M	A	S	O	N	D	J	M	A	S	O	N	D	J	M	A	S	O	N	D	J	M			
June-Oct		-0.6	-0.7	-0.1	0.0	-0.5	-0.4	-0.6	0.7	0.8	0.9	1.0	0.5	0.6	0.7	1.2	1.2	1.6	0.2	0.7	1.8	0.9	1.2	1.4	2.3	0.7	
J		0.7	0.8	0.5	1.3	0.7	0.7	0.5	1.4	0.7	1.0	1.1	1.1	1.3	0.8	1.4	0.7	1.1	1.0	0.5	0.6	0.7	1.2	1.2	1.6	0.4	
J		1.6	0.7	1.7	2.1	2.7	1.9	1.1	0.6	1.6	1.0	0.8	2.1	2.1	2.4	2.5	1.9	3.2	2.5	3.0	3.1	2.1	4.5	4.0	3.5	3.4	
A		2.5	1.2	2.0	3.1	3.7	2.8	2.5	2.3	2.7	2.5	2.1	3.6	3.3	3.1	3.5	3.6	3.8	3.8	4.6	4.1	3.8	5.1	4.8	4.4	4.7	
S		3.3	2.0	1.6	1.5	2.5	2.9	2.0	1.5	1.7	2.3	1.4	2.8	2.6	2.7	2.3	2.4	2.0	2.6	2.6	3.1	2.8	3.4	2.9	3.2	3.8	
O		1.9	0.8	0.7	0.4	0.6	1.0	1.1	1.2	0.9	1.2	0.7	1.5	1.2	1.1	1.3	1.8	1.6	1.4	1.9	1.6	1.9	2.0	1.5	1.6	1.4	
N		-0.2	-0.5	0.1	-0.6	0.1	-0.1	0.2	-0.1	0.3	0.2	0.4	-0.2	0.0	0.4	-0.2	0.6	0.6	0.8	0.2	-0.4	1.4	0.9	0.7	0.4	0.1	
D		-0.4	-0.8	-0.5	-0.7	-0.3	-0.4	-0.2	-0.2	-0.9	-0.4	-0.6	-0.6	-0.1	-0.4	-0.5	-0.7	-1.0	-0.6	-0.8	-0.5	-0.1	-0.4	-0.1	-0.2	-0.1	
June-Oct		1.5	1.0	1.2	2.0	2.1	1.9	1.5	1.2	1.5	1.6	1.2	2.2	2.1	2.0	2.2	2.0	2.6	2.3	2.6	2.6	2.2	3.2	2.9	2.8	2.4	
J		1.5	1.0	1.2	2.0	2.1	1.9	1.5	1.2	1.5	1.6	1.2	2.2	2.1	2.0	2.2	2.0	2.6	2.3	2.6	2.6	2.2	3.2	2.9	2.8	2.4	
M		1.5	1.0	1.2	2.0	2.1	1.9	1.5	1.2	1.5	1.6	1.2	2.2	2.1	2.0	2.2	2.0	2.6	2.3	2.6	2.6	2.2	3.2	2.9	2.8	2.4	
A		-0.0	-0.5	-0.4	-0.3	-0.1	-0.3	0.2	0.7	0.0	-0.0	0.6	-0.9	-0.3	0.9	0.1	1.1	0.4	1.4	0.8	0.6	0.6	0.5	0.6	0.3	0.1	
M		0.0	0.0	0.1	0.5	-0.4	0.2	0.3	-0.1	-0.3	0.2	0.7	0.0	-0.0	0.6	-0.9	0.1	1.1	0.4	1.4	0.8	0.6	0.6	0.5	0.6	0.3	
J		0.9	1.0	0.9	1.5	0.5	1.6	1.1	1.6	1.1	1.3	2.2	1.2	1.9	1.6	1.5	2.3	2.0	1.5	1.3	2.6	2.8	3.2	2.7	1.8	3.5	
J		4.1	2.6	2.6	2.8	3.1	3.1	3.6	3.4	3.5	2.6	2.6	4.4	4.8	4.8	4.7	4.8	4.7	4.2	4.8	6.8	6.7	6.1	5.4	5.7	7.1	5.8
A		5.2	4.0	4.4	5.4	6.2	6.1	5.6	4.3	5.8	4.6	4.1	6.9	6.2	6.0	5.8	6.7	8.2	6.9	5.4	5.2	4.7	4.4	6.6	6.7	7.5	7.6
S		4.8	3.6	3.6	3.0	4.2	4.4	5.0	3.9	3.6	3.2	3.4	4.5	4.5	4.5	5.4	5.2	4.7	5.4	5.8	5.7	5.5	5.1	5.6	4.5	4.6	4.8
O		3.0	1.7	1.7	1.3	1.5	1.6	2.4	2.5	2.1	2.3	2.7	2.4	2.3	2.8	2.2	3.3	2.5	2.9	3.3	2.3	2.8	2.0	3.0	3.1	2.7	2.5
N		1.2	0.6	0.4	-0.2	0.5	0.0	0.5	0.3	0.5	0.4	0.3	0.6	0.7	0.9	0.9	1.1	0.9	0.9	1.1	0.8	1.1	0.5	1.9	1.5	1.5	1.7
D		0.7	-0.1	-0.6	-0.1	-0.6	-0.1	-0.1	-0.2	-0.1	-0.2	-0.1	-0.2	-0.1	-0.2	-0.1	-0.1	-0.1	-0.1	-0.1	-0.1	-0.1	-0.1	-0.1	-0.1	-0.1	
June-Nov		2.7	2.2	2.0	2.6	2.7	2.9	2.6	2.3	2.5	2.4	2.3	3.3	3.5	3.3	3.2	3.2	4.0	3.5	3.8	3.6	3.3	3.7	4.2	3.6	4.8	3.3
J		-0.3	-0.4	-0.3	-0.2	-0.1	-0.2	-0.1	-0.1	-0.1	-0.1	-0.1	-0.1	-0.1	-0.1	-0.1	-0.1	-0.1	-0.1	-0.1	-0.1	-0.1	-0.1	-0.1	-0.1	-0.1	
F		-0.9	-0.8	-0.9	-0.8	-0.9	-0.8	-0.9	-0.8	-0.9	-0.8	-0.9	-0.9	-0.9	-0.9	-0.9	-0.9	-0.9	-0.9	-0.9	-0.9	-0.9	-0.9	-0.9	-0.9	-0.9	
M		-0.9	-0.9	-0.9	-0.9	-0.9	-0.9	-0.9	-0.9	-0.9	-0.9	-0.9	-0.9	-0.9	-0.9	-0.9	-0.9	-0.9	-0.9	-0.9	-0.9	-0.9	-0.9	-0.9	-0.9	-0.9	
A		-0.8	-0.6	0.5	-0.7	-0.9	-0.8	-1.1	-0.8	-1.2	-0.7	-0.8	-0.8	-1.0	-1.0	-0.9	-0.9	-0.7	-0.8	-0.5	-0.8	-0.9	-0.8	-0.9	-0.8	-0.8	
M		0.4	0.3	0.7	0.1	0.6	0.9	0.5	0.0	-0.3	0.4	0.3	1.1	0.5	0.3	0.7	0.0	0.7	0.0	0.1	0.6	0.0	0.2	0.3	0.1	0.3	
J		1.5	1.0	1.0	1.6	1.4	1.9	0.9	0.2	0.2	1.7	1.5	2.7	1.8	1.4	2.1	2.6	2.7	2.4	2.7	3.8	2.4	2.7	3.3	4.4	2.9	2.1
A		4.4	5.0	4.5	4.5	3.6	4.0	4.7	4.5	3.5	3.5	4.9	6.4	5.7	4.4	5.1	6.5	4.5	6.3	7.3	8.0	8.0	7.4	8.9	6.4	7.0	8.0
S		6.6	7.2	6.3	6.9	7.1	7.4	6.1	5.5	6.7	5.2	5.6	9.1	8.2	7.7	8.1	7.3	8.9	8.1	10.0	7.8	6.7	9.0	9.5	8.4	7.7	8.3
O		5.9	5.2	4.1	5.2	6.0	6.5	6.0	5.4	3.6	4.5	4.1	7.6	5.8	5.3	6.4	6.7	5.7	7.1	6.5	7.0	6.8	7.5	7.0	6.5	7.4	8.5
N		3.7	2.0	2.6	1.9	1.6	2.9	1.1	1.7	2.4	2.5	2.2	3.4	4.0	3.3	2.0	3.1	3.8	3.0	3.5	3.6	2.4	3.7	3.5	3.4	3.4	4.4
D		0.7	-0.1	-0.2	0.1	-0.1	0.5	0.1	0.1	0.7	-0.9	0.6	-0.6	0.6	0.1	0.5	0.6	0.5	0.7	0.2	1.3	1.1	1.2	1.1	1.0	0.8	0.2
May-Nov		3.1	2.8	2.8	2.6	3.1	3.0	3.4	2.5	2.6	2.3	2.6	3.7	4.1	3.8	3.1	3.6	4.3	3.8	4.4	3.9	4.7	5.5	5.5	4.5	4.5	5.4
J		-0.3	-0.3	-0.3	-0.2	-0.0	0.1	0.1	0.0	-0.1	-0.1	-0.1	-0.1	-0.1	-0.1	-0.1	-0.1	-0.1	-0.1	-0.1	-0.1	-0.1	-0.1	-0.1	-0.1	-0.1	
F		-0.4	-0.2	-0.3	-0.2	-0.1	-0.1	-0.1	-0.1	-0.1	-0.1	-0.1	-0.1	-0.1	-0.1	-0.1	-0.1	-0.1	-0.1	-0.1	-0.1	-0.1	-0.1	-0.1	-0.1	-0.1	
M		0.2	0.9	-0.2	1.1	-0.1	0.1	0.8	-0.8	-0.9	-0.4	-0.5	0.2	-1.0	0.6	0.5	0.3	-0.3	-0.4	0.2	0.1	-0.1	-0.3	-0.6	-0.6	-0.6	-0.6
A		1.5	1.0	1.1	0.1	0.6	1.7	0.2	0.0	0.5	0.7	1.0	1.4	1.2	0.7	1.2	1.6	1.5	0.5	0.7	0.5	0.1	0.0	-0.1	-0.1	-0.1	
M		2.3	3.3	2.4	2.1	3.3	3.4	3.3	3.6	3.6	4.0	4.4	4.0	4.8	4.0	4.9	3.9	3.6	3.3	6.1	6.6	3.9	5.1	4.2	3.9	4.2	4.5
J		6.0	7.2	7.7	6.9	7.8	7.1	6.0	5.2	5.1	6.4	8.1	7.2	7.1	8.0	7.6	8.5	8.7	9.8	10.5	9.3	10.0	11.0	10.6	10.2	12.1	11.5
A		9.8	8.3	10.5	9.8	10.0	10.2	10.0	10.0	10.0	10.0	10.0	10.0	10.0	10.0	10.0	10.0	10.0	10.0	10.0	10.0	10.0	10.0	10.0	10.0	10.0	
S		8.3	7.7	8.4	7.1	8.6	7.3	8.1	8.1	8.5	8.7	9.1	9.2	9.6	9.8	9.2	9.8	10.5	9.9	10.5	11.5	10.8	10.5	11.0	11.5	12.0	
O		5.0	3.8	5.1	4.1	3.8	4.7	5.2	5.6	5.6	5.4	4.9	4.7	5.8	6.4	5.9	5.2	5.7	6.0	6.1	6.8	4.4	5.9	5.5	6.2	5.0	5.0
N		2.8	1.9	2.7	1.8	2.1	2.6	2.2	2.6	2.9	2.0	2.6	3.1	2.9	3.0	3.0	3.2	2.5	3.8	3.2	3.4	3.5	2.6	2.9	2.1	2.0	2.2
D		1.3	0.5	-0.1	-0.2	0.5	0.1	0.7	-0.9	0.6	-0.6	0.6	0.6	0.1	0.5	0.6	1.5	0.7	0.2	1.3	0.4	0.7	0.8	0.7	0.6	1.1	1.0
May-Nov		4.9	5.0	5.0	4.7	5.2	5.3	5.7	4.9	4.9	4.2	5.5	5.2	6.3	6.4	6.1	5.6	6.3	6.6	7.2	7.7	7.5	5.5	6.4	6.7	5.7	5.3
J		1.5	1.2	-0.2	0.3	0.3	0.2	0.2	0.8	0.7	0.7	1.2	1.3	1.1	1.6	1.1	1.0	1.5	0.7	1.2	1.4	1.0	0.7	0.9	1.8	1.3	1.4
F		1.1	-0.1	0.1	0.1	0.1	0.1	0.1	0.1	0.1	0.1	0.1	0.1	0.1	0.1	0.1	0.1	0.1	0.1	0.1	0.1	0.1	0.1	0.1	0.1	0.1	0.1
M		0.2	0.9	-0.2	1.1	-0.1	0.1	0.8	-0.8	-0.9	-0.4	-0.5	0.2	-1.0	0.6	0.5	0.3	-0.4	0.2	0.1	0.0	-0.6	-0.6	-0.6	-0.6		

Figure 18. Satellite SST May to November monthly anomalies averaged over NAFO Divisions 2G, 2H, 2J, 3K and 3L, cropped at the shelf break (see Figure 15 or Figure 16). The scorecards are colour-coded according to the monthly normalized anomalies based on the 1991–2020 climatologies for each month, but the numbers are the monthly average temperatures in °C. The 1991–2020 mean and standard deviation are indicated for each month on the right side of the table.

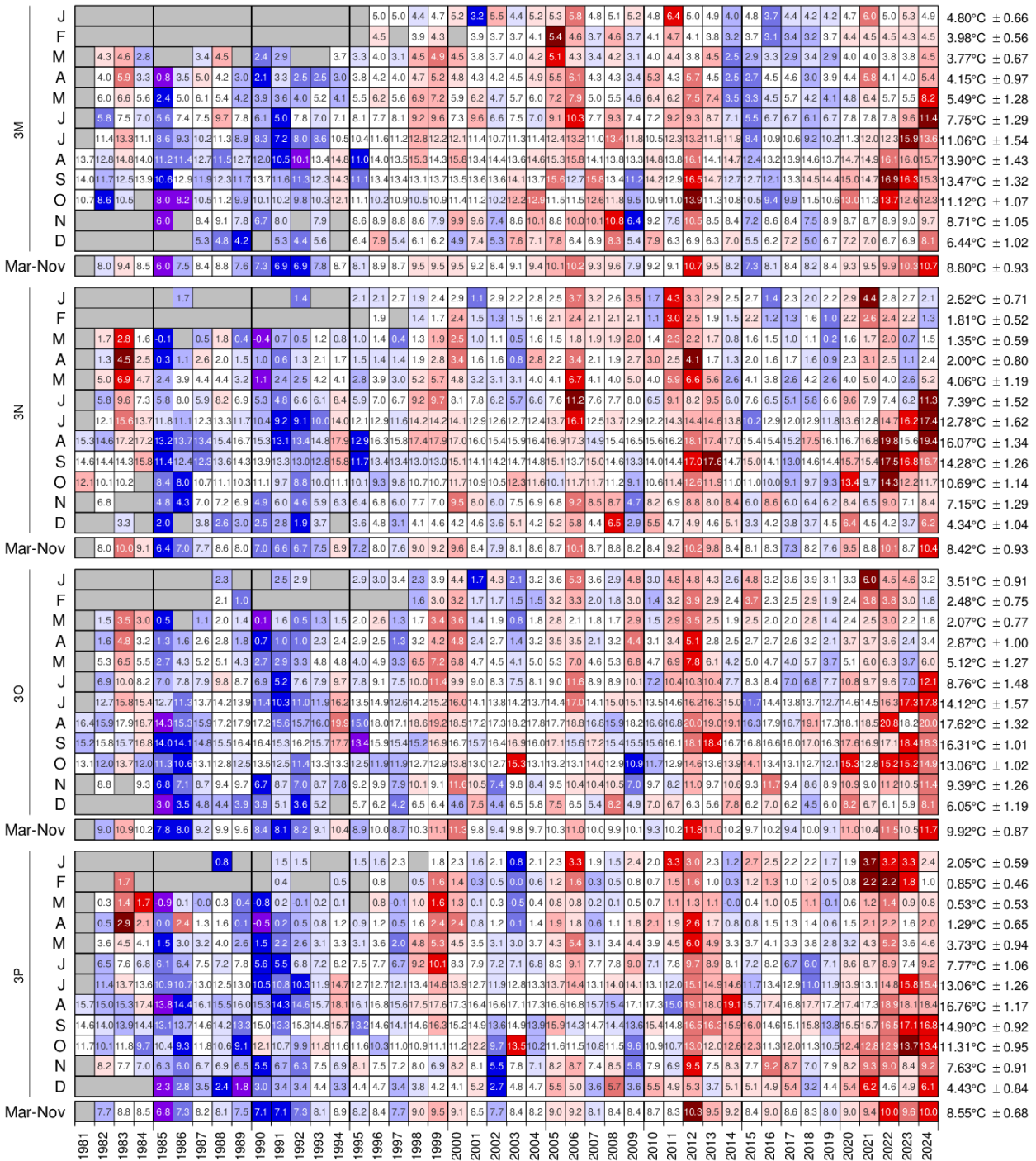


Figure 19. Satellite SST May to November monthly anomalies averaged over NAFO Divisions 3M, 3N, 3O and 3P, cropped at the shelf break (see Figure 15 or Figure 16). The scorecards are colour-coded according to the monthly normalized anomalies based on the 1991–2020 climatologies for each month, but the numbers are the monthly average temperatures in °C. The 1991–2020 mean and standard deviation are indicated for each month on the right side of the table.

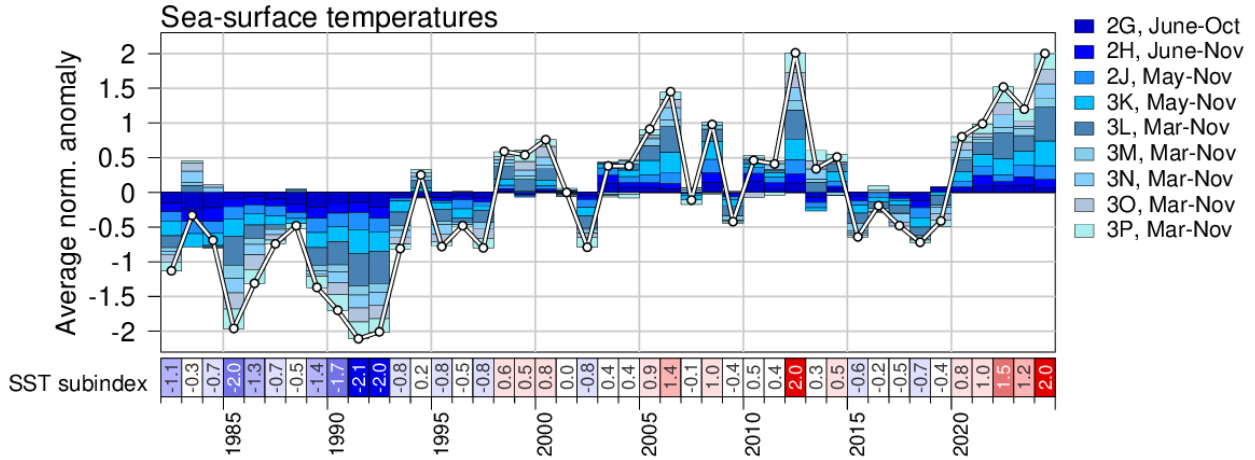


Figure 20: Northwest Atlantic SST index built from the sum of the seasonal anomalies for all NAFO divisions (bottom rows of panels in Figure 17). This index contributes to the NL climate index described in the summary (Figure 4646).

5.1 Marine heatwaves

Marine heatwaves (MHWs) are defined as prolonged discrete anomalously warm water events or, quantitatively, by temperatures exceeding the 90th percentile of temperatures for that day of year during at least 5 consecutive days (Hobday et al., 2016; Oliver et al., 2021). The 90th percentile thresholds area is calculated using the standard 1991–2020 climatology period of the daily averages over each subarea based on the NAFO divisions in the Newfoundland and Labrador region.

MHWs are commonly discussed in terms of intensity (I), i.e., the difference between temperature and the daily climatology. Single events are then summarized using four standard metrics: duration (D), average intensity (I_{mean}), maximum intensity (I_{max}), and integrated intensity (I_{cum}). These metrics were calculated over daily polygon average time series using the [Python implementation](#) of Hobday et al., (2016) written by Eric Oliver. Following Hobday et al., (2018), MHWs with I_{max} values greater than 1, 2, 3, and 4 times the difference between the 90th percentile and the climatology are respectively referred to as moderate, strong, severe and extreme events. Sea surface temperature has higher variability in summer and lower variability in winter, which results in a seasonal bias: summer and winter moderate thresholds correspond to different intensity values. To facilitate the comparison of events during different seasons, we therefore calculate c , the intensity normalized by the difference between the 90th percentile and the climatology, and the corresponding standard event metrics. This normalized intensity is a continuous equivalent to the Hobday et al., (2018) category system. Event metrics for individual years are thus aggregated into annual metrics shown in Figure 21 (sum of durations, ΣD ; annual maximum of the normalized intensity, \hat{c}_{max} ; annually integrated normalized intensity, Σc_{cum} ; and the MHW event count).

There were 4 notable MHW events in the Newfoundland and Labrador region during 2024. The first was a short strong event peaking in June in the 2J region (Figure 22). The second was a long summer event (June-August) most clearly defined in region 3N ($D = 89$ days), but also visible in the nearby regions (3K, 3L, 3M, 3O). The third was a short strong event in region 2J (September-October), in the north of the zone. The last event ranked severe in the 3K region, but this is due to the intensity peak in January 2025 of an otherwise strong event that began in November. Overall, 2024 was an active MHW year in the Newfoundland and Labrador region with all but NAFO region 3P having annually integrated normalized intensity Σc_{cum} greater than 200 days: this result was mostly driven by their durations, rather than the intensity of single events. The total number of events detected was also more than twice the interannual average.

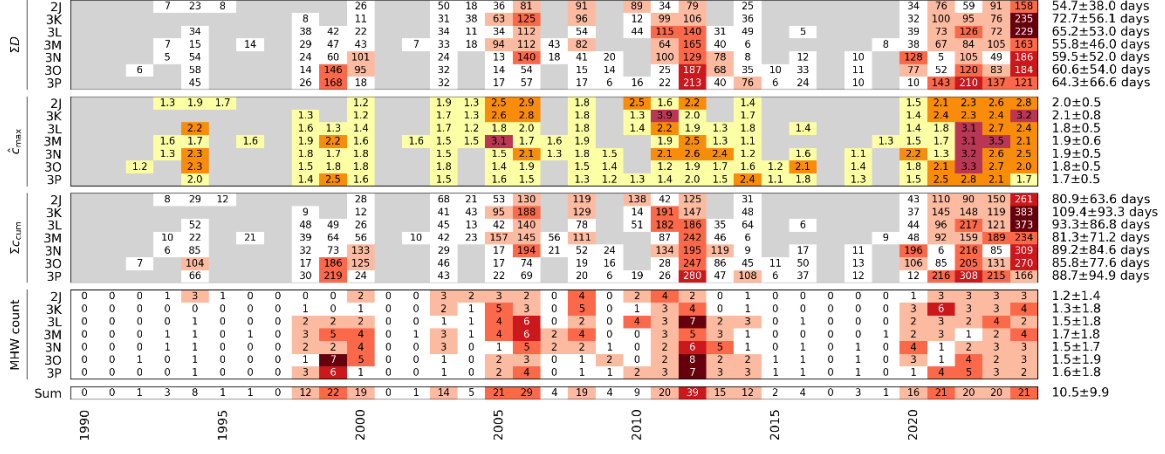


Figure 21. Aggregated MHW metrics by region. From top to bottom are shown ΣD , \hat{c}_{max} , Σc_{cum} , and the number of MHW events. Boxes are colour-coded according to their values. To emphasize larger events, values up to the mean of each panel are coloured white and shades of red darken with increasing values by one standard deviation for each shade. The \hat{c}_{max} panel is colour-coded to the corresponding MHW category: yellow (moderate), orange (strong), burgundy (severe) or purple (extreme). The mean and standard deviation are shown to the right for each station. All results are based on daily satellite SST data.

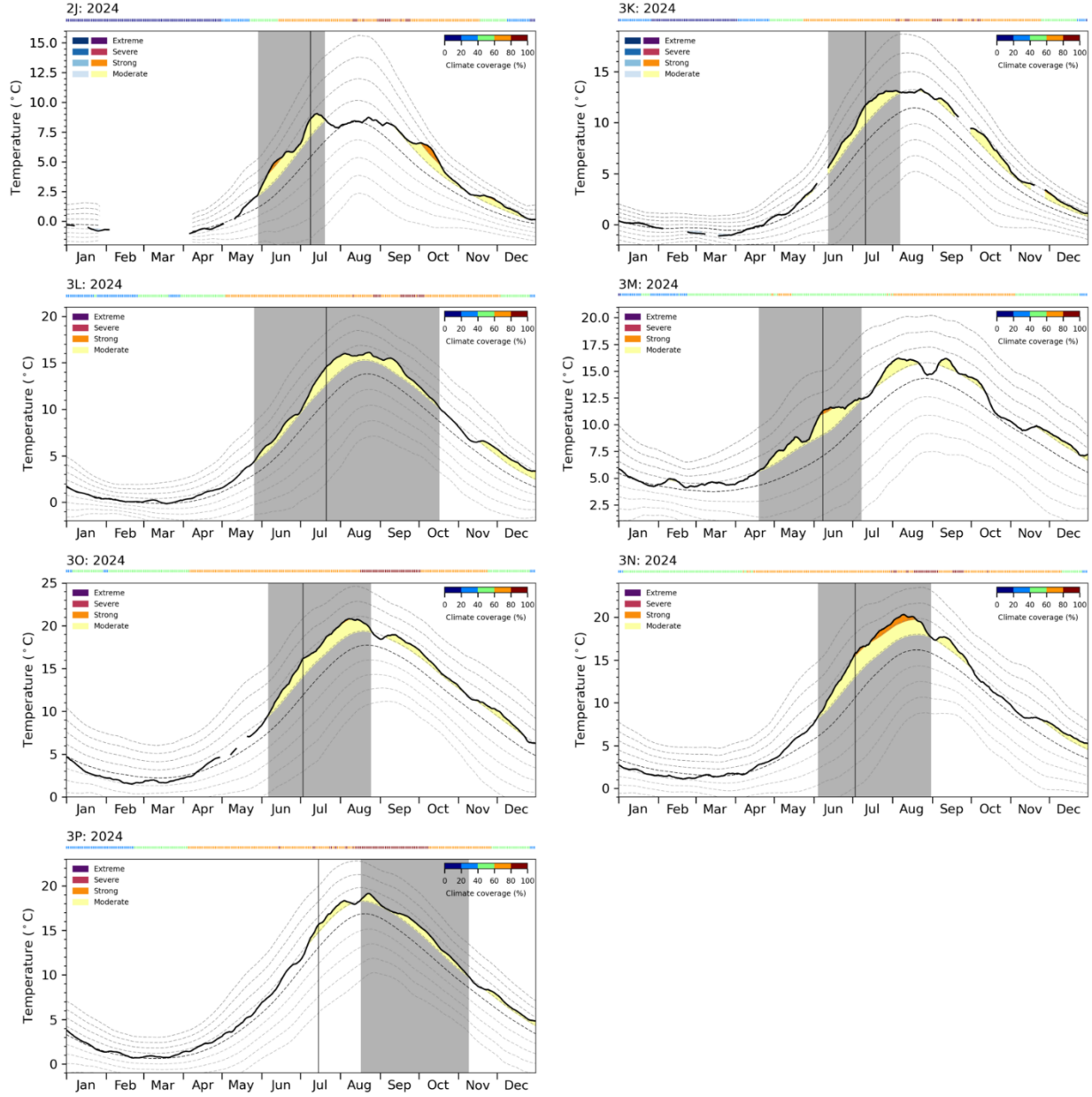


Figure 22. Temperature time series (solid black) for the 2J3KLN MOP NAFO regions during 2024. The thresholds for MHW and MCS categories are shown (dashed gray lines) on each side of the climatology (dashed black line). When temperature exceeds MHW or MCS thresholds, the area between the thresholds and the time series is coloured according to the corresponding MHW or MCS category as detailed in the upper left corner. Coloured tick marks above the graph show the daily percentage of available data on which to base the thresholds over the climate reference period, with colours matching the scale in upper right corner. The gray patch indicates the time span of the MHW event of highest cumulative intensity, and a vertical line shows the annual intensity maximum.

6 Ocean conditions on the Newfoundland and Labrador shelf

The following section presents observations of various ocean parameters at long-term monitoring Station 27, along standard hydrographic sections, and over the ocean bottom.

6.1 Long-term observations at Station 27

Station 27 ($47^{\circ}32.8'N$, $52^{\circ}35.2'W$) is located in the Avalon Channel off Cape Spear, NL (Figure 1). It is one of longest hydrographic time series in Canada with frequent, near-monthly, occupations since 1948. In 2024, the station was occupied 27 times including 16 Conductivity-Temperature-Depth (CTD)-only casts, 12 full AZMP physical-biogeochemical samplings and 8 Expendable Bathymeterograph (XBT) measurements.

Since 2017, an automatic profiling system installed on a surface buoy (type Viking) usually provides extended temporal coverage of temperature (T) and salinity (S) at Station 27. The buoy was deployed in July 2024, but unfortunately the mini-winches used to collect CTD profile data were non-operational. Multiple attempts were made to repair the mini-winches at sea but they proved unsuccessful. No CTD profiles were collected in 2024 by the buoy.

Station occupations were used to obtain the annual evolution of temperature and salinity at Station 27, as well as the anomaly compared to the 1991–2020 climatology, shown in Figure 2323 and Figure 2424. These figures demonstrate the seasonal warming of the top layer (~20 m), with temperature peaking in August before being mixed during the fall. The CIL (Petrie et al., 1988), a remnant of the previous winter cold layer and defined by temperatures below $0^{\circ}C$ (thick black line in Figure 2323) is also evident below 100 m throughout the summer. Interestingly, the coldest water body within the CIL (darkest shades of blue in the middle panel of Figure 2323) is mostly found in the summer between mid-June and mid-August, suggesting advection of cold waters from the Labrador Shelf and the Arctic to the Newfoundland Shelf. The surface layer is generally freshest between August and mid-October, with salinities below 31 (Figure 2424). These low near-surface salinities are a prominent feature of the salinity cycle on the Newfoundland Shelf and are largely due to the melting of coastal sea ice. The presence of such a large volume of freshwater late in the summer season also points to advection from northern areas (Labrador and the Arctic).

Aside from one profile taken in January, no measurements were taken at Station 27 until mid-May 2024 (Figure 2323 and Figure 2424, top and bottom panels). Fresh conditions persisted throughout most of May to December, except from mid-November to December where positive salinity anomalies were present from 40–160 m (Figure 2424, bottom panel). Warm anomalies developed at the surface (0–20 m) in early August and continued to the end of the year, eventually reaching depths of 100 m (Figure 2323, bottom panel). A short negative temperature anomaly occurred in July from 0–40 m. At the same time and location, salinity switched from anomalously fresh to anomalously saline. The CIL generally followed the climatology, with the upper layer deepening from 60 m to 140 m from May to December (Figure 2323, top and middle panels). Unlike the climatology, the 2024 CIL did not extend to the sea floor in November and December.

Over 2024, the annual temperature anomaly (defined as the average of monthly anomalies) for the vertically averaged (0–176 m) temperature was positive (+1.2 SD), while the vertically-averaged salinity was slightly fresh at -1.2 SD (Figure 2525 and Figure 2626). The fresh anomaly of the early 1970s

(Figure 2525, bottom panel), commonly referred to as the Great Salinity Anomaly in the North Atlantic (Dickson et al., 1988), now looks very minor compared to the freshening happening at Station 27 since the late 2010s. This is partly due to a change in the mean state towards a freshening of the NL shelf. The decrease in salinity at Station 27 coincides with the substantial loss (melting) of Arctic sea ice in recent years (Yashayaev, 2024). Normalized anomalies of temperature and salinity for all years since 1980 and for different depth ranges (0–176 m, 0–50 m and 150–176 m) are reported in scorecards in Figure 2626.

The summer (May-July) CIL statistics at Station 27 since 1951 are presented in Figure 2727. Here the CIL mean temperature corresponds to the average of all temperatures below 0°C. The CIL thickness as well as the CIL core temperature (the minimum temperature of the CIL) and its depth are also presented in Figure 2727. After the prevalence of a warm CIL in the early 2010s (with some of the warmest years since the mid-1970s), there was a cooler period between about 2014 and 2017. The CIL was warmer than normal between 2018 and 2024, except in 2020 when it was normal. The SD of these metrics are reported in a scorecard in Figure 2626.

The monthly mean mixed layer depth (MLD) at Station 27 was also estimated from the density profiles as the depth of maximum buoyancy frequency (N) calculated from the monthly averaged density profiles ($\rho(z)$):

$$N^2 = \frac{-g}{\rho_0} \frac{\Delta\rho(z)}{\Delta z},$$

with $g = 9.8 \text{ ms}^{-2}$ as the gravitational acceleration, z the depth and ρ_0 the mean density. Here N^2 is calculated using the Gibbs-SeaWater (GSW) Oceanographic Toolbox (McDougall & Barker, 2011).

Climatological monthly MLD values, as well as monthly MLDs during 2024, are presented in Figure 2828. The climatological annual cycle shows a gradual decrease of the MLD from December-January to July-August. In 2024, the MLD was shallower than the average in January (no data from February to April), close to normal in spring and summer, and shallower than average in November and December. Annual mean values of the MLD and its 5-year moving average are shown in Figure 2929 (solid gray line and dashed-black line, respectively). In general, there is a strong interannual and decadal oscillation in MLD, but the striking feature is a step-like increase in the 1990s. From 2019 to 2024, there has been a decrease in MLD. A scorecard of annual and seasonal MLD anomalies since 1980 can be found in Figure 2626.

Stratification is an important characteristic of the water column since it influences, for example, the transfer of solar heat to deeper layers and the vertical exchange of biogeochemical tracers between the deeper layers and the surface. The seasonal development of stratification is also an important process influencing the formation and evolution of the CIL on the shelf regions of Atlantic Canada. It insulates the lower water column from the upper layers, thus slowing the vertical heat flux from the seasonally heated surface layer.

Stratification at Station 27 is calculated from monthly average density profiles using discrete differences between two averaged depth ranges. Two definitions of the stratification indices are calculated for Station 27. The first one uses density differences (i.e. $\Delta\rho/\Delta z$) between 0–5 m and 48–53 m (labelled 0–50 m definition) and the second one between 8–13 m and 148–153 m (labelled 10–150 m definition). See bottom two scorecards in Figure 2626. Measurements taken from non-bottle instrument types were discarded in the top two depth levels to mitigate the influence of problem surface measurements. The reason for these two definitions is that historical near-surface measurements in the 1950s and 1960s were made at discrete depths of $z=0, 25. In the 1970s and 1980s, these discrete depths were changed to $z=0, 10, 20, 30, 50\text{ m}$. Finally, since the widespread use of electronic measurements using CTDs mounted on rosettes started in the 1980s, near-surface ($z=0$) measurements of density are usually discarded, and each high-resolution cast usually starts between 2–5 m depth to avoid electronic noise contamination or damage to the rosette by surface waves or ship motion. There is thus no simple definition that can ensure continuity$

of the metric from the 1950s to present. Here the definition 0-50 m will mostly focus on the 1950-1990 period, while the definition 10-150 m will be representative of the period 1960-present. Note that the 0-50 m definition is also calculated until present, but it considers the average over 0-5 m as the surface measurement, making it difficult to directly compare with historical data. When reporting annual averages, yearly stratification values are omitted if there are fewer than 3 months of data available. When reporting seasonal averages, only one measurement must be present.

The 2024 and climatological evolution of the 0-50 m stratification throughout the year are shown in Figure 3030. The stratification is generally weakest between December and April, before rapidly increasing at the onset of spring until it peaks in August. Stratification was close to normal in May and October. Relatively high stratification was observed from June to August as well as November and December (Figure 3030). These anomalously high stratification values are coherent with the shallow MLD observed during those months (Figure 2828).

The interannual evolution of the stratification anomaly since 1950 is shown in Figure 3131. Strong decadal variations exist in the two different definitions of stratification. For the 0-50 m range, an increase in stratification from the 1950s to about 2000 is observed, followed by a slight decrease until 2019. For the 10-150m definition, no real trends are discernible, but a step-wise increase seems to occur in the early 1990s, which is also apparent in the 0-50 definition. We have shown this increase by presenting the average stratification between 1950-1990 and 1990-present (Figure 3131). In 2024, the seasonal and annual stratification means were high relative to the 1991-2020 climatology (excluding the 0-50 m winter stratification). A scorecard of annual and seasonal stratification anomalies since 1980 can be found in Figure 2626.

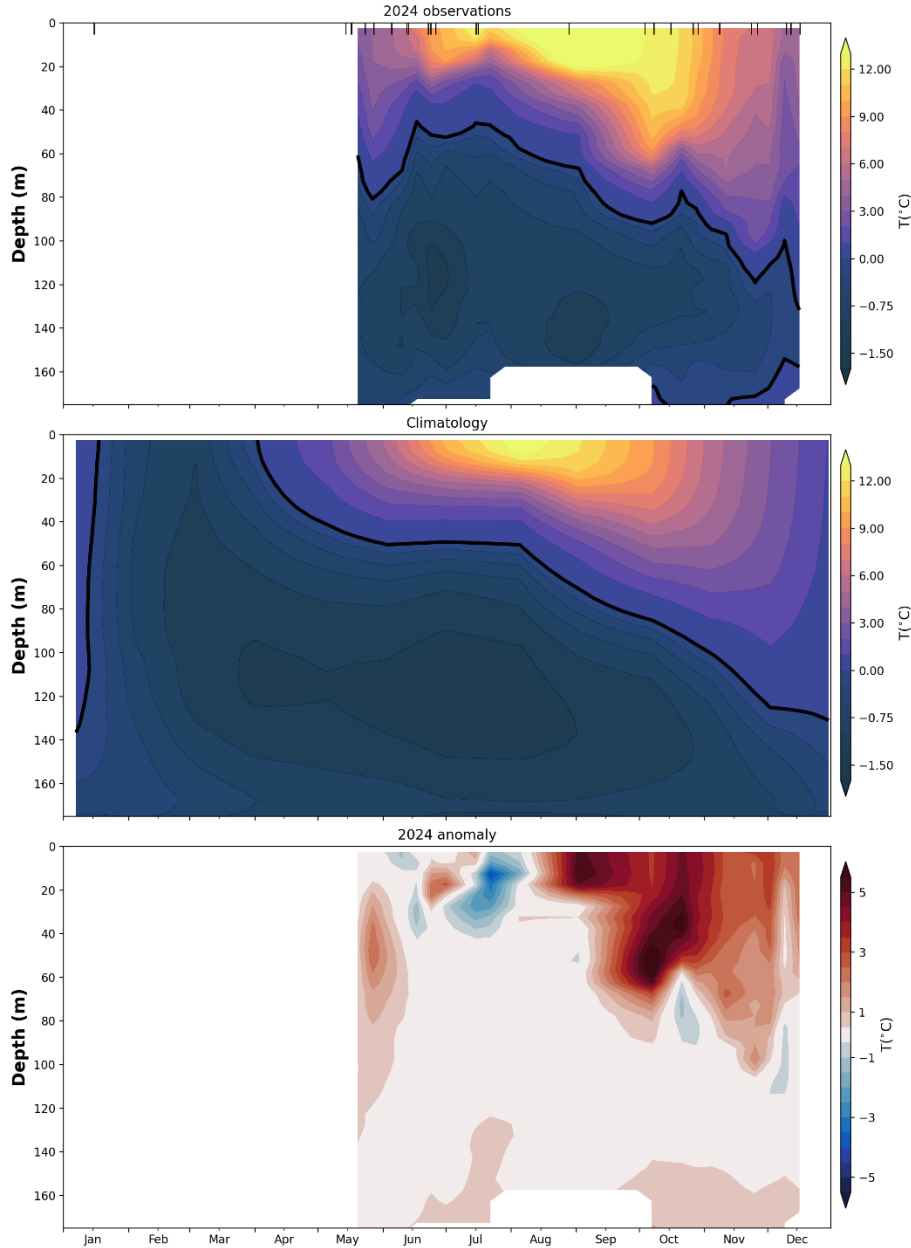


Figure 2323: Annual evolution of temperature at Station 27. The 2024 contour plot (top panel) is generated from weekly averaged profiles from all available data, including station occupations (indicated by black tick marks on top of panel). The solid black contour delineates the cold intermediate layer (CIL), defined as water below 0°C. The 1991–2020 weekly climatology is plotted in the middle panel. Note the uneven colourbar used in the two first panels: below 0°C, 0.25°C increments are used, while 1°C increments are used above 0°C. The anomaly (bottom panel) is the difference between the 2024 field and the climatology.

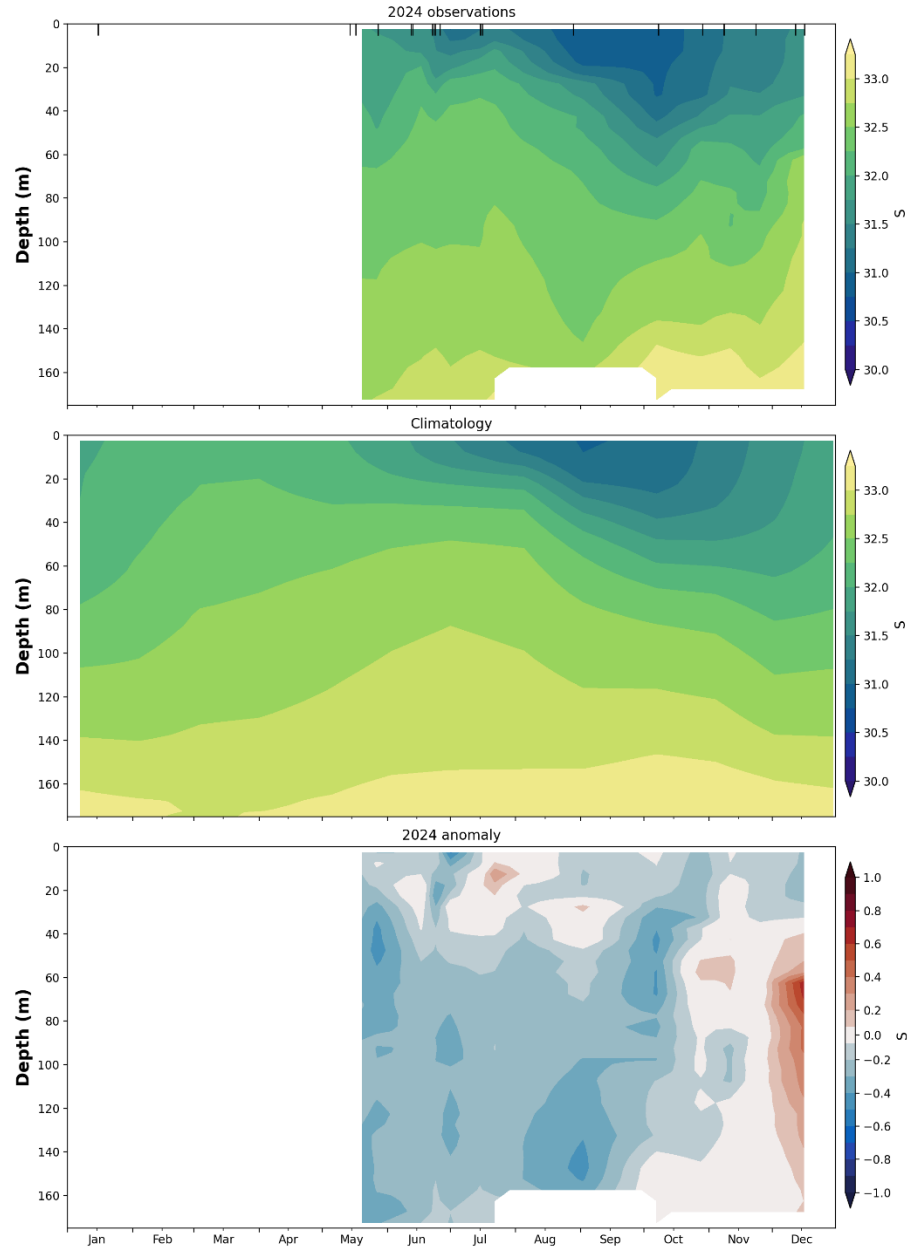


Figure 2424: Same as in Figure 2323, but for salinity.

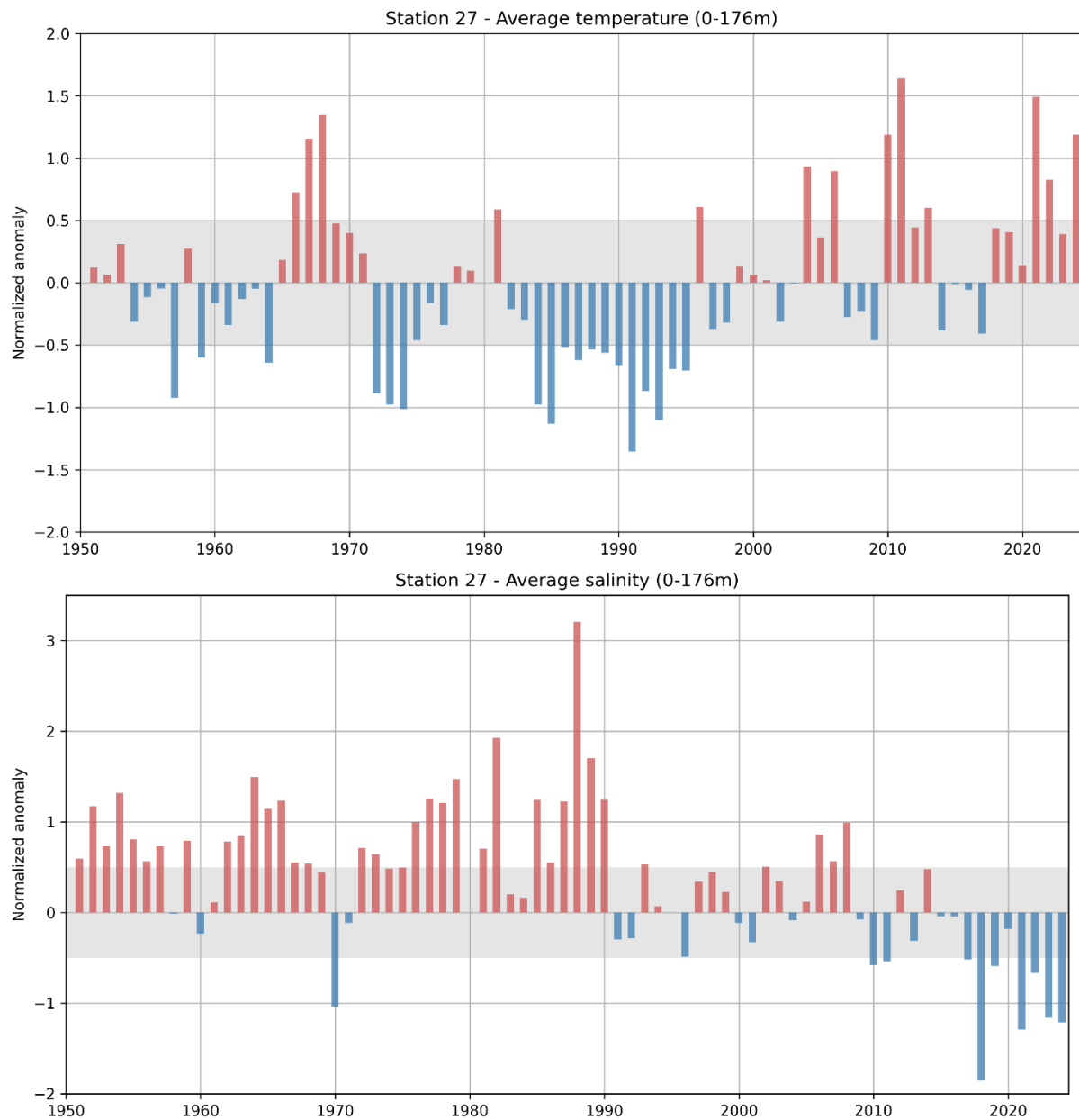


Figure 2525: Annual normalized anomaly of vertically averaged (0–176 m) temperature (top) and salinity (bottom) at Station 27 calculated from all occupations since 1951. Only years where at least 8 months of the year are sampled are presented. Shaded gray areas represent the climatological (1991–2020) average ± 0.5 SD range considered “normal”. These two time series contribute to the NL climate index described in the summary (Figure 4646).

Figure 2626: Annual normalized anomalies of hydrographic parameters for Station 27. The different boxes from top to bottom are: vertically averaged temperature and salinity for different depth ranges, cold intermediate layer (CIL) properties, mixed layer depth (MLD), stratification between 0 and 50m, and stratification between 10 and 150m for the 4 seasons and annual average. The cells are color-coded according to Figure 2. Gray cells indicate an absence of data. Note that the salinity anomaly sign is the opposite as reported in the NL climate index (NLCI) (Figure 4646).

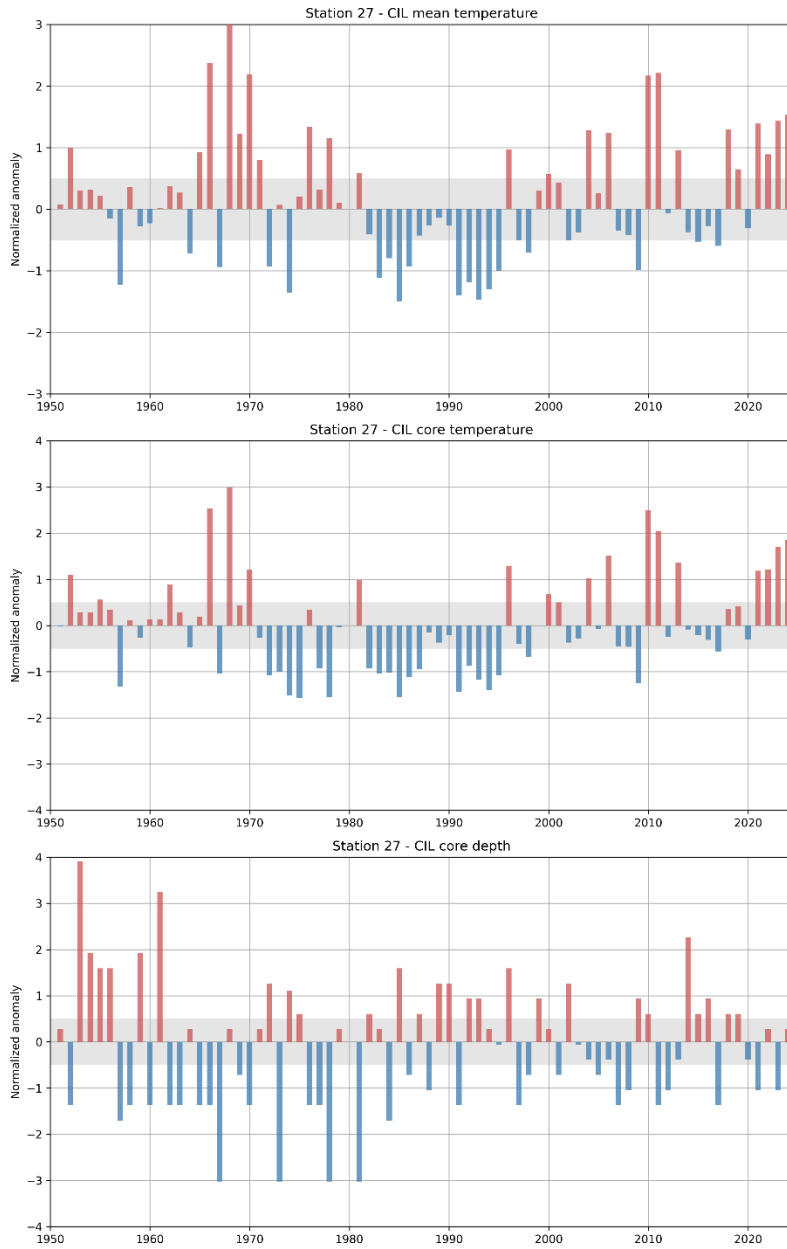


Figure 2727: Normalized anomalies of summer (May-July) cold intermediate layer (CIL) statistics at Station 27 since 1951. Only years where at least 8 months of the year are sampled are presented. The top panel shows the CIL mean temperature, the middle the CIL core temperature (minimum temperature of the CIL) and the bottom panel the depth of the CIL core. Shaded gray areas represent the climatological (1991–2020) average ± 0.5 SD range considered “normal”. The CIL core temperature anomalies (middle panel) contribute to the NL climate index described in the summary (Figure 4646).

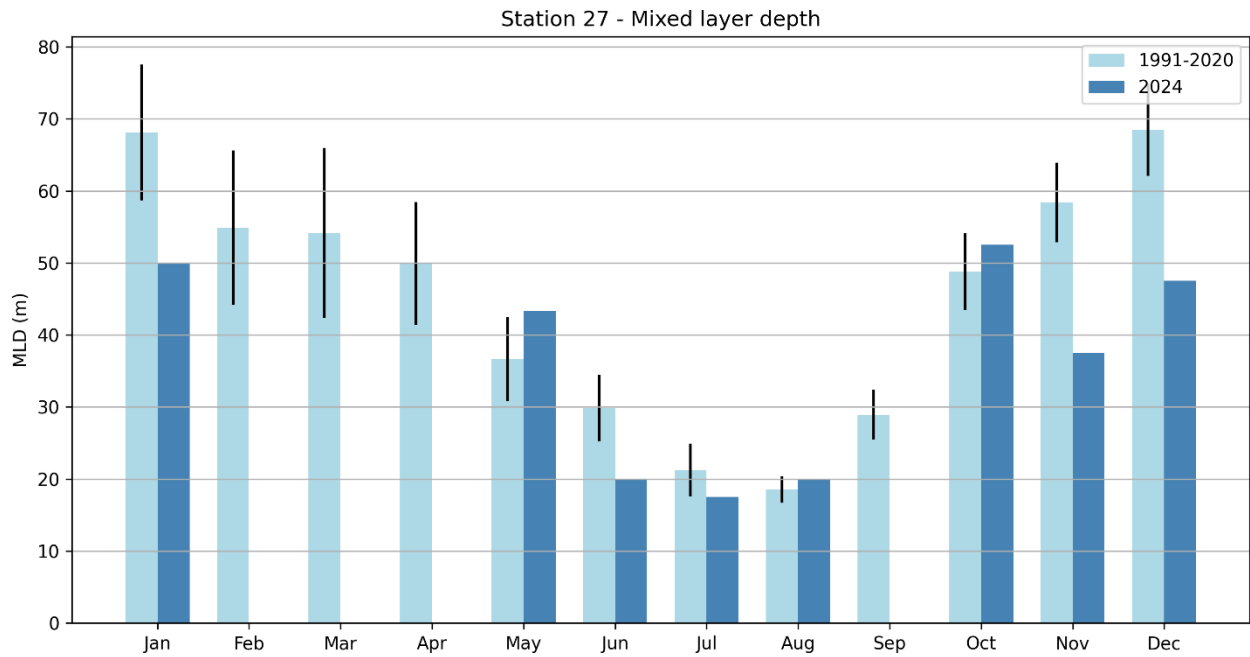


Figure 2828: Bar plot of the monthly averaged mixed layer depth (MLD) at Station 27. The 1991–2020 climatology is shown in light blue while the update for 2024 is shown in dark blue. The black lines represent 0.5 SD above and below the climatology. No observations were made in February–April and in September.

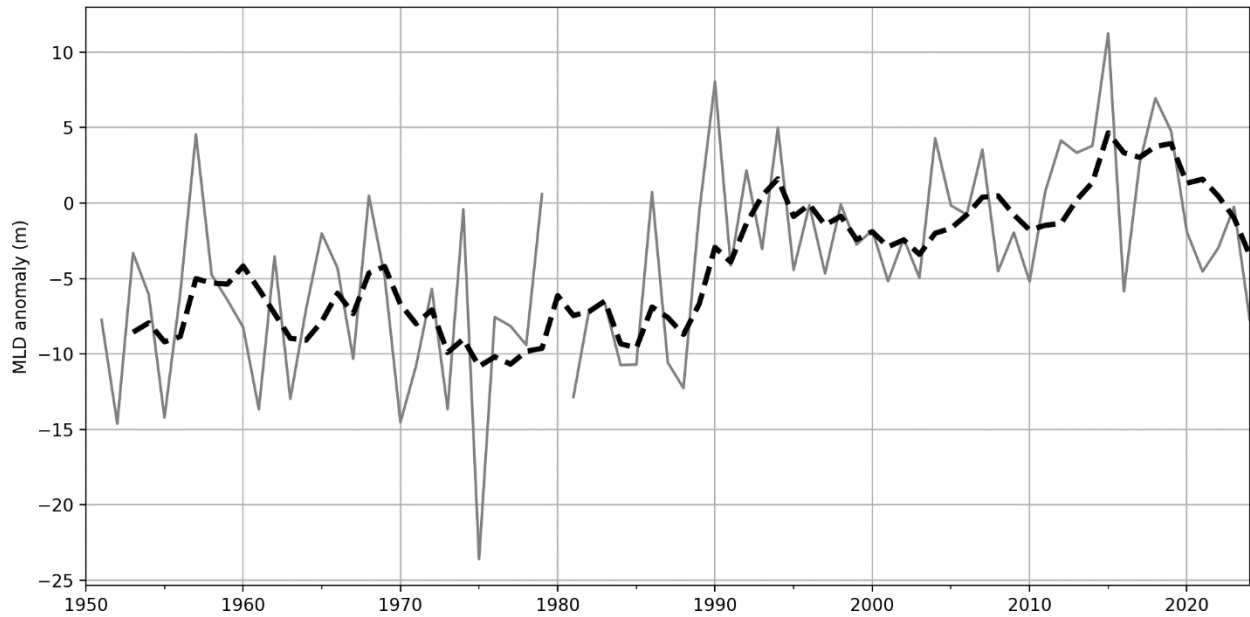


Figure 2929: Time series of the annual mixed layer depth (MLD) average at Station 27 since 1950 (gray solid line) and its 5-year running mean (dashed-black line).

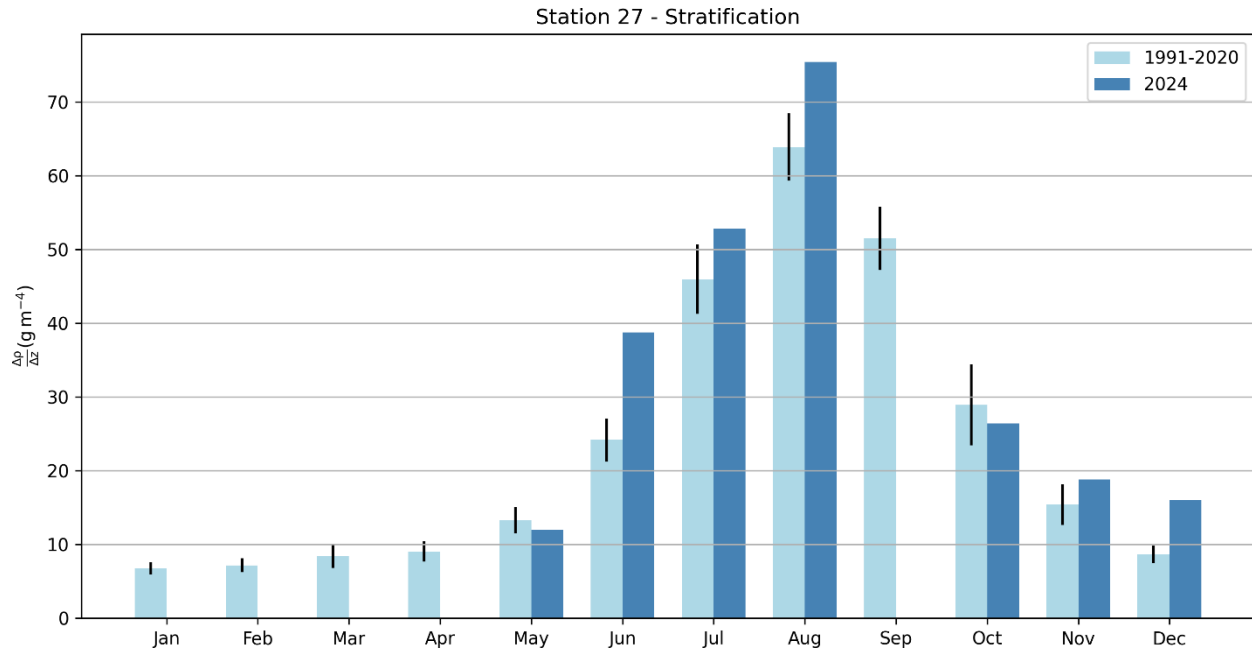


Figure 3030: Bar plot of the monthly average stratification (defined as the density difference between 0 and 50 m) at Station 27. The 1991–2020 climatology is shown in light blue while the update for 2024 is shown in dark blue. The black lines represent 0.5 SD above and below the climatology. No observations were made from January–April and September.

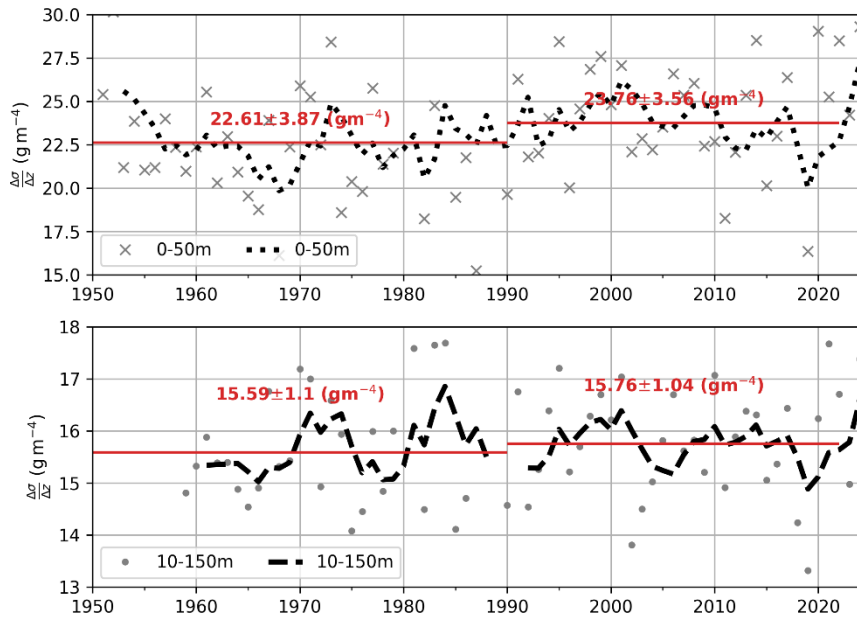


Figure 3131: Time series of the annual average stratification at Station 27 between 0 and 50m (gray crosses; top) and 10 and 150m (gray dots; bottom) since 1950. For each panel, the 5-year running mean is shown as a dotted/dashed black line. Note the different vertical axis for the two panels. The average annual stratification from 1950 to 1990 and 1990 to 2023 is shown in red.

6.2 Standard hydrographic sections

In the early 1950s, several countries under the auspices of the International Commission for the Northwest Atlantic Fisheries (ICNAF) carried out systematic monitoring along hydrographic sections in NL waters. In 1976, ICNAF normalized a suite of oceanographic monitoring stations along sections in the Northwest Atlantic Ocean from Cape Cod (USA) to Egedesminde (West Greenland) (ICNAF, 1978). In 1998 under the AZMP, the Seal Island (SI), Bonavista Bay (BB), Flemish Cap (47°N) (FC) and Southeast Grand Bank (SEGB) historical stations were selected as core monitoring sections. The White Bay section (WB) continued to be sampled during the summer as a long time series ICNAF/NAFO section (see Figure 1).

Two ICNAF sections on the mid-Labrador Shelf, the Beachy Island (BI) and the Makkovik Bank (MB) sections, were selected to be sampled during the summer if survey time permitted. Starting in the spring of 2009, a section crossing south-west over St. Pierre Bank (SWSPB) and one crossing south-east over St. Pierre Bank (SESPB) were added to the AZMP surveys.

The spring 2024 survey (planned to be onboard the CCGS Capt. Jacques Cartier) was not completed due to a refit delay. The summer 2024 survey (June 25 – July 16 onboard the CCGS John Cabot) sampled sections BB, FC, MB, SI, WB, and S27, while the fall 2024 survey (October 28 – November 25 onboard the RRS Discovery) sampled sections BB, FC, SEGB, SI, and SWSPB. In this manuscript we present the summer cross-sections of temperature and salinity and their anomalies along the SI, BB and FC sections to represent the vertical temperature and salinity structure across the NL Shelf during 2024.

6.2.1 Temperature and Salinity Variability

The water mass characteristics observed along the standard sections crossing the NL Shelf are typical of Arctic-origin waters with a subsurface temperature range of -1.5°C to 2°C and salinities from 31.5 to 33.5. Labrador Slope water flows southward along the shelf edge and into the Flemish Pass and Flemish Cap regions. With temperatures in the range of 3°C to 4°C and salinities in the range of 34 to 34.75, this water mass is generally warmer and saltier than the shelf waters. Surface temperatures normally warm to between 10°C and 12°C during late summer, while bottom temperatures remain <0°C over much of the Grand Banks, increasing to between 1°C and 3.5°C near the shelf edge below 200 m and in the deep troughs between the banks. In the deeper (>1,000 m) waters of the Flemish Pass and across the Flemish Cap, bottom temperatures generally range from 3°C to 4°C. In general, the near-surface water mass characteristics along the standard sections undergo seasonal modification from annual cycles of air-sea heat flux, wind-forced mixing, and the formation and melting of sea ice. These mechanisms cause intense vertical and horizontal temperature and salinity gradients, particularly along the frontal boundaries separating the shelf and slope water masses. The seasonal changes in the temperature and salinity fields along the Bonavista section are presented in Colbourne et al., (2015).

Summer temperature and salinity structures along the SI, BB and FC (47°N) are presented in Figure 3232 to Figure 3434. The dominant thermal feature along these sections is associated with the cold and relatively fresh CIL overlying the shelf. This water mass is separated from the warmer and denser water of the continental slope region by strong temperature and salinity fronts. The cross-sectional area of the CIL is bounded by the 0°C isotherm and highlighted as a thick black contour in the temperature panels. The CIL parameters are regarded as robust indicators of ocean climate conditions on the eastern Canadian Continental Shelf. While the CIL area undergoes significant seasonal variability, the changes are highly coherent from the Labrador Shelf to the Grand Banks. The CIL remains present throughout most of the summer until it gradually decays during the fall as increasing winds and storm episodes deepen the surface mixed layer.

In 2024, all sections show the presence of a very thin (<15m) surface layer with temperature anomalies reaching +3°C above normal (Figure 3232, Figure 3333, Figure 3434, top left panels). Below this thin surface layer, close to normal and slightly positive temperature anomalies can be seen at SI and BB. At FC and BB, small areas of negative temperature anomalies are located directly below the warm surface, excluding the Flemish Pass and Flemish Cap where positive temperature anomalies are present. The CIL temperature in all three sections was slightly higher than normal and the CIL area was smaller than the climatology, partially due to positive temperature anomalies at depth in both SI and BB. Along the SI section, the CIL maximum depth was shallower than normal.

The corresponding salinity cross sections show a relatively fresh (<33) upper water layer over the shelf with sources from Arctic outflow on the Labrador Shelf, in contrast to the saltier Labrador Slope water further offshore with values >34 (Figure 3232 to Figure 3434, right panels). In 2024, negative salinity anomalies can be seen where the CIL occurs in all three sections. Negative salinity anomalies are also present at shallow depths in the Flemish Pass and Flemish Cap with slightly positive salinity anomalies beneath them.

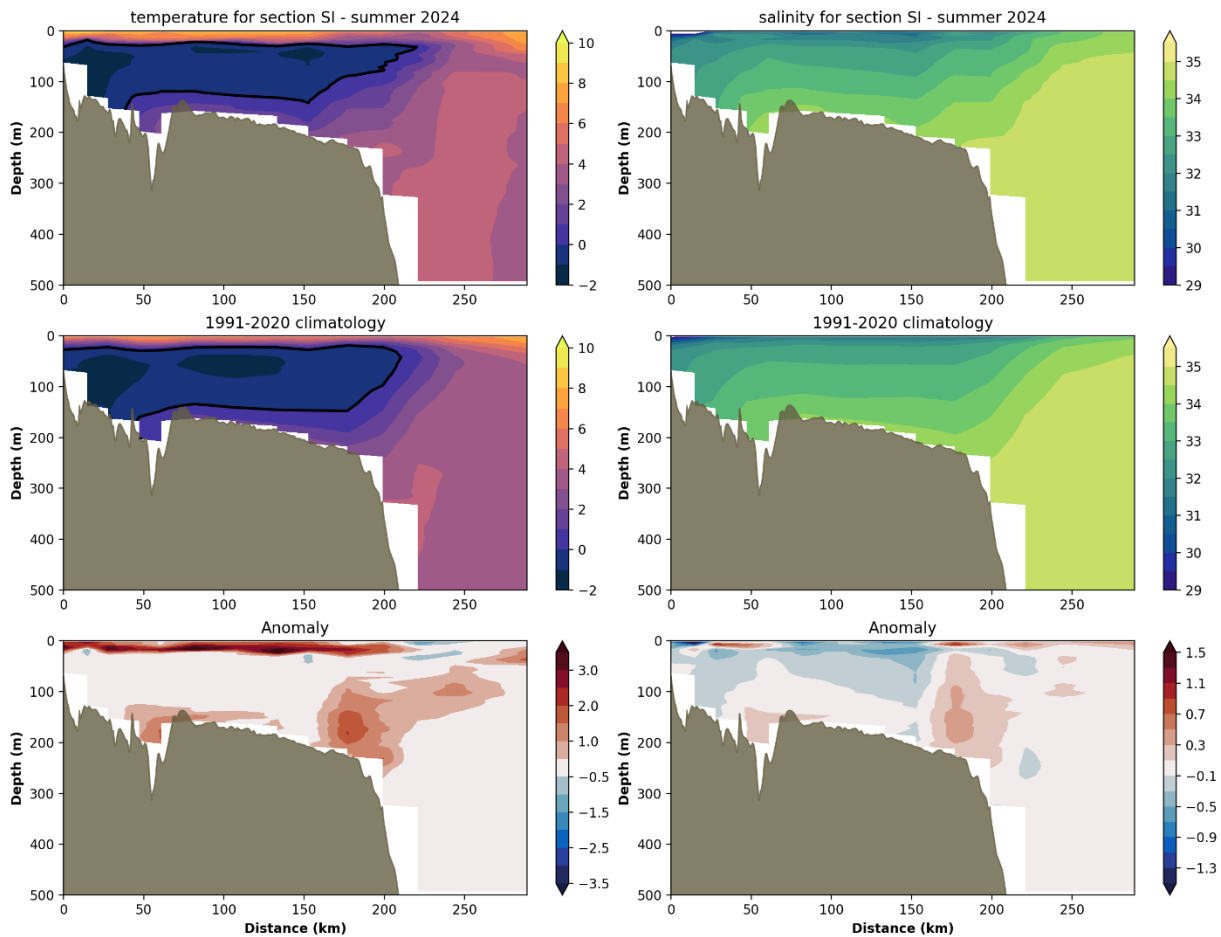


Figure 3232: Contours of temperature (°C), left column, and salinity, right column, during summer 2024 (top row), with climatological averages (middle row) for the Seal Island (SI) hydrographic section (see map Figure 1 for location). Their respective anomalies for 2024 are plotted in the bottom panels.

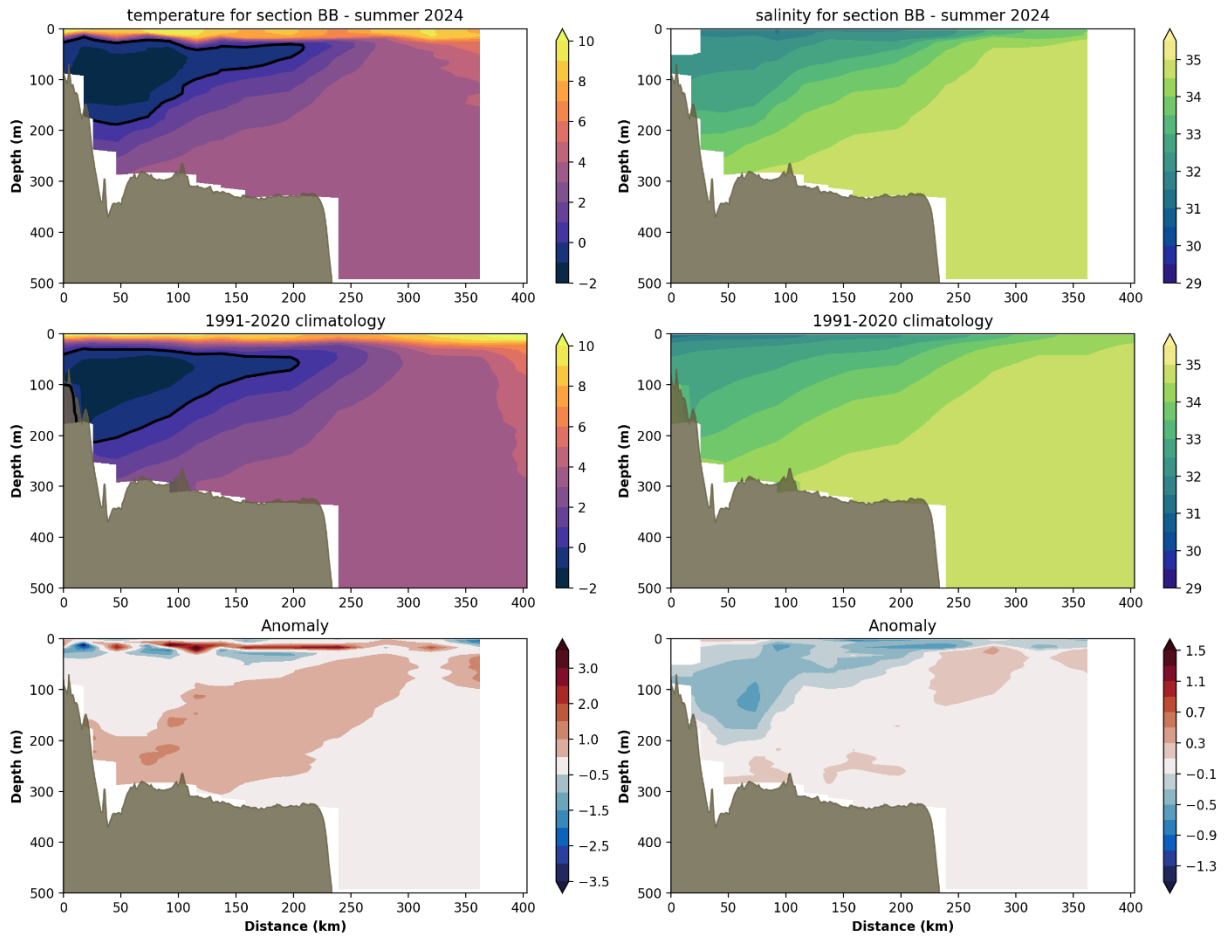


Figure 3333: Contours of temperature ($^{\circ}\text{C}$), left column, and salinity, right column, during summer 2024 (top row), with climatological averages (middle row) for the Bonavista (BB) hydrographic section (see map Figure 1 for location). Their respective anomalies for 2024 are plotted in the bottom panels.

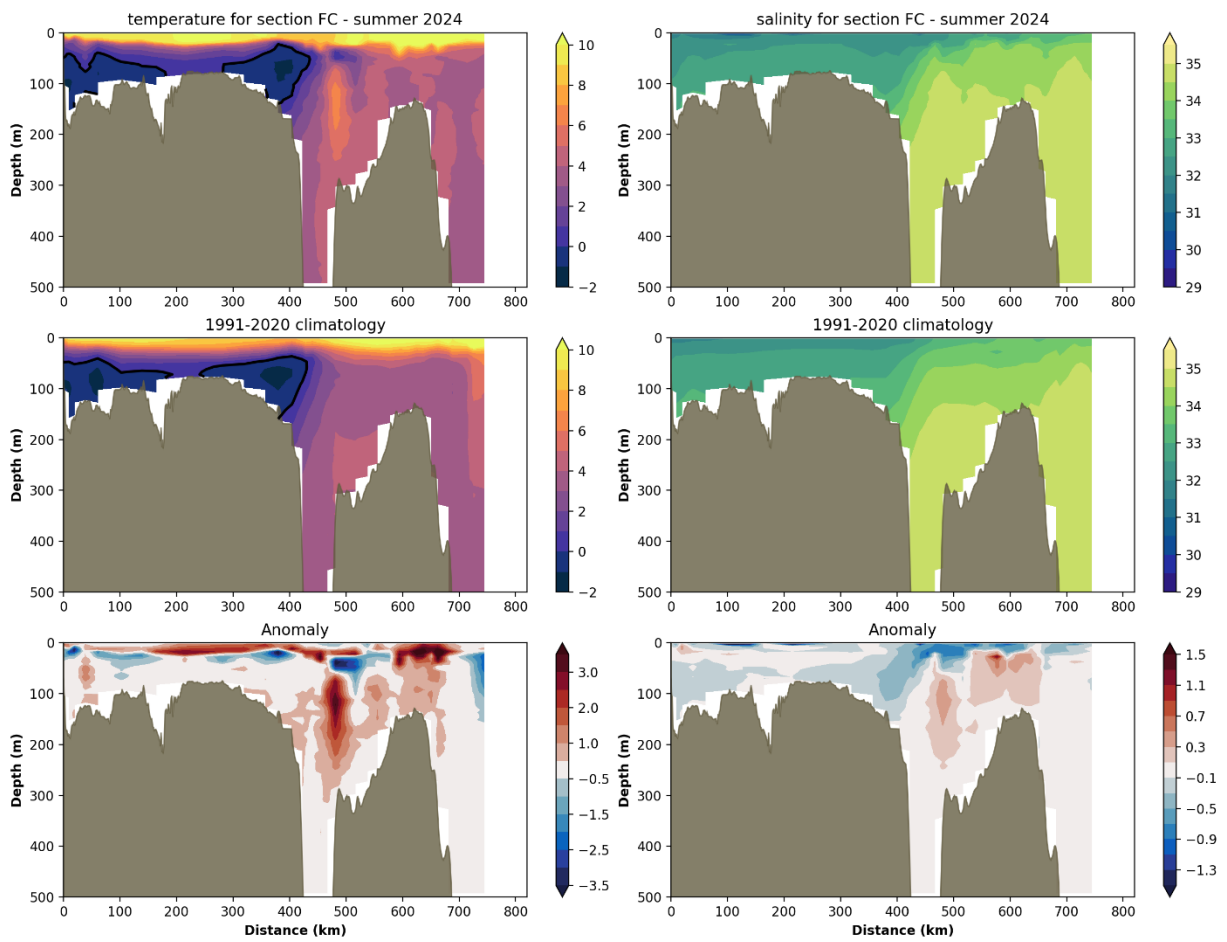


Figure 3434: Contours of temperature ($^{\circ}\text{C}$), left column, and salinity, right column, during summer 2024 (top row), with climatological averages (middle row) for the Flemish Cap (FC) hydrographic section (see map Figure 1 for location). Their respective anomalies for 2024 are plotted in the bottom panels.

6.2.2 Cold Intermediate Layer Variability

Two different methodologies were used to select temperature profiles used to determine the summer CIL area and core temperature. First, for years when AZMP trips were successfully completed (typically after 1995), profiles associated with the trip were isolated using the “STATION_NAME” variable from CASTS. Second, for years when no AZMP trip was completed or properly labeled in the metadata (prior to 1995, and during 2022 for example), a 0.25° radius circle surrounding the nominal position of each standardized station on the section was used to isolate all temperature profiles from CASTS taken between June and August. Each of the profiles was then vertically interpolated to fill any vertical gaps and averaged into a single profile per station. After these profiles were identified (i.e., based on station names or by a search in a radius around the nominal location of the station), the procedure for calculating the CIL metrics remains the same.

The climatology of each section was determined by averaging all annual summer temperature profiles for each station between 1991 and 2020. Then, for each individual year when the CIL metrics are derived, any missing profile from a station in a given year was filled with the climatological profile from that station. After visual inspection, and based on expert judgement, yearly CIL area and core temperature were set to NaNs (Not-a-Number) if the sampling did not properly resolve the CIL (e.g. if too many stations are missing in the inshore part of the section). If the sampling was deemed sufficient, temperature measurements between stations were then horizontally interpolated to a constant 1km grid cell size and depth-averaged into 5m bins. The number of grid cells below 0°C was then multiplied by the now-constant grid size to determine the CIL area. This was repeated between 1980 and 2024.

Statistics of summer CIL anomalies (CIL area, CIL core temperature and CIL core depth) for the three sections discussed above (SI, BB and FC) are presented in a scorecard in Figure 3535. The years where data are re-constructed using profiles collected between June and August are identified in the bottom row of the scorecards with small black dots. Because this method uses the average between June and August, the core CIL temperature is not derived. The climatological average cross-sectional areas of the summer CIL along these sections are $25\pm6 \text{ km}^2$, $24\pm7 \text{ km}^2$ and $20\pm5 \text{ km}^2$, respectively. The averaged anomalies of the CIL cross-sectional area for these three sections are summarized in Figure 3636 as a time series going back to 1950. In general, the summer CIL has been predominantly warmer and smaller than average since the mid-1990s, with a cold phase extending from about 2012 or 2014 to 2017. However, the most striking aspect of this long time series is the warm conditions that prevailed in the mid-1960s and mid-1970s, followed by a cold period that lasted from the mid-1980s to the mid-1990s.

In 2024, the CIL area was slightly negative (-1.0 SD for SI, -0.7 for BB, and -0.6 SD for FC). Averaged together, this leads to a slightly negative CIL subindex of -0.7 SD for 2024 (Figure 3636). The slightly negative anomaly is possibly due to mild 2024 winter conditions (Figure 5). This is because the summer CIL is a remnant of the previous winter’s conditions that are advected from the north during the rest of the year, and its properties are isolated from the summer atmospheric warming.

Figure 3535: Scorecards of the cold intermediate layer (CIL) summer statistics along the Seal Island, Bonavista and Flemish Cap hydrographic sections. The CIL area is defined as all water below 0°C (see black contours in Figure 3232 to Figure 3434) and the CIL core temperature as the minimum temperature of the CIL. Color codes for the CIL area have been reversed (positive is blue and negative is red) because a large CIL represents cold conditions, and vice-versa. Grayed cells indicate an absence of data. When possible, the AZMP station labeled in the data files are used, but in some instances (indicated here by black dots in the last row of each table) the average June-August profile of all available casts in at $0.25^\circ \text{x} 0.25^\circ$ (lat x lon) box around the nominal station locations are used to reconstruct the section.

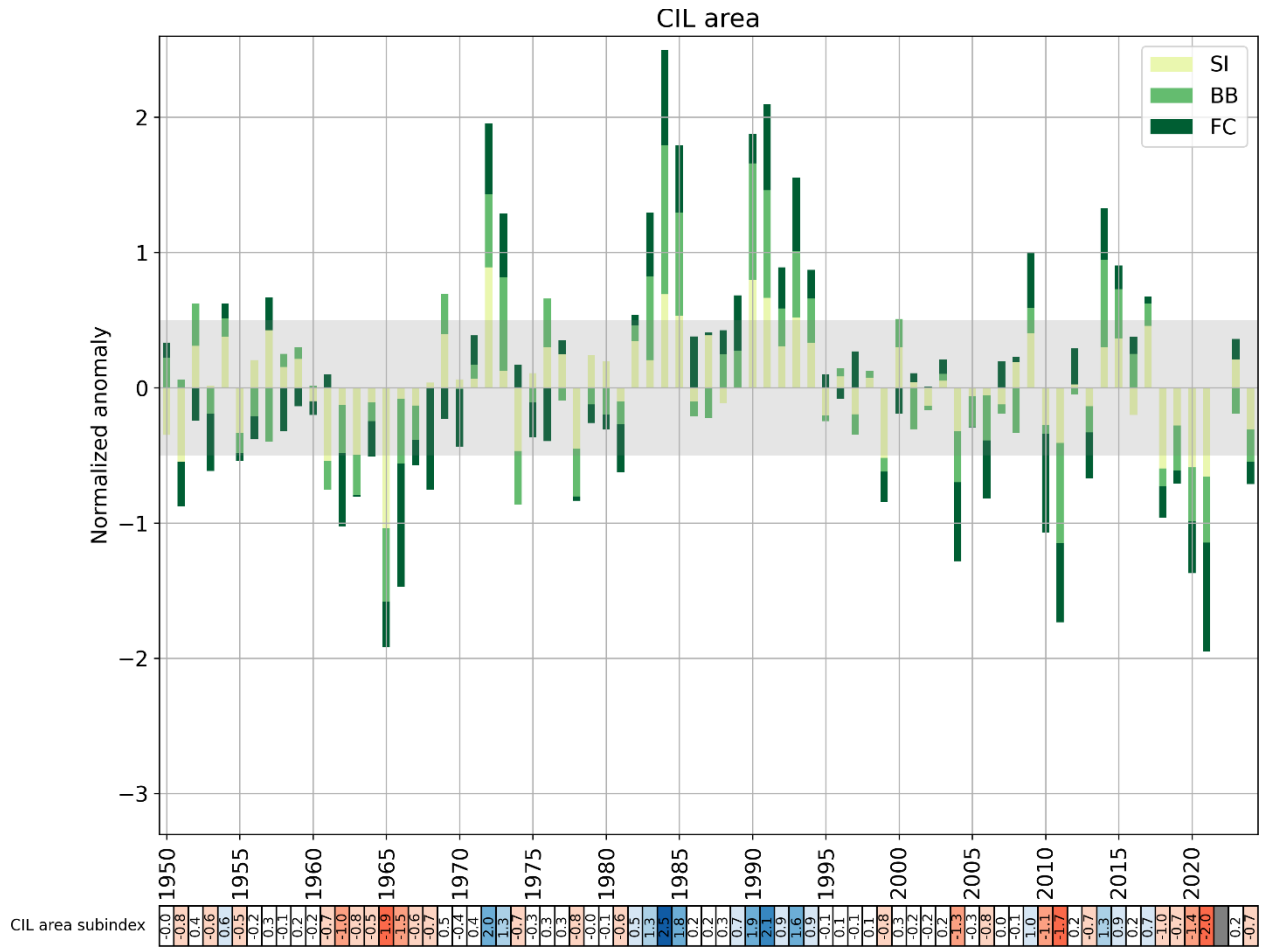


Figure 3636: Normalized anomalies of the mean CIL area for hydrographic sections Seal Island (SI), Bonavista Bay (BB) and Flemish Cap (FC). This time series corresponds to the average of the three sections, in which the contribution of each section is represented (values for each separate section since 1980 can be found in Figure 3535). The shaded area corresponds to the 1991–2020 average ± 0.5 SD, a range considered “normal”. The numerical values of this time series are reported in a color-coded scorecard at the bottom of the figure. Here negative anomalies (generally corresponding to warmer conditions) are colored red and positive anomalies blue. Years with no data present are colored grey. This time series is one component of the NL climate index (Figure 4646).

6.3 Bottom observations in NAFO sub-areas

Canada has been conducting stratified random bottom trawl surveys in NAFO Sub-areas 2 and 3 on the NL Shelf since 1971. Areas within each division, with a selected depth range, were divided into strata, and the number of fishing stations in an individual stratum was based on an area-weighted proportional allocation (Doubleday, 1981). Temperature profiles (and since 1990, salinity profiles) are available for most fishing sets in each stratum. These surveys provide large spatial-scale oceanographic data sets for the Newfoundland and Labrador Shelf. NAFO Subdivision 3Ps on the Newfoundland south coast and Divisions 3LNO on the Grand Banks are surveyed in the spring, and Divisions 2HJ off Labrador in the north, 3KL off eastern Newfoundland, and 3NO on the southern Grand Bank are surveyed in the fall. The hydrographic data collected on these surveys are routinely used to assess the spatial and temporal variability in the thermal habitat of several fish and invertebrate species. Many products based on the data are used to characterize the oceanographic bottom habitat. Among these are contour maps of the bottom temperatures and their anomalies, the area of the bottom covered by water in various temperature ranges, etc. In addition, species-specific ‘thermal habitat’ indices are often used in marine resource assessments for snow crab and northern shrimp.

Maps and statistics of bottom temperature and salinity observations, originally introduced by (Cyr et al., 2019), are now taken from the Canadian Atlantic Bottom Observations of Temperature-Salinity (CABOTS) data product (Coyne & Cyr, 2025). This methodology is recalled here. First, all available seasonal (April-June for spring, July-September for summer – not shown in this report –, and October-December for fall) temperature and salinity profiles are taken from the CASTS dataset (Coyne et al., 2023). A 0.05° latitude by 0.05° longitude grid is defined using GEBCO_2023 gridded bathymetry (GEBCO Compilation Group, 2023). Cycling over each grid cell, all profile measurements taken within 25m of the recorded depth and less than 2° distance from the point of interpolation are isolated. Profile measurements with land barriers between them and the point of interpolation are not considered. If three or more profile measurements meet all of these requirements, inverse distance-weighted interpolation with adaptive power determination (Lu & Wong, 2008) is then used to determine the associated grid cell value. Lastly, bottom observations are restricted to those between 10m and 1,000m depth, that is below the surface and shallower than down the continental slope where the data coverage is much lower. This procedure was performed for all years and all seasons between 1980 and 2024, from which the climatological seasonal averages (averages over 1991-2020) were derived.

Before calculating statistics on bottom observations (e.g. mean temperature or salinity, area of the sea floor covered by a certain temperature range, etc.), missing observations on the annual maps (for example when no observations are available for a specific year) are filled with the climatology. This allows us to calculate these metrics on the same seafloor area (especially important for areas covered by a certain temperature range). We note that this method is conservative as it will tend to pull anomalies towards zero. As part of CABOTS, we provide the percentage area of each NAFO division covered so users can assess the confidence of the observations for a certain year and season. Annual anomalies are calculated as the difference between annual observations and climatology.

6.3.1 Spring Conditions

Maps of spring climatological temperature and salinity, together with 2024 observations and anomalies for NAFO divisions 3LNOPs, are presented in Figure 3737 and Figure 3838, respectively (with the center panel showing also the station occupation coverage).

Bottom temperatures are generally colder in the northern part of the Grand Banks (3L) and warmer in the shallower southern part of the Grand Banks (3NO) and along the slopes (Figure 3737, left panel). In 2024, bottom temperatures were warmer than average in 3L, 3O (especially along the shelf break), and the

eastern parts of 3Ps excluding the Hermitage Channel. 3N bottom temperature anomalies were close to normal or slightly negative in 2024. Spring bottom salinities in 3LNO generally range from 32 to 33 over the central Grand Bank, and from 33 to 35 closer to the shelf edge (Figure 3838, left panel). In 3Ps, salinities are between 32 and 33 over shallower areas and above 34.5 in the Laurentian Channel. In 2024, salinities were close to normal in most of the Grand Banks, excluding the 3O shelf break and Northwest 3L where positive anomalies occurred, and the 3N shelf break where there were negative anomalies. Outside of the Hermitage Channel, most of 3Ps was slightly fresh in 2024.

Climate indices based on normalized spring bottom temperature anomalies (mean temperature and temperature in areas shallower than 200 m), as well as the area of the sea floor covered by water above 2°C and below 0°C between 1980 and 2024 are shown in a color-coded scorecard in Figure 3939. Overall, the colors visually highlight two contrasting periods of this time series: the cold period of the late 1980s / early 1990s (mostly blue cells) and the warm period of the early 2010s (mostly red cells). This warm period lasted between 2010 and 2013 (2011 being the warmest at 2.2 SD above normal in 3LNO) before returning towards to normal values between 2015 and 2019 (2014 was slightly cold). Between 2015 and 2019 the bottom area that was covered by <0°C water was also normal. While no information was available for 2020, 2021 and 2022 were the fourth and second warmest years in 3LNO, respectively. Bottom temperatures were back to normal in 3LNO in 2023, but increased again in 2024.

Division 3Ps bottom temperatures exhibit some similarities to those from 3LNO, with two periods of warm years, 1999–2000 and 2005–06, separated by a colder period (2003 is the coldest year on record since 1991 at -1.9 SD). With the exception of 2017 (which was normal), 2020 (no data), and 2023 (no data), all years between 2010 and 2022 were warmer than normal. 2021 and 2022 are the warmest years on record since 1980 at +2.8 SD and +2.9 SD, respectively. 2022 also established a new record for the area of the seafloor covered with water >2°C at +1.9 SD, beating the 2021 record of +1.8 SD. Although not as warm as 2021 and 2022, all 2024 bottom statistics remained positive (Figure 3939).

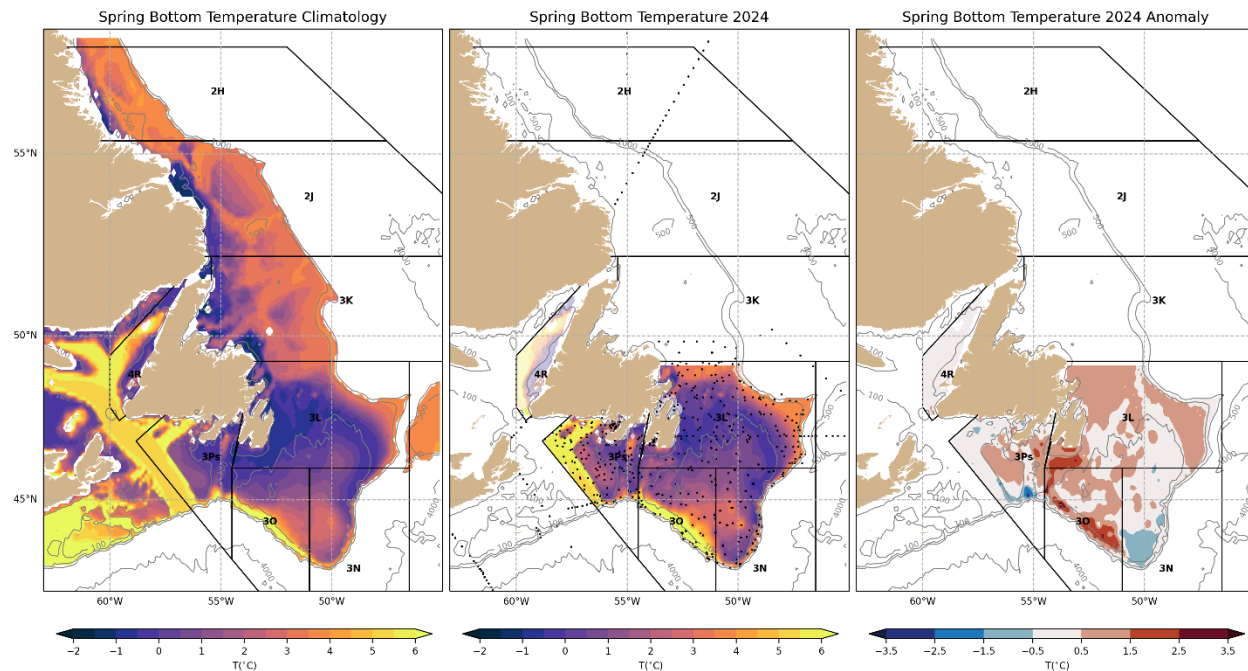


Figure 3737: Maps of the climatological (1991–2020) mean spring bottom temperature (left), and spring 2024 bottom temperature (center) and anomalies (right) for NAFO Divisions 3LNOPs only. The locations of observations used to derive the temperature field are shown as black dots in the center panel. When applicable, the portions of the shelf missing bottom temperatures were filled with the climatology (see methodology) and are left semi-transparent.

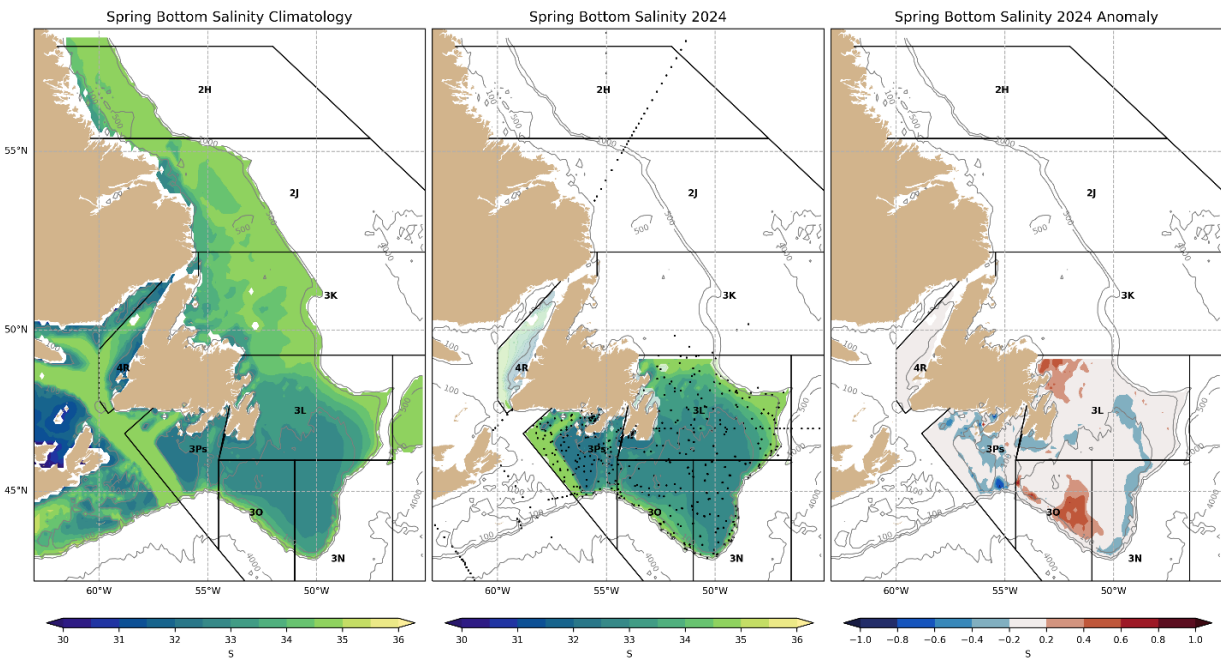


Figure 3838: Maps of the climatological (1991–2020) mean spring bottom salinity (left), and spring 2024 bottom salinity (center) and anomalies (right) for NAFO Divisions 3LNOPs only. The locations of observations used to derive the salinity field are shown as black dots in the center panel. When applicable, the portions of the shelf where missing bottom salinities were filled with the climatology (see methodology) are left semi-transparent.

Figure 3939: Scorecards of normalized spring bottom temperature anomalies (mean temperature, mean temperature for area shallower than 200 m, and area of sea floor covered by water above 2°C and below 0°C, respectively) for 3LNO and 3Ps.

6.3.2 Fall Conditions

Maps of fall climatological temperature and salinity, together with 2024 observations and anomalies for NAFO Divisions 2HJ3KLNO, are presented in Figure 4040 and Figure 4141 respectively (see center panel for station occupation coverage). Bottom temperatures are generally cold ($<0^{\circ}\text{C}$) in shallow areas of 2HJ3KLNO and warmer on the slopes and the troughs, and on the southern areas of the Grand Banks that lie at depths shallower than the CIL (e.g. $<50\text{m}$). In 2024, anomalies are generally warm or close to normal along the Labrador coast where the CIL typically hugs the seafloor, as well as the northern Grand Banks (Division 3L). Temperature anomalies are especially high along the 3O shelf break ($>3.5^{\circ}\text{C}$), while slightly negative temperature anomalies are present in much of 3N.

Bottom salinities in divisions 2HJ and 3K generally display an inshore-offshore gradient between <33 close to the coast and 34 to 35 at the shelf edge (Figure 4141, left panel). The Grand Banks (3LNO) bottom salinities range from <33 to 35, with the lowest values on the southeast shoal. In 2024 the bottom salinities were close to normal in most of the Labrador coast. Slightly positive salinity anomalies occurred in northern 3L and southern 3K, while negative anomalies were present in some parts of 3N. In 3O, positive salinity anomalies were located along the shelf break, matching the location of positive temperature anomalies.

Normalized bottom temperature anomalies (mean temperature and temperature in areas shallower than 200 m), as well as area of the sea floor covered by water above 2°C or below either 0°C or 1°C between 1980 and 2024 are shown in a color-coded scorecard in Figure 4242. A clear cold period is visible from the early 1980s to the mid-1990s, with the coldest anomalies reached in NAFO Divisions 2J and 3K. This was followed by a warmer period peaking in 2010 and 2011, the warmest years on records for these divisions. After a slight return to normal-to-cold anomalies between 2012 and 2017, bottom temperatures have been generally above or close to normal since. In 2024, bottom temperature anomalies were close to normal or positive in all divisions, with 2024 3LNO bottom temperature being the fifth highest on record (+1.4 SD), mostly driven by the positive temperature anomalies seen along the 3O shelf break. In 3LNO, the bottom area with water below 0°C was also at its second lowest on record (-1.5SD; Figure 4242),

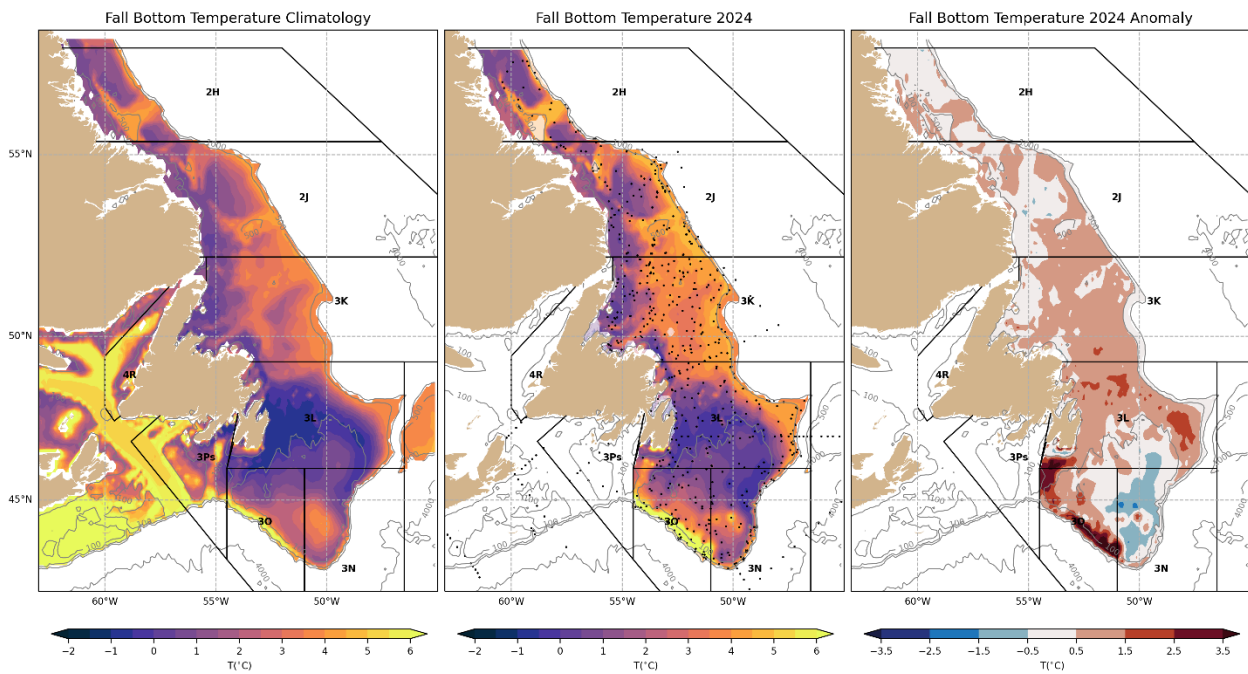


Figure 4040: Maps of the climatological (1991–2020) mean fall bottom temperature (left), and fall 2024 bottom temperature (center) and anomalies (right) for NAFO Divisions 2HJ3KLNO only. The locations of observations used to derive the temperature field are shown as black dots in the center panel. When applicable, the portions of the shelf where missing bottom temperatures were filled with the climatology (see methodology) are left semi-transparent.

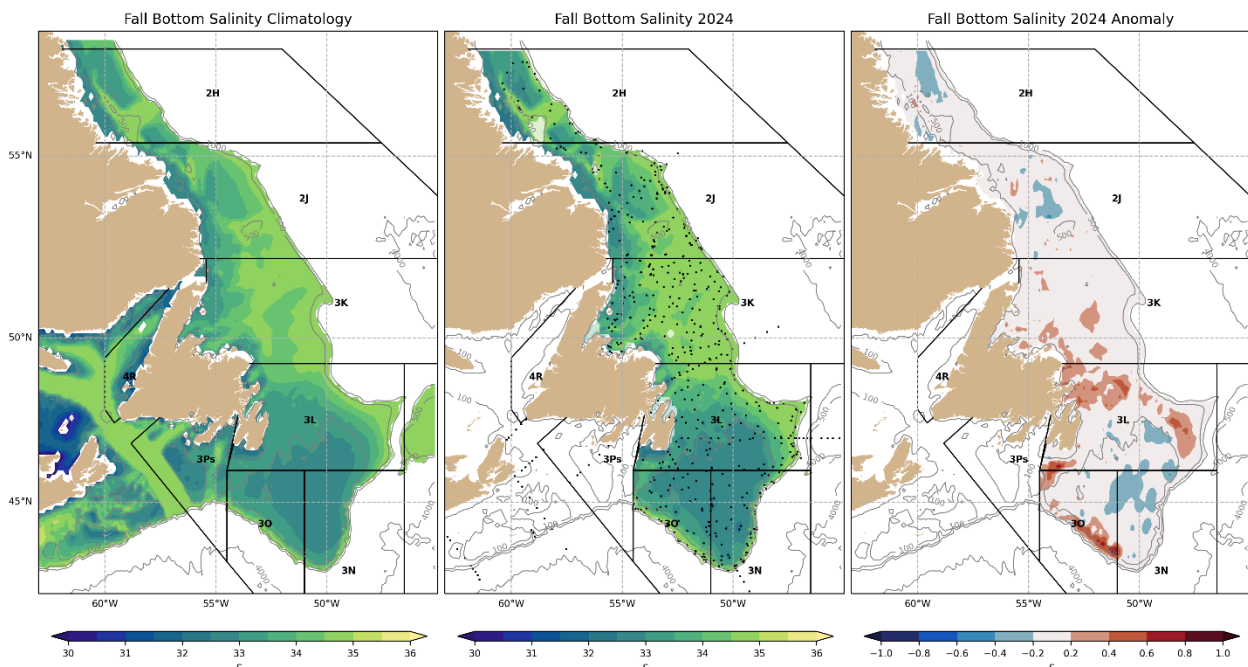


Figure 4141: Maps of the climatological (1991–2020) mean fall bottom salinity (left), and fall 2024 bottom salinity (center) and anomalies (right) for NAFO Divisions 2HJ3KLNO only. The locations of observations used to derive the salinity field are shown as black dots in the center panel. When applicable, the portions of the shelf where missing bottom salinities were filled with the climatology (see methodology) are left semi-transparent.

-- NAFO division 2H --																																															
80	81	82	83	84	85	86	87	88	89	90	91	92	93	94	95	96	97	98	99	00	01	02	03	04	05	06	07	08	09	10	11	12	13	14	15	16	17	18	19	20	21	22	23	24	\bar{x}	sd	
T _{bot}	-0.2	-0.2	-2.5			-1.2			-1.9			0.1	0.0	0.2	-1.4		1.3	-0.2	0.4	1.6	1.8	0.4	-0.4	-0.2	-0.7	-1.7	0.2	0.4	0.5	1.0	0.2	1.3	0.4	2.2	0.4												
T _{bot<200m}	0.1	0.2	-2.7			-1.3			-2.1			0.5	-0.1	0.1	-1.7		1.1	-0.2	0.0	1.4	1.7	0.2	-0.7	-0.4	0.0	-0.2	-1.4	0.2	0.8	0.8	1.0	0.4	1.4	0.0	1.2	0.5											
Area > 2°C	0.1	1.0	-2.0			-1.4			-1.9			0.9	-0.4	0.7	-1.5		1.0	-0.6	-0.5	1.0	1.0	0.2	-0.9	-0.5	0.4	-0.3	1.7	0.9	1.0	1.0	1.0	0.2	-0.6	34.1	8.3												
Area < 1°C	-0.1	-1.0	2.0			1.4			1.9			-0.9	0.4	-0.7	1.5		-1.0	0.6	0.5	-1.0	-1.0	-0.2	0.9	0.5	-0.4	0.3	1.7	-0.9	-1.0	-1.0	-0.2	0.6	8.6	8.3													
% Cov	74	85	62	84	11	74	60	76	48	12	12	82	73	12	14	0	36	90	90	90	15	89	10	19	90	17	90	12	90	90	90	90	86	84	90	89	90	89	85	77	82						
-- NAFO division 2J --																																															
T _{bot}	-1.0	-0.3	1.8	-1.9	-2.9	-2.4	-0.3	-2.1	-0.5	-1.3	-1.8	-1.5	-2.3	-2.2	-1.6	0.1	0.0	0.1	0.4	-0.6	0.3	-0.1	0.8	1.2	1.0	-0.2	1.1	0.0	0.0	1.7	1.7	0.0	0.0	-0.6	-0.7	0.1	-0.5	0.7	1.0	0.1	1.0	0.0	0.0	0.8	2.3	0.5	
T _{bot<200m}	-0.8	-0.3	-1.3	1.8	-2.8	-1.8	-0.2	1.9	-0.4	-1.0	-1.4	-1.5	-2.2	-2.0	-1.4	0.3	-0.2	-0.1	0.4	-0.5	0.3	-0.2	0.6	1.0	1.1	-0.5	1.0	-0.2	-0.1	1.7	1.9	-0.1	-0.1	-0.8	-0.6	0.7	-0.4	0.6	1.4	0.1	0.9	-0.3	-0.6	0.2	1.1	0.6	
Area > 2°C	-0.9	-0.3	-2.1	-1.7	-2.7	-2.1	-0.2	-2.0	-0.2	-1.5	-1.9	-1.8	-2.0	-2.0	-1.6	0.3	0.0	-0.1	1.0	-0.5	0.4	0.0	0.7	0.9	1.0	-0.5	1.0	-0.3	-0.4	1.3	1.3	-0.2	-0.2	-0.7	-0.7	1.0	-0.6	1.0	1.3	0.4	1.1	-0.1	-0.4	0.2	63.5	12.3	
Area < 1°C	0.9	0.3	2.1	1.8	2.7	2.1	0.2	2.0	0.2	1.5	1.9	1.8	2.0	2.0	1.6	-0.3	0.0	0.1	-1.0	0.5	-0.4	0.0	-0.7	-0.9	-1.0	0.5	-1.0	0.3	0.4	-1.3	-1.3	0.2	0.2	0.7	0.7	-1.0	0.6	-1.0	-1.3	-0.4	-1.1	0.1	0.4	-0.2	16.4	12.3	
% Cov	90	86	87	91	87	87	87	88	87	88	90	89	89	90	68	90	90	90	90	90	90	90	90	90	90	90	90	90	90	90	90	90	90	90	90	90	82	91	90								
-- NAFO division 3K --																																															
T _{bot}	-0.5	-0.3	-1.2	-1.2	-1.9	-2.4	-0.3	-1.4	-0.6	-0.9	-1.9	-1.4	-2.3	-2.1	-1.8	-0.8	-0.3	0.2	0.1	0.5	0.0	-0.1	0.2	0.4	1.2	0.7	-0.1	1.0	0.5	-0.1	1.4	2.1	0.1	0.1	-0.5	-0.3	-0.4	-0.9	0.8	0.9	0.7	1.3	0.4	0.4	1.3	2.4	0.5
T _{bot<200m}	-0.7	-0.4	-1.7	-1.7	-2.0	-2.0	0.0	-1.6	-0.9	-0.7	-1.2	-1.7	-1.9	-1.9	-1.5	0.1	0.2	-0.3	-0.4	0.2	-0.7	0.1	0.4	-0.3	1.0	0.5	-0.3	1.3	-0.4	-0.1	1.8	1.9	-0.1	-0.5	-0.9	-0.2	0.6	-0.4	1.0	1.5	0.9	1.1	-0.3	-0.8	0.2	0.8	0.6
Area > 2°C	-0.6	-0.3	1.0	-1.2	-1.3	-2.1	0.2	-0.9	-0.2	-0.3	-2.2	-1.2	-1.8	-2.1	-1.6	-0.2	0.3	-0.3	-0.4	0.0	-0.5	-0.2	0.3	0.1	1.4	0.6	-0.5	1.3	-0.2	-0.3	1.5	1.6	-0.5	-0.2	-0.6	-0.4	0.5	-0.8	1.3	1.5	1.1	1.3	-0.3	0.0	0.4	82.3	10.8
Area < 1°C	0.6	0.3	1.0	1.2	1.4	2.1	-0.2	0.9	0.2	0.3	2.2	1.2	1.8	2.1	1.6	0.2	-0.3	0.3	0.4	0.0	0.5	0.2	-0.3	-0.1	-1.4	-0.6	0.5	-1.3	0.2	0.3	-1.5	1.6	0.5	0.2	0.6	0.4	-0.5	0.8	-1.3	-1.5	-1.1	-1.3	0.3	0.1	-0.4	19.4	10.8
% Cov	90	90	79	87	91	92	89	90	88	88	92	94	95	95	93	90	95	96	94	93	94	94	94	87	94	94	94	93	92	94	95	92	94	94	94	94	92	93	93	94	94	94					
-- NAFO division 3LNO --																																															
T _{bot}	0.7	-0.1	-0.3	-0.4	-1.3	-1.6	0.1	-0.9	-0.5	-0.7	-0.8	-1.3	-1.2	-2.1	-1.8	-0.2	-0.1	-0.2	0.8	1.9	-0.2	0.1	-0.2	-0.2	0.6	0.2	0.4	-0.1	-0.6	0.6	1.6	2.1	0.4	-0.2	-0.3	-0.2	0.0	-1.3	-0.1	-0.4	1.8	1.0	0.1	1.4	1.3	0.5	
T _{bot<200m}	0.7	-0.1	-0.3	-0.4	-1.3	-1.5	0.2	-0.9	-0.4	-0.7	-0.5	-1.3	-1.1	-1.9	-1.6	-0.1	0.1	-0.3	0.8	2.1	-0.2	0.1	-0.1	-0.3	0.5	0.2	0.4	-0.2	-0.9	0.7	1.7	2.1	0.4	-0.2	-0.3	-0.2	0.1	-1.3	-0.2	-0.6	1.7	0.8	0.0	1.2	0.9	0.5	
Area > 2°C	0.3	-0.3	0.0	-0.5	-0.9	1.6	0.8	-0.8	-0.5	-0.7	-0.6	-1.2	-1.0	-2.1	1.8	0.3	-0.1	-0.2	0.6	2.0	-0.3	0.1	0.1	-0.2	0.6	0.1	0.4	-0.3	0.9	0.7	1.5	2.0	0.0	-0.3	-0.1	0.1	0.2	-1.3	-0.3	-0.7	1.9	0.8	-0.3	0.9	98.0	20.6	
Area < 1°C	0.6	-0.1	0.4	0.8	1.2	1.3	-0.2	0.4	0.2	0.8	0.4	1.6	1.3	1.9	1.9	-0.1	0.0	0.3	-0.4	-1.1	0.5	-0.1	-0.6	-0.1	-1.3	-0.5	-1.0	-0.2	-0.6	-1.3	0.1	0.0	0.4	0.2	0.2	1.4	-0.5	0.7	-1.4	-1.0	-0.3	-1.5	62.3	23.7			
% Cov	90	91	81	92	93	94	95	94	94	91	96	96	97	98	97	99	99	99	99	99	99	99	99	98	98	98	99	99	99	99	98	99	99	99	97	98	98	64	97	98	97						

Figure 4242: Scorecards of normalized fall bottom temperature anomalies (mean temperature, mean temperature for area shallower than 200 m, and area of sea floor covered by water above 2°C and below 0°C, respectively) for 2H, 2J, 3K and 3LNO.

6.3.3 Summary of bottom temperatures

When standardized anomalies of spring and fall bottom temperatures (first row of all scorecards in Figure 3939 and Figure 4242) are combined in a bar plot, the low frequency patterns of the bottom temperature on the NL shelf become apparent (Figure 4343). The coldest period encompasses the mid-1980s to the mid-1990s. Such cold anomalies are not observed later in the time series. Bottom temperatures from 2012 to 2017 were roughly normal, following the rather warm period of the mid-1990s to the mid-2010s. 2021 is the warmest year on record for the bottom temperature (+2.2 SD) and 2022 the third warmest (+1.1 SD). Bottom temperature dropped to normal in 2023 (+0.2 SD) but was above normal in 2024 at +0.8 SD.

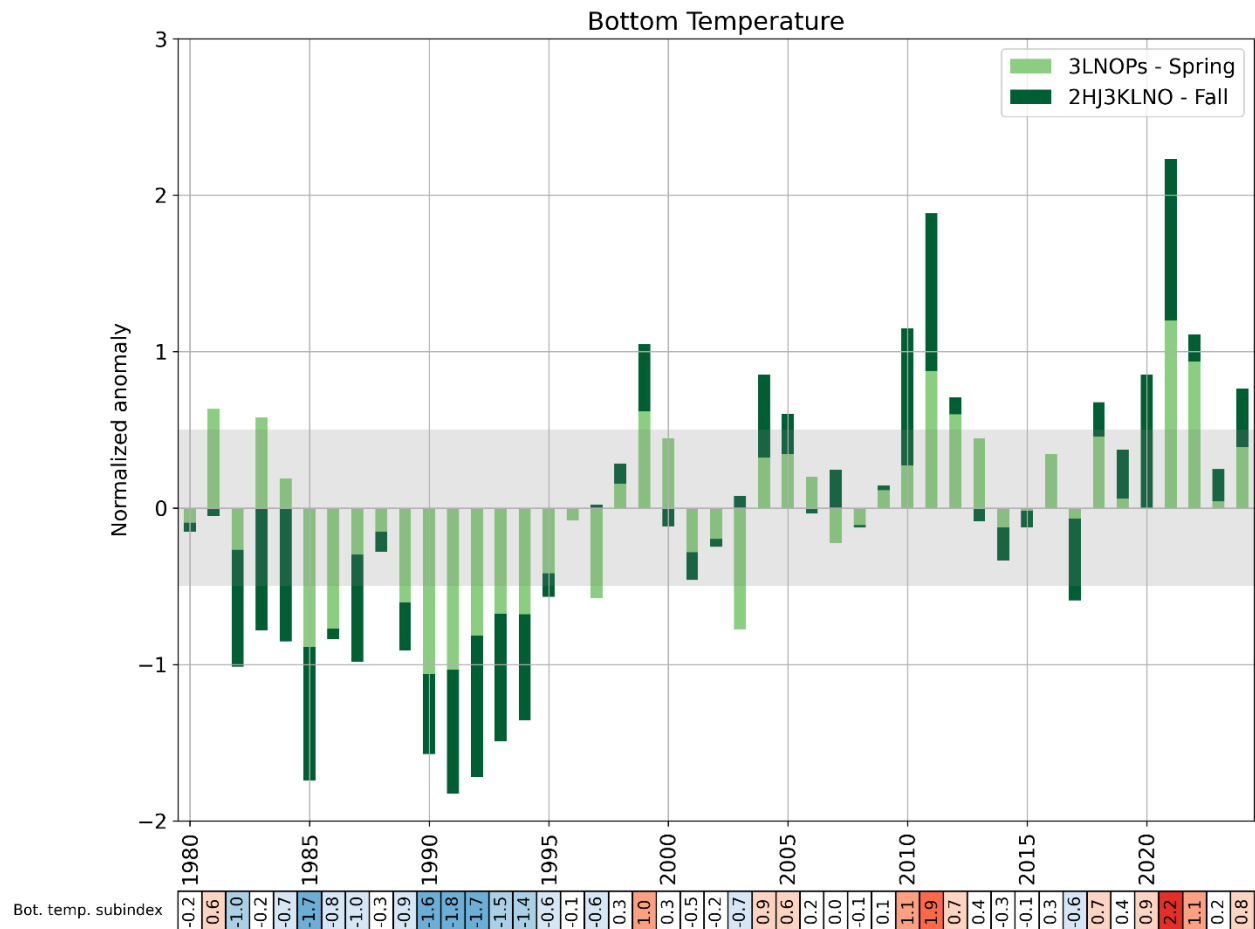


Figure 4343: Normalized anomalies of bottom temperature in NAFO Divisions 3LNOPs (spring) and 2HJ3KLNO (fall). This time series corresponds to the average of the two seasons, in which each contribution is represented. The shaded area corresponds to the 1991–2020 average ± 0.5 SD, a range considered “normal”. The numerical values of this time series are reported in a color-coded scorecard at the bottom of the figure. This time series is one component of the NL climate index (Figure 4646).

7 Labrador Current transport

The circulation in the NL region is dominated by the south-eastward flowing Labrador Current system, which floods the eastern shelf areas with cold and relatively fresh subpolar waters (Figure 4444). This flow can significantly affect physical and biological environments off Atlantic Canada on seasonal and interannual time scales. On the shelf, the Coastal Labrador Current (Florindo-López et al., 2020) originates near the northern tip of Labrador where the outflow from the Hudson Strait combines with the eastern Baffin Island Current and flows southeastward along the Labrador coast. During its southward journey on the Labrador shelf, it is strongly influenced by the seabed topography, following the various cross shelf saddles and inshore troughs. A separate offshore branch of the Labrador Current flows southeastward along the western boundary of the Labrador Sea. This current is part of the large-scale Northwest Atlantic circulation consisting of the West Greenland Current that flows northward along the West Coast of Greenland, a branch of which turns westward and crosses the northern Labrador Sea forming the northern section of the Northwest Atlantic subpolar gyre.

Further south, near the northern Grand Banks, the Coastal Labrador Current becomes broader and less defined. In this region, most of the inshore flow combines with the offshore branch and flows eastward, with a portion of the combined flow following the bathymetry southward around the southeast Grand Bank, and the remainder continuing east and southward around the Flemish Cap (Figure 4444). A smaller inshore component flows through the Avalon Channel and around the Avalon Peninsula, and then westward along the Newfoundland south coast. Off the southern Grand Bank the offshore branch flows westward along the continental slope, some of which flows into the Laurentian Channel and eventually onto the Scotian shelf. This extension of the Labrador Current on the Scotian shelf is referred to as the Scotian shelf break current. Additionally, there are strong interactions between the offshore branch of the Labrador Current and large-scale circulation. A significant portion of the offshore branch combines with the North Atlantic Current and forms the southern section of the subpolar gyre. Further east, the Flemish Cap is located in the confluence zone of subpolar and subtropical western boundary currents of the North Atlantic. Labrador Current water flows to the east along the northern slopes of the Cap and south around the eastern slopes of the Cap. In the eastern Flemish Pass, warmer high salinity North Atlantic Current water flows northward contributing to a topographically induced anticyclonic gyre over the central portion of the Cap.

Satellite altimetry data are used over a large spatial area to calculate the annual-mean anomalies of the Labrador Current transport (Han et al., 2014). A total of nine cross-slope satellite altimetry tracks are used to cover the Labrador Current on the NL shelf break from approximately 47°N to 58°N latitude (Figure 4444). Similarly, five tracks from approximately 55°W to 65°W longitude are used for the Scotian shelf break current. The nominal cross-slope depth ranges used for calculating the transport are from 200 to 3,000 m isobaths over the NL shelf break and from 200 to 2,000 m isobaths over the Scotian shelf break.

An empirical orthogonal function (EOF) analysis of the annual-mean transport anomalies was carried out. An index was developed from the time series of the first EOF mode and normalized by dividing the time series by its SD. The mean transport values are provided based on ocean circulation model output along the NL shelf break (Han et al., 2008) and over the Scotian shelf break (Han et al., 1997). The mean transport of the Labrador Current along the NL shelf break is 13 Sv ($1 \text{ Sv} = 10^6 \text{ m}^3 \text{ s}^{-1}$) with a SD of 1.4 Sv, and the mean transport of the Scotian shelf break current is 0.6 Sv with a SD of 0.3 Sv. The mean transport values will be updated as new model output becomes available. The SD values will be updated as knowledge on nominal depth improves.

The Labrador Current transport along the NL shelf break was out of phase with that of the Scotian shelf break current for most of the years over 1993–2024 (Figure 4545). The transport over the NL shelf break

was strong in the early- and mid-1990s, weak in the mid-2000s and early-2010s, and became strong again in late 2010s and early 2020s. In contrast, the transport over the Scotian shelf break fluctuated in a nearly opposite way. The Labrador Current transport index was positively and negatively correlated with the winter NAO index over the NL and Scotian shelves breaks, respectively.

The annual-mean transport of the Labrador Current over the Labrador and northeastern Newfoundland Slope in 2024 was normal, and weaker than that in the preceding two years. The transport on the Scotian Slope in 2024 was at a record high (+2.3 SD). A positive transport on the Scotian slope indicates that fresher and colder Labrador Slope water may reach the Scotian shelf and the mouth of the Laurentian Channel.

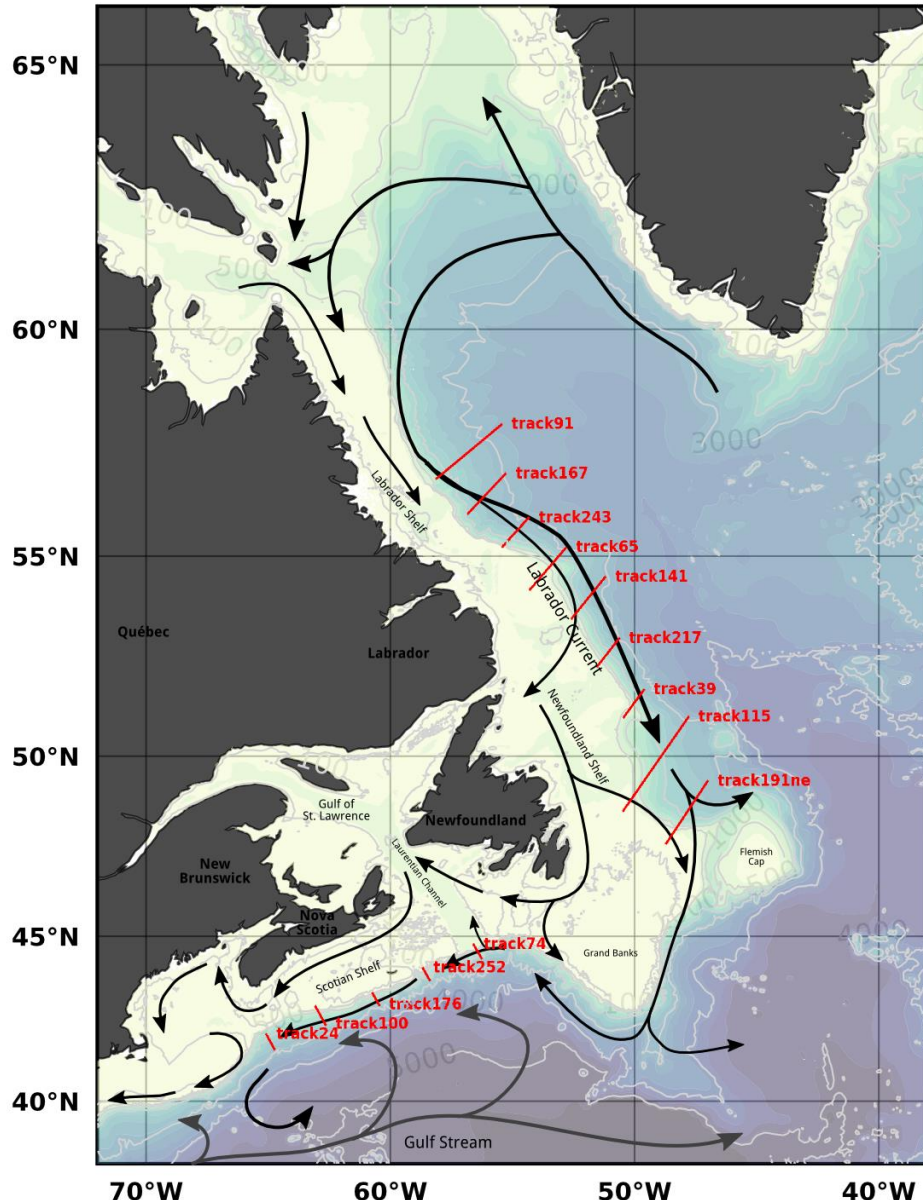


Figure 4444: Map showing the Northwest Atlantic bottom topography (depth contour values in light gray) and schematic flow patterns (arrows). The transport is calculated across the cross-slope sections (red lines) identified by their satellite ground tracks numbers. The series of northern tracks are used for the Labrador Current calculation on the NL shelf, while the series of tracks in the south are used for the Scotian shelf break current transport.

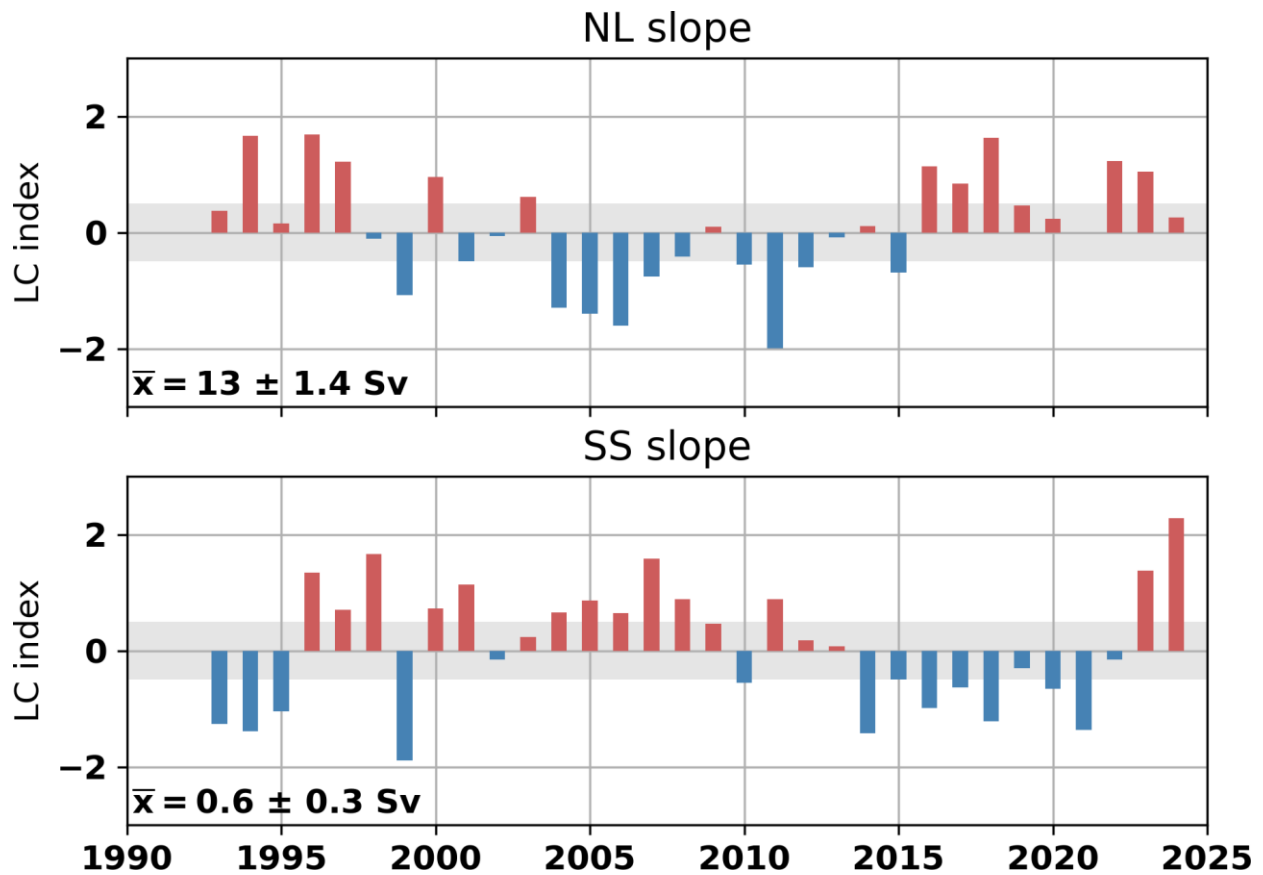


Figure 4545: Normalized index of the annual-mean transport of the Labrador Current on the NL shelf break (top) and Scotian shelf break (bottom). Long-term averages over 1993–2024 (with standard deviation) are $13.0 \pm 1.4 \text{ Sv}$ for the Labrador Current and $0.6 \pm 0.3 \text{ Sv}$ for the Scotian shelf break current. Shaded gray areas represent the $\pm 0.5 \text{ SD}$ range considered “normal”.

8 Summary

The NL climate index (NLCI) (Cyr & Galbraith, 2021), summarizes selected time series discussed throughout this report (Figure 4646). The NLCI runs between 1951 to present and is updated annually. This index is presented here in the form of a scorecard followed by a stacked bar plot of 10 equally weighted time series:

- Winter NAO index (starts in 1951; see Figure 3);
- Air temperatures at five sites (starts in 1950; see Figure 6);
- Sea ice season duration and maximum area for the northern Labrador, southern Labrador and Newfoundland shelves (starts in 1969; see Figure 12)
- Number of icebergs crossing 48°N (starts in 1950; see Figure 13);
- SSTs in NAFO Division 2GHJ3KLNOP (starts in 1982; see Figure 20);
- Vertically averaged temperature at Station 27 (starts in 1951; see Figure 2525);
- Vertically averaged salinity at Station 27 (starts in 1951; see Figure 2525);
- CIL core temperature at Station 27 (starts in 1951; see Figure 2727);
- Summer CIL areas on the hydrographic sections Seal Island, Bonavista Bay and Flemish Cap (starts in 1950; see Figure 3636); and
- Spring and fall bottom temperature in NAFO Divisions 3LNOPs and 2HJ3KLNO, respectively (starts in 1980; see Figure 4343).

The NLCI can be interpreted as a measure of the overall state of the climate system with positive values representing warm and fresh conditions with less sea ice and conversely negative values representing cold and salty conditions.

The NLCI highlights the different climate regimes prevailing since the early 1950s. For example, the relatively warm 1960s were followed by cold conditions in the early 1970s and most importantly from the mid-1980s to the mid-1990s which was the coldest decade on record. The warming trend from the early 1990s that peaked in 2010 was followed by recent cooling that culminated in 2015. While the NLCI for years 2016 to 2019 were normal (with a certain spread between positive and negative subindices within those years), the NLCI has been positive since 2020, including 2021 (+1.3) which is tied with 2010 for the warmest year on record. 2024 was the fourth warmest year on record (+1.1), continuing the warming trend. The NLCI and its subindices are available at <https://doi.org/10.20383/101.0301> [consulted 2025-01-23] (Cyr & Galbraith, 2020).

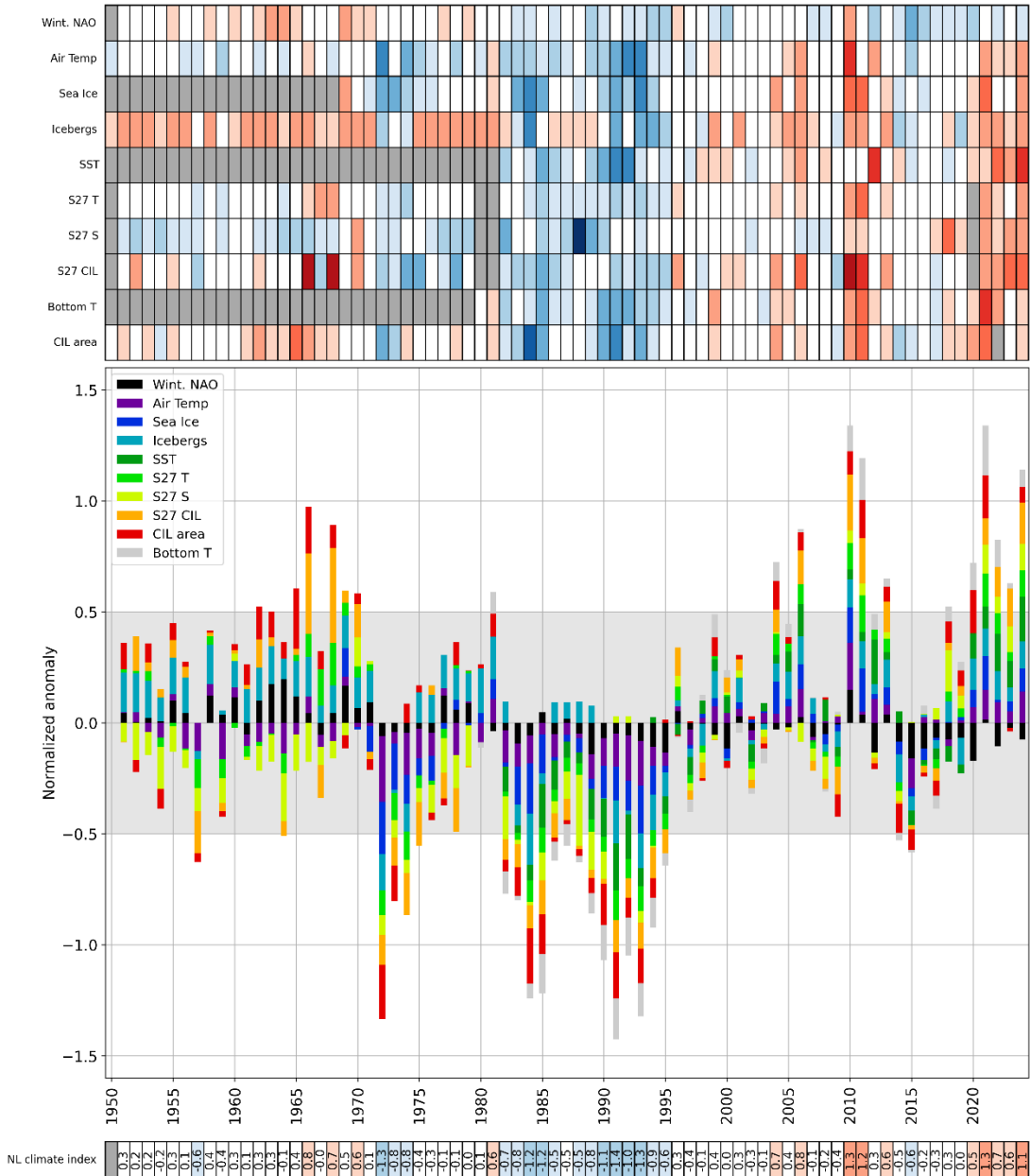


Figure 4646: Newfoundland and Labrador climate index derived by averaging the normalized anomalies of various time series presented in this report. The scorecard in the top panel represents the 10 subindices used to construct the climate index, color-coded according to their value (blue negative, red positive, white neutral). The sign of some indices (NAO, ice, icebergs, salinity and CIL area) has been reversed when positive anomalies are generally indicative of colder conditions. Grey cells in the scorecards indicate the absence of data. The central panel represents the climate index in a stacked-bar fashion, in which the total length of the bar is the average of the respective subindices and in which their relative contribution to the average is adjusted proportionally. The scorecard at the bottom of the figure shows the color-coded numerical values of the climate index. Note that the salinity anomaly sign is the opposite of that reported in the S27 scorecard (Figure 2626).

8.1 Highlights of 2024

- Based on the NL climate index, 2024 was overall warm at +1.1 (4th warmest rank).
- While winter NAO was slightly positive (normally indicative of colder winter conditions), most other sub-indices of the NLCI showed warm anomalies, especially SST.
- Sea surface temperatures were at their warmest on record (tied with 2012), and established new monthly and seasonal records across different NAFO divisions.
- Scotian Shelf transport for 2024 was the highest on record (+2.3 Sv), and above normal for the second year in a row after being normal or below normal since 2014.

9 Acknowledgements

This work is a contribution to the scientific program of the Atlantic Zone Monitoring Program. We thank the many scientists and technicians at the Northwest Atlantic Fisheries Centre for collecting and providing much of the data contained in this analysis and the Marine Environment Data Section of Fisheries and Oceans Canada in Ottawa for providing most of the historical data. We also thank the captain and crew of the CCGS John Cabot and RRS Discovery for oceanographic data collection during the summer and fall of 2024, respectively. We thank Heather Andres and Nancy Soontiens for reviewing the document.

References

- Casey, K. S., Brandon, T. B., Cornillon, P., & Evans, R. (2010). The Past, Present, and Future of the AVHRR Pathfinder SST Program. In V. Barale, J. Gower, & L. Alberotanza (Eds.), *Oceanography from Space: Revisited* (pp. 273–287). Springer Netherlands.
- Colbourne, E., Holden, J., Craig, J., Senciall, D., Bailey, W., Stead, P., & Fitzpatrick, C. (2015). Physical Oceanographic Conditions on the Newfoundland and Labrador Shelf During 2014. *DFO Can. Sci. Advis. Sec. Res. Doc.*, 2015/053, v + 37 p.
- Colbourne, E., Narayanan, S., & Prinsenberg, S. (1994). Climatic changes and environmental conditions in the Northwest Atlantic, 1970-1993. *ICES Journal of Marine Science Symposia*, 198, 311–322.
- Coyne, J., & Cyr, F. (2025). *Canadian Atlantic Bottom Observations Temperature-Salinity (CABOTS)*. Federated Research Data Repository. <https://doi.org/10.20383/103.0969>
- Coyne, J., Cyr, F., Donnet, S., Galbraith, P. S., Geoffroy, M., Hebert, D., Layton, C., Ratsimandresy, A., Snook, S., Soontiens, N., & Walkusz, W. (2023). Canadian Atlantic Shelf Temperature-Salinity (CASTS). *Federated Research Data Repository*. <https://doi.org/10.20383/102.0739>
- Cyr, F., Colbourne, E., Holden, J., Snook, S., Han, G., Chen, N., Bailey, W., Higdon, J., Lewis, S., Pye, B., & Senciall, D. (2019). Physical Oceanographic Conditions on the Newfoundland and Labrador Shelf during 2017. *DFO Can.Sci. Advis. Sec. Res. Doc.*, 2019/051, iv + 58 pp.
- Cyr, F., Coyne, J., Snook, S., Bishop, C., Galbraith, P. S., Chen, N., & Han, G. (2024). Physical Oceanographic Conditions on the Newfoundland and Labrador Shelf during 2023. In *Can. Tech. Rep. Hydrogr. Ocean Sci.* (Vol. 382).
- Cyr, F., & Galbraith, P. S. (2020). Newfoundland and Labrador climate index. In *Federated Research Data Repository*.
- Cyr, F., & Galbraith, P. S. (2021). A climate index for the Newfoundland and Labrador shelf. *Earth System Science Data*, 13(5), 1807–1828. <https://doi.org/10.5194/essd-13-1807-2021>
- Cyr, F., & Galbraith, P. S. (2023). Newfoundland-Labrador Shelf. Ch. 4.3. In C. González-Pola, K. M. H. Larsen, P. Fratantoni, & A. Beszczynska-Möller (Eds.), *ICES Report on Ocean Climate 2021* (p. 123 p.). ICES Cooperative Research Reports No. 358. <https://doi.org/10.17895/ices.pub.24755574>
- Dickson, R. R., Meincke, J., Malmberg, S. A., & Lee, A. J. (1988). The “great salinity anomaly” in the northern North Atlantic 1968–1982. *Progress in Oceanography*, 20(2), 103–151.

- Doubleday, W. G. (1981). Manual on groundfish surveys in the Northwest Atlantic. In *NAFC Sco. Coun. Studies 2* (p. 56 p.).
- Drinkwater, K. F., Myers, R. A., Pettipas, R. G., & Wright, T. L. (1994). Climatic data for the Northwest Atlantic: the position of the shelf/slope front and the northern boundary of the Gulf Stream between 50°W and 75°W, 1973–1992. *Canadian Data Report of Fisheries and Ocean Sciences*, 125, iv +103 p.
- Florindo-López, C., Bacon, S., Aksenov, Y., Chafik, L., Colbourne, E., & Penny Holliday, N. (2020). Arctic ocean and hudson bay freshwater exports: New estimates from seven decades of hydrographic surveys on the Labrador shelf. *Journal of Climate*, 33(20), 8849–8868. <https://doi.org/10.1175/JCLI-D-19-0083.1>
- Galbraith, P. S., Blais, M., Lizotte, M., Cyr, F., Bélanger, D., Casault, B., Clay, S., Layton, C., Starr, M., Chassé, J., Azetsu-scott, K., Coyne, J., Devred, E., Gabriel, C., Johnson, C. L., Maillet, G., Pepin, P., Plourde, S., Ringuette, M., & Shaw, J. (2024). Oceanographic conditions in the Atlantic zone in 2023. *Can. Tech. Rep. Hydrogr. Ocean Sci.*, 379, v+38 p.
- Galbraith, P. S., Chassé, J., Shaw, J.-L., Dumas, J., & Bourassa, M. (2024). Physical Oceanographic Conditions in the Gulf of St . Lawrence during 2023. *Can. Tech. Rep. Hydrogr. Ocean Sci.*, 378, v + 91 p.
- Galbraith, P. S., Chassé, J., Shaw, J.-L., Lefavire, D., & Bourassa, M.-N. (2025). Physical Oceanographic Conditions in the Gulf of St. Lawrence during 2024. In *Can. Tech. Rep. Hydrogr. Ocean Sci.* (Issue XXX).
- Galbraith, P. S., Larouche, P., Caverhill, C., Galbraith, P. S., Larouche, P., & Carla, C. (2021). A Sea-Surface Temperature Homogenization Blend for the Northwest Atlantic. *Canadian Journal of Remote Sensing*, 47(4), 554–568. <https://doi.org/10.1080/07038992.2021.1924645>
- Galbraith, P. S., Sévigny, C., Bourgault, D., & Dumont, D. (2024). Sea Ice Interannual Variability and Sensitivity to Fall Oceanic Conditions and Winter Air Temperature in the Gulf of St. Lawrence, Canada. *Journal of Geophysical Research: Oceans*, 129(7). <https://doi.org/10.1029/2023JC020784>
- GEBCO Compilation Group. (2023). *GEBCO 2023 Grid*. <https://doi.org/10.5285/f98b053b-0cbc-6c23-e053-6c86abc0af7b>
- Han, G., Chen, N., & Ma, Z. (2014). Is there a north-south phase shift in the surface Labrador Current transport on the interannual-to-decadal scale? *Journal of Geophysical Research: Oceans*, 119(1), 276–287. <https://doi.org/10.1002/2013JC009102>

- Han, G., Hannah, C. G., Loder, J. W., & Smith, P. C. (1997). Seasonal variation of the three-dimensional mean circulation over the Scotian Shelf. *Journal of Geophysical Research: Oceans*, 102(1), 1011–1025. <https://doi.org/10.1029/96jc03285>
- Han, G., Lu, Z., Wang, Z., Helbig, J., Chen, N., & de Young, B. (2008). Seasonal variability of the Labrador Current and shelf circulation off Newfoundland. *Journal of Geophysical Research*, 113(C10), C10013. <https://doi.org/10.1029/2007JC004376>
- Hebert, D., Layton, C., Brickman, D., & Galbraith, P. S. (2024). Physical Oceanographic Conditions on the Scotian Shelf and in the Gulf of Maine during 2023. *Canadian Technical Report of Hydrography and Ocean Sciences*, IN PRESS, vi + 71 p.
- Hobday, A. J., Alexander, L. V., Perkins, S. E., Smale, D. A., Straub, S. C., Oliver, E. C. J., BenthuySEN, J. A., Burrows, M. T., Donat, M. G., Feng, M., Holbrook, N. J., Moore, P. J., Scannell, H. A., Sen Gupta, A., & Wernberg, T. (2016). A hierarchical approach to defining marine heatwaves. *Progress in Oceanography*, 141, 227–238. <https://doi.org/10.1016/j.pocean.2015.12.014>
- Hobday, A. J., Oliver, E. C. J., Gupta, A. Sen, BenthuySEN, J. A., Burrows, M. T., Donat, M. G., Holbrook, N. J., Moore, P. J., Thomsen, M. S., Wernberg, T., & Smale, D. A. (2018). Categorizing and naming marine heatwaves. *Oceanography*, 31(2 Special Issue), 162–173. <https://doi.org/10.5670/oceanog.2018.205>
- ICNAF. (1978). List of ICNAF Standard Oceanographic Sections and Stations. *ICNAF Selected Papers Number 3*, 109–117. <https://doi.org/10.1111/j.1949-8594.1914.tb16026.x>
- International Ice Patrol. (2020). *International Ice Patrol Annual Count of Icebergs South of 48 Degrees North, 1900 to Present, Version 1*. <https://doi.org/10.7265/z6e8-3027>
- Jonasson, O., Gladkova, I., Ignatov, A., & Kihai, Y. (2024). *GHRSST NOAA/STAR ACSPO v2.81 0.02 degree L3S Daily Dataset from LEO Satellites (GDS version 2)*. NOAA National Centers for Environmental Information. Dataset. <https://doi.org/10.25921/d8ef-8597>
- Kerr, R. A. (2000). A North Atlantic Climate Pacemaker for the Centuries. *Science*, 288(5473), 1984–1985.
- Larouche, P., & Galbraith, P. S. (2016). A Sea-Surface Temperature Homogenization Blend for the Northwest Atlantic. *Canadian Journal of Remote Sensing*, 42(3), 243–258.
- Lu, G. Y., & Wong, D. W. (2008). An adaptive inverse-distance weighting spatial interpolation technique. *Computers and Geosciences*, 34(9), 1044–1055. <https://doi.org/10.1016/j.cageo.2007.07.010>
- McDougall, T. J., & Barker, P. M. (2011). *Getting started with TEOS-10 and the Gibbs Seawater (GSW) Oceanographic Toolbox* (Issue May). SCOR/IAPSO WG127.

Oliver, E. C. J., Benthuysen, J. A., Darmaraki, S., Donat, M. G., Hobday, A. J., Holbrook, N. J., Schlegel, R. W., & Sen Gupta, A. (2021). Marine Heatwaves. *Annual Review of Marine Science*, 13, 313–342. <https://doi.org/10.1146/annurev-marine-032720-095144>

Petrie, B., Akenhead, S. A., Lazier, S. A., & Loder, J. (1988). The cold intermediate layer on the Labrador and Northeast Newfoundland Shelves, 1978–86. *NAFO Science Council Studies*, 12, 57–69.

Petrie, B., Pettipas, R. G., & Petrie, W. M. (2007). An Overview of Meteorological, Sea Ice and Sea-Surface Temperature Conditions off Eastern Canada during 2006. *Canadian Science Advisory Secretariat, 2007/022*, iv + 38pp.

Report of the International Ice Patrol in the North Atlantic - 2024 Season. (2024).

[https://www.navcen.uscg.gov/sites/default/files/pdf/iip/Report of the International Ice Patrol in the North Atlantic 2024.pdf](https://www.navcen.uscg.gov/sites/default/files/pdf/iip/Report%20of%20the%20International%20Ice%20Patrol%20in%20the%20North%20Atlantic%202024.pdf)

Theriault, J. C., Petrie, B., Pepin, P., Gagnon, J., Gregory, D., Helbig, J., Herman, A., Lefavre, D., Mitchell, M., Pelchat, B., Runge, J., & Sameoto, D. (1998). Proposal for a northwest zonal monitoring program. *Canadian Technical Report of Hydrographic and Ocean Sciences*, 194, vii + 57 p.

Thyng, K. M., Greene, C. A., Hetland, R. D., Zimmerle, H. M., & DiMarco, S. F. (2016). True colors of oceanography: Guidelines for effective and accurate colormap selection. *Oceanography*, 29(3), 9–13. <https://doi.org/10.5670/oceanog.2016.66>

Vincent, L. A., Wang, X. L., Milewska, E. J., Wan, H., Yang, F., & Swail, V. (2012). A second generation of homogenized Canadian monthly surface air temperature for climate trend analysis. *Journal of Geophysical Research*, 117(D18110).
<https://doi.org/10.1029/2012JD017859>

Yashayaev, I. (2024). Intensification and shutdown of deep convection in the Labrador Sea were caused by changes in atmospheric and freshwater dynamics. *Communications Earth and Environment*, 5(1). <https://doi.org/10.1038/s43247-024-01296-9>